special issue
2023march

ENGINSOFT

futurities

The Simulation Based Engineering & Sciences Magazine

Heading towards Moving Particle Simulation

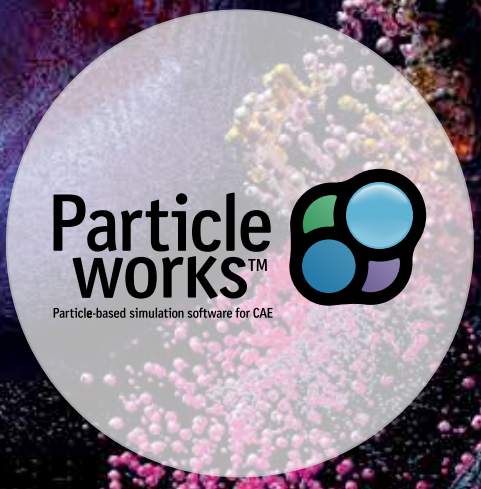

Futurities
Special Issue - March 2023
To receive a free copy of the next magazine, please contact our Marketing office at: marketing@enginsoft.com

EnginSoft S.p.A.
24126 BERGAMO c/o Parco Scientifico Tecnologico
Kilometro Rosso - Edificio A1, Via Stezzano 87 • Tel. +39 035 368711
50127 FIRENZE Via Panciatichi, 40 • Tel. +39 055 4376113
35129 PADOVA Via Giambellino, 7 • Tel. +39 049 7705311
72023 MESAGNE (BRINDISI) Via A. Murri, 2 - Z.I. • Tel. +39 0831 730194
38123 TRENTO fraz. Mattarello - Via della Stazione, 27 • Tel. +39 0461 915391
10133 TORINO Corso Marconi, 20 • Tel. +39 011 6525211

www.enginsoft.com
e-mail: info@enginsoft.com

Futurities is a quarterly magazine published by EnginSoft SpA

COMPANY INTERESTS
EnginSoft GmbH - Germany
EnginSoft UK - United Kingdom
EnginSoft Turkey - Turkey
EnginSoft USA
Particleworks Europe
www.enginsoft.com

CONSORZIO TCN www.consorziotcn.it • www.improve.it
M3E Mathematical Methods and Models for Engineering www.m3eweb.it
AnteMotion antemotion.com

ASSOCIATION INTERESTS
NAFEMS International www.nafems.it • www.nafems.org
TechNet Alliance www.technet-alliance.com

ADVERTISING
For advertising opportunities, please contact our Marketing office at: marketing@enginsoft.com

RESPONSIBLE DIRECTOR
Stefano Odorizzi

PRINTING
Grafiche Dalpiaz - Trento

Autorizzazione del Tribunale di Trento
n° 1353 RS di data 2/4/2008

Contents

AUTOMOTIVE

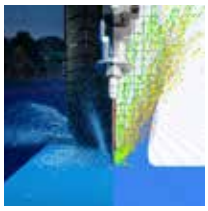

CIVIL

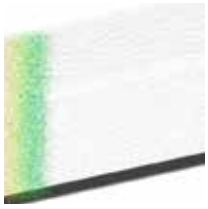

LUBRICATION

CONSUMER PRODUCTS

E-MOTOR COOLING

FOCUS ON

ENERGY

ENGINE

FOCUS ON

Meshfree liquid flow simulation

Methodology, features and applications

Moving Particle Simulation (MPS) is a meshless method of Computational Fluid Dynamics (CFD) specifically conceived to analyse liquid flows, from the most common liquids like water and oil, to the most complex ones such as highly viscous consumer products, adhesives, polymers, and foods or even semi-solid materials like grease or organic waste.

There are many CFD software packages on the market, each with a long development and validation history, that are highly suitable for a wide range of industrial applications.

The key advantages of MPS, however, lie in the words “meshless” and “particle-based”. These mean that MPS offers a “faster-track” from the physical reality that we wish to understand to the digital model we will use to describe that same reality. MPS models can be built directly using the most complex geometries without needing to spend numerous hours on adjusting a 3D CAD and generating computational grids.

Discretizing the fluid using particles (or, more specifically, by using calculation points that are free to move according to the Navier-Stokes equations) makes the solution highly stable. The native GPU solver and the impressive speed-to-cost ratio of modern GPUs make the solution of complex real-world cases feasible within industrial time constraints using limited hardware resources, such as a desktop workstation.

In other words, MPS removes some of the barriers that previously limited access to CFD and its benefits.
It enables CFD to be used for applications in which it was previously unfeasible to use conventional CFD, and it enables CFD to be used earlier in the design process when there is still sufficient time, space, and opportunity to improve and innovate. In addition, its rendering CFD generally simpler and more accessible, and complex CFD faster and more feasible (a few days or hours rather than weeks) does not mean sacrificing the accuracy and reliability of results.

This publication is a collection of papers addressing different industrial sectors and covering applications ranging from lubrication of transmissions, cooling of engines, prevention of aquaplaning, and fire extinguishing, to the electrification of mobility solutions and the study of snow drifts.

It should be noted, however, that this collection is a very incomplete representation of years of simulation and model development since it presents only a tiny proportion of the results of years of collaboration

between simulation engineers and testing or field engineers who have validated the method by comparing simulation results with experimental data and with both expected and unexpected results.

The common thread unifying these papers was the need to find a way to simulate a system, process, or item that was impossible to simulate in other ways; the need to find a solution to an industrial case within industrial time constraints and using reasonable resources and a scientific method.

The authors are linked by their common desire to develop and validate a method for future use by their companies as an asset for innovation and in order to stay one step ahead of their competitors.

Particleworks: Meshfree liquid flow simulation software

Particleworks is CAE software based on the Moving Particle Simulation (MPS) method for the simulation of liquid flows. It solves the Navier-Stokes equations using a deterministic Lagrangian method while its main fields of application are free-surface flows, and liquid jets or spray.

Particleworks discretizes the fluid using particles and eliminates the need for a computational grid. Its meshless nature and intuitive interface make the simulation process simple and fast, even for complex geometries with moving parts. It is widely used in different industrial sectors: automotive, aerospace, consumer goods, power generation, the Food & Beverage industry, machining, and others.

The software's development is industry-driven and benefits from the close collaboration between industry, the Prometech Software development team, and the inventor of the MPS method, Prof. Seiichi Koshizuka of the University of Tokyo.

In addition to the simulation of liquid flows Particleworks includes modules that simulate heat conduction and conjugate heat transfer; airflow and multi-phase liquid-gas flow; and a Discrete Element Method solver to compute the flow of granular materials and their interactions with liquids.

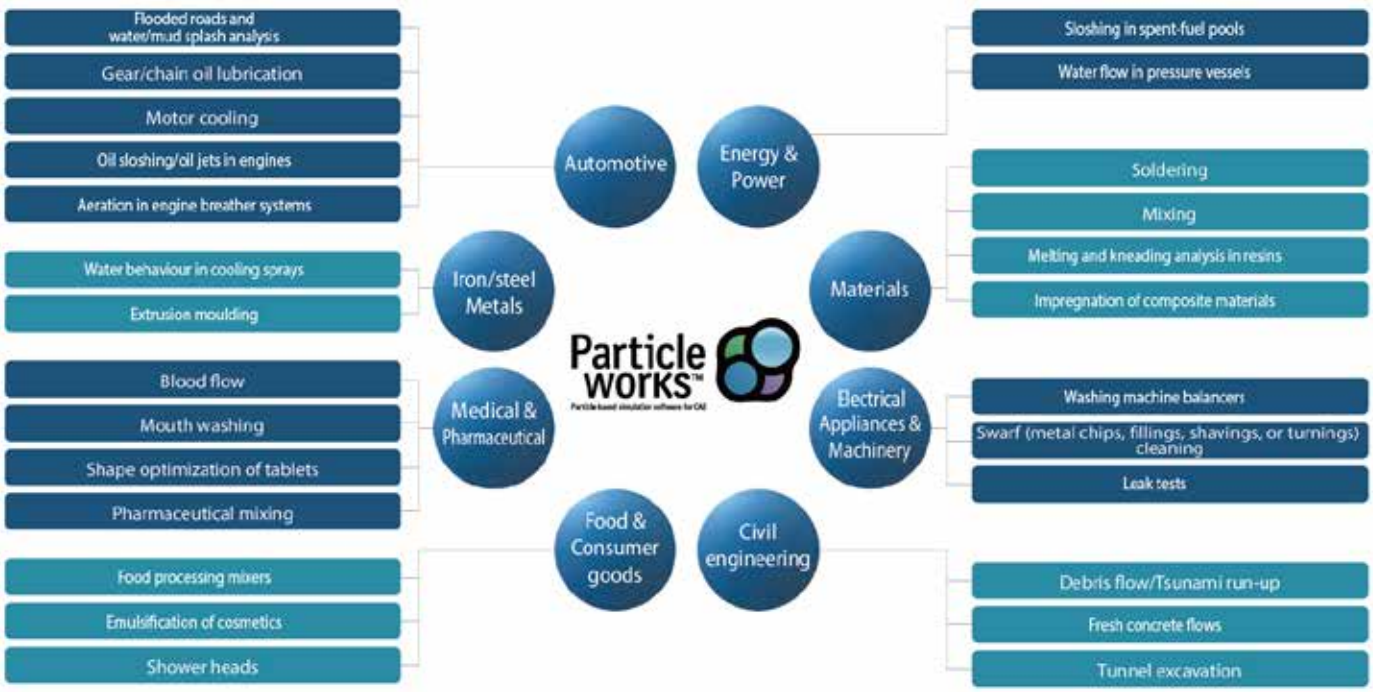

For more information:

particleworks-europe.com | info@particleworks-europe.com

About Prometech Software, Inc.

Prometech Software was founded by experienced professionals and researchers at the University of Tokyo in 2004. With the company's unique technology based on the Moving Particle Simulation (MPS) and Multi-GPU acceleration, Prometech provides simulaton software and solutions to support engineering industries including chemical, rubber, steel, process manufacturing.

In addition to simulation technology of complicated physical phenomena which has been researched in the field of computer science, Prometech Software Inc. provides interactive high-quality computational realities to the manufacturing, video production and entertainment industries by using high-speed HD drawing technology. Prometech's core business is providing groundbreaking particle-based physical simulations by the use of top of the edge hardware. Prometech is creating a new world by joining both engineering simulations (CAE) and visualization and video productions.

PROMETECH.

www.prometech.co.jp

ENGINSOFT

www.enginsoft.com

About EnginSoft

EnginSoft is one of the leading technology transfer companies in the field of Simulation Based Engineering Science (SBES). Since its foundation in 1984, through our expansion in the sector in the mid-Seventies, to the present day with a global presence, EnginSoft has always been at the forefront of technological innovation.

EnginSoft is unique in its field simultaneously having specific and advanced skills in all disciplines in which simulation technologies are utilized, combined with the vital complementary statistical approaches, scientific computing know-how and simulation process and data management (SPDM) knowledge and experience to assist customers to safely and effectively navigate, exploit and manage the vast and complex data and information obtained both from SBES applications and from direct physical testing.

Particleworks Europe

Particleworks Europe is a joint venture between Prometech Software Inc. and EnginSoft S.p.A. The JV aims to establish, promote and manage the European distribution of Particleworks and of Granuleworks.

In addition to and in order to support and enhance this network, Particleworks Europe is constituting the European competence centre for these technologies, both to help distributors and to assist customers.

Particleworks Europe aims at aggregating the needs and requirements of target customers to ensure their rational inclusion in the development roadmap of the related software technologies.

Particleworks EUROPE

www.particleworks-europe.com

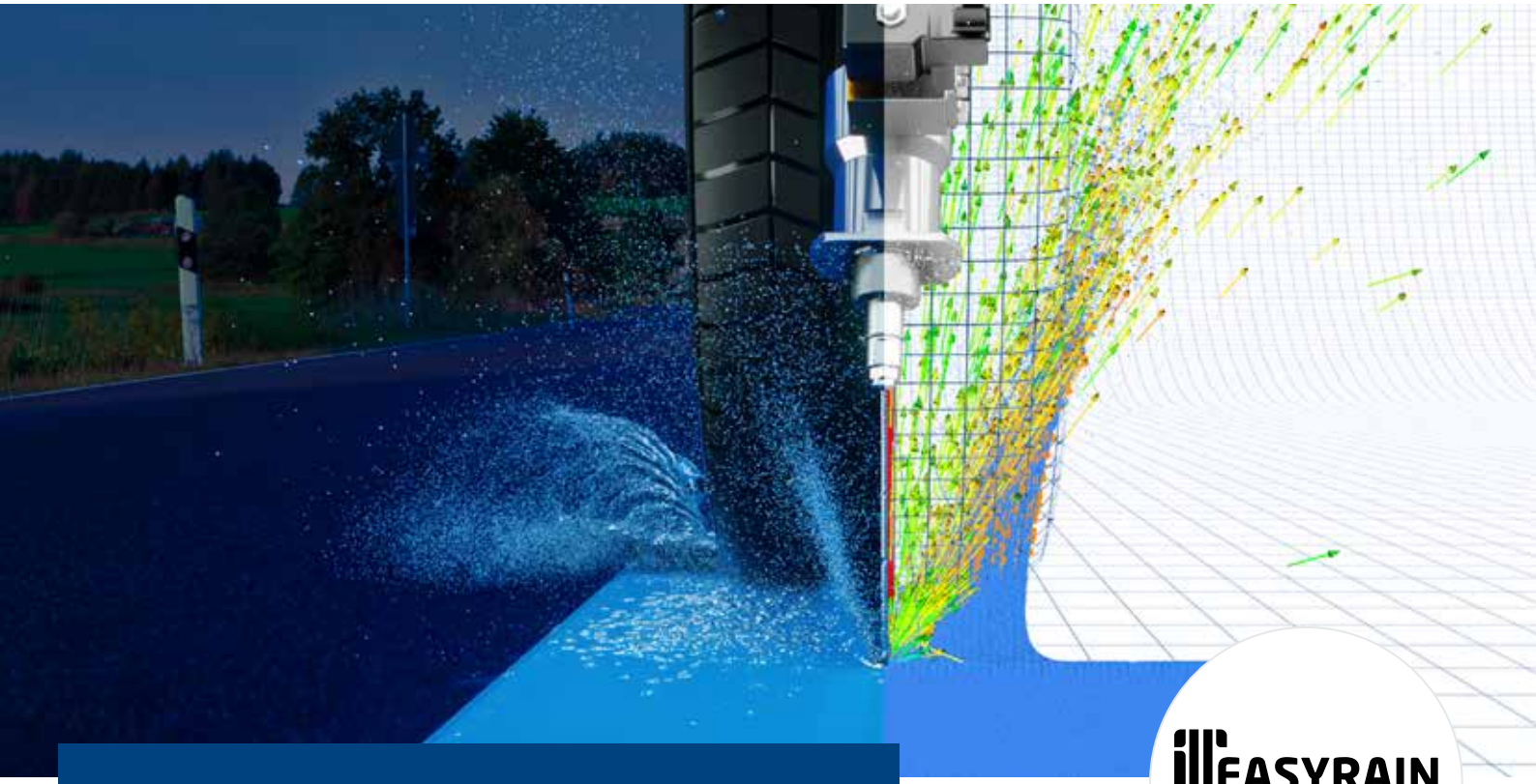

Optimization of water spray parameters by 3D CFD particle simulation for an automotive anti-aquaplaning system

by Federico Accardo[1], Paolo Alberto Fina[1] and Michele Merelli[2]
1. EASYRAIN - 2. EnginSoft

One in four accidents in the United States (according to the National Highway Traffic Safety Administration) is due to adverse weather conditions.

The same study reports that wet roads are more dangerous than icy and snowy roads (46% of accidents versus 30%). Aquaplaning and hydroplaning occur when water, accumulated on the road surface or splashed by vehicles ahead, forms a thin layer between the asphalt and the car tyre.

This layer prevents the tyre from properly adhering and gripping, making the vehicle uncontrollable and often causing accidents. In this paper, we discuss the digital modelling and simulation of the EASYRAIN Aquaplaning Intelligent Solution (AIS) using mesh-free moving particle simulation (MPS). We used MPS to study the impact of the pressurized water jet of the AIS system. First, we verified the jet forces predicted by the CFD methodology with experimental configurations and compared the MPS results with the results of track tests. Furthermore, we analysed the influence of different working parameters

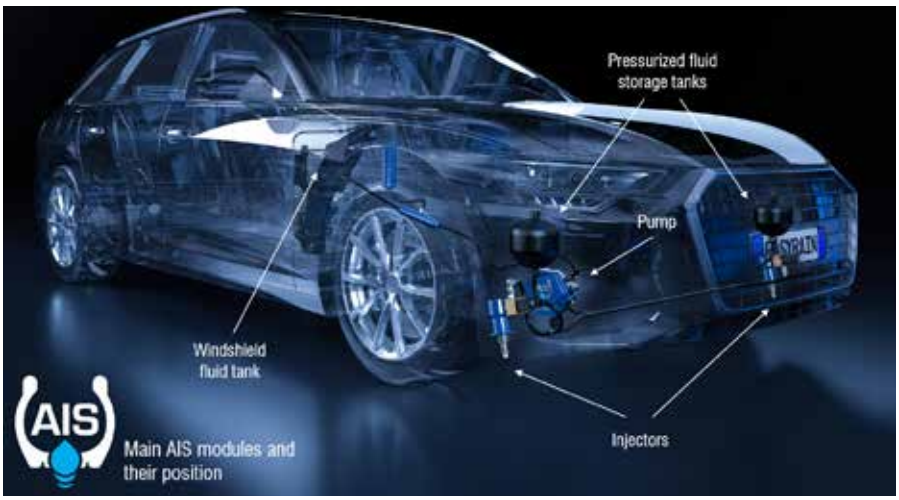

Fig. 1. Overview of the AIS solution and its hydraulic system.

(such as water jet pressure, spray angle and injector position) on the efficiency of aquaplaning prevention. Considering the speed of a car, it is important to take into account aerodynamic effects and their influence on the jet. For this reason, we used a finite volume solver embedded in the CFD software itself and fully coupled with the liquid phase MPS. Thanks to the reported validations and experimental correlations, EASYRAIN can thus design and improve the AIS system without the need for time-consuming physical prototypes and expensive track tests, resulting in the best solution for a wide range of car bodies and hydraulic systems.

EASYRAIN mission and vision: saving lives by reducing aquaplaning

Aquaplaning occurs when a thin layer of water accumulates between the car tyre and the road surface. This causes a loss of grip that results in an unresponsive vehicle. Founded in Italy in 2013, EASYRAIN's main mission is to save lives by developing advanced safety solutions to prevent aquaplaning. EASYRAIN's flagship product is the Aquaplaning Intelligent Solution (AIS), a safety device that can be fitted to a wide range of vehicles (including autonomous and electric vehicles).

The AIS directs a controlled jet of water in front of the front tyres to break up the water layer, effectively counteracting aquaplaning and restoring tyre grip and vehicle control. The Aquaplaning Intelligent Solution (AIS) is shown in Fig. 1. It consists of two injectors, pressurized fluid tanks, and a pump. The system is connected to the windshield fluid tank, which holds most of the water.

EASYRAIN is also developing EASYRAIN Digital Platform (EDP) and EASYRAIN Cloud (ERC). EDP is a platform that hosts virtual sensors that recognize dangerous road conditions, based on vehicle network data combined with EASYRAIN's patented algorithm. The Digital Aquaplaning Information (DAI), the first virtual sensor to be developed within the platform, recognizes dangerous wet road conditions and provides three levels of warning to the vehicle. ERC is a cloud service to expand and enhance the performance of AIS and EDP.

Moving particle CFD and simulation overview

We present a simulation to analyse the water sprayed by the AIS nozzles. The digital prototype of the injector is created using a mesh-free MPS (moving particle simulation) CFD approach. MPS is an innovative CFD (computational fluid dynamics) method for simulating free surface flows and liquid jets [1]. As this method does not require a computational grid, it streamlines and accelerates the simulation of complex geometries and moving parts. As far as vehicle simulation is concerned MPS is widely used to analyze the soiling of windows and other critical regions [2], or to optimize tyres to reduce splashes towards the car body [3].

As schematized in Fig. 2. the simulation focuses on the area close to the front tyre. An inflow is placed at the injector and water is initialized on the road surface, representing the water layer that

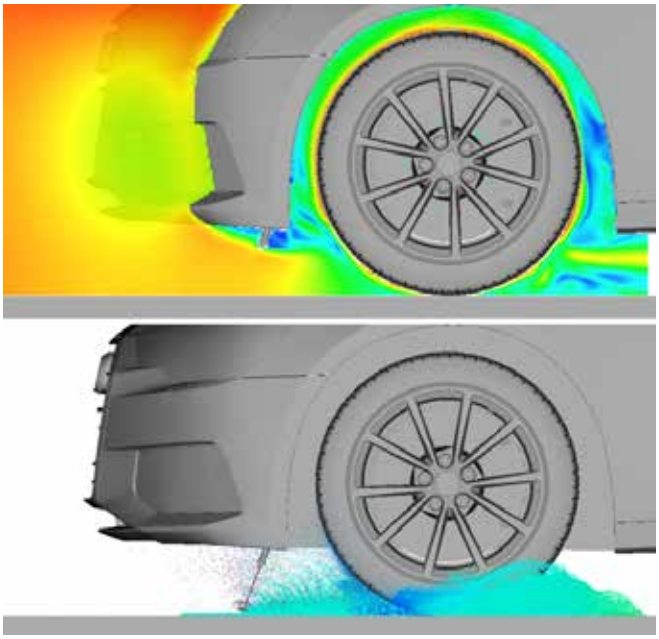

Fig. 2. The images show the simulated region and the car component considered. The top image shows the velocity profile of the finite volume method calculated in the software; the bottom image shows an example of the moving particle simulation showing the jet and the tyre interacting with the puddle.

induces aquaplaning. The car then moves towards the puddle; the tyre rotation is also modelled. Prior to the MPS simulation, by taking advantage of a finite volume solver incorporated in the Particleworks MPS software, we modelled the aerodynamics of the system using the same simulation configuration without either meshing or preparing any geometry (the software calculates an automatic Cartesian grid). Although the built-in FVM (finite volume method) allows for a coupled MPS-FVM simulation, we decided that the one-way coupling approach might be more suitable to reduce simulation time. After stabilization of the FVM simulation, the airfield was transferred to the MPS simulation.

With regard to the numerical settings of the simulation, an appropriate particle size of 0.6mm was selected: small enough to capture the jet profile while still allowing reasonable simulation times. At its peak, the simulation took into account 10M particles (particles were removed from the domain when they splashed out of the area of interest). The transient simulation analysed 2-3s; the corresponding hardware time was approximately 3-4 days (on 1xGPU, NVIDIA RTX3090).

Validation of simulation results: force prediction on flat plate and aquaplaning

Before using the CFD methodology for R&D considerations and improvements to the AIS system, the model was validated by EASYRAIN with experimental observations.

First a flat-plate pressure gauge was modelled in Particleworks. The forces on the flat plate were compared with the experimental values. The simulation setup is briefly shown. The inflow is positioned in the injection area and the pressure profile is written in the software to match the pump characteristics and working conditions.

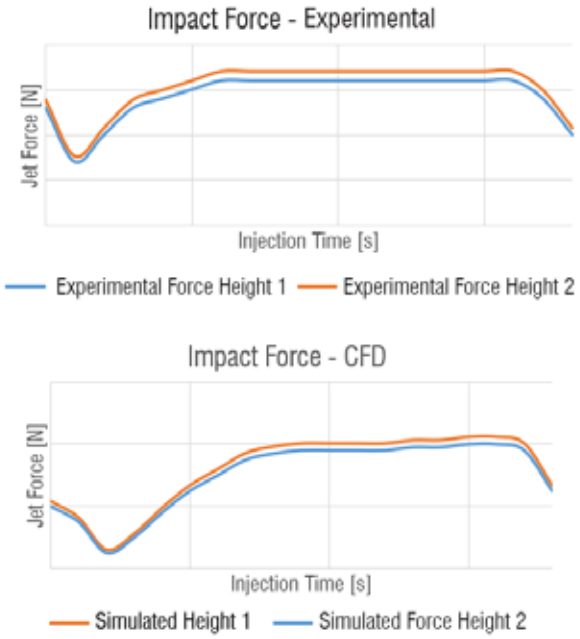

Fig. 3. Top: Experimental forces measured on a flat plate while varying the height of the AIS nozzle, Bottom: MPS predictions for corresponding jet heights.

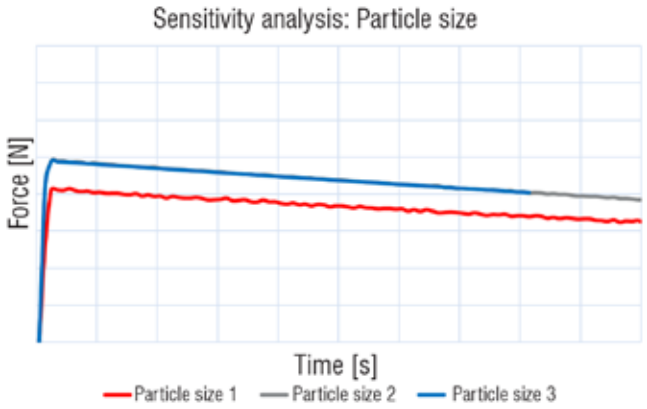

Fig. 4. MPS prediction of flat-plate force during AIS activation. A clear convergence with decreasing particle size is observed.

The main objectives of this simulation were to verify:

- The influence of particle size on force predictions
- The correspondence between the pressure profile and predicted force on the plate
- The influence of the casting height (relative to the plate) on the measured forces

In Fig. 3 we show the comparison between the flat-plate experimental data and MPS force predictions during AIS jet activation. The simulated trend closely resembles the experimental signal. Moreover, the influence of the water height on the jet forces is quantitatively significant: the relative difference between the two heights falls within an error range of 3%, compared to the experimental values.

To further corroborate the MPS results, we performed a sensitivity analysis on them by varying the particle sizes (Fig. 4). This process is commonly found in CFD analysis to verify the mesh independence of computational predictions. As can be seen, by decreasing the particle size and improving the resolution of the MPS simulation, we achieved convergence on the predicted forces.

After the flat-plate correlation, EASYRAIN compared the video footage on the track with the flow prediction simulated by the software. By simulating conditions (speed, puddle depth) known to be critical for aquaplaning, EASYRAIN was able to verify whether the same critical conditions were observed in the digital model. As can be seen, the opening capabilities of the jet stream are captured closely by the software. In addition, the simulation also predicts other phenomena that directly affect the performance of the jet; this information remains confidential.

Digital comparison between prototypes (AIS Proto-1 vs AIS Proto-2)

For development reasons, the AIS underwent several technical modifications prior to the CFD simulations. Specifically, the pumping system was updated, resulting in a significantly different pressure curve during AIS activation (Fig. 5).

Since track data was only available for AIS Proto-1, Particleworks enabled an initial evaluation of the influence of the modifications on the performance of AIS Proto-2.

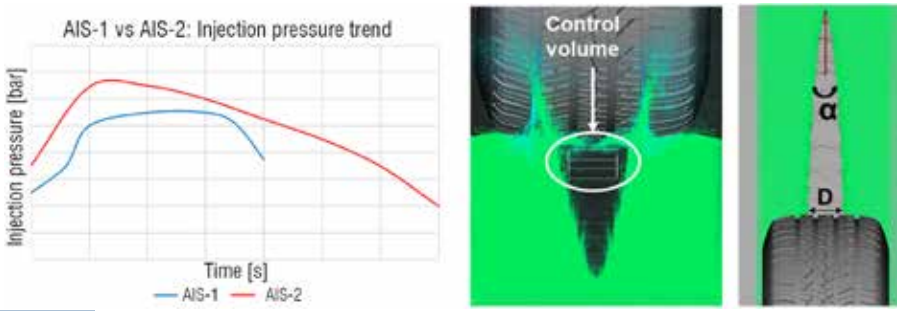

Fig. 5. Left: comparison of the pressure profile between AIS Proto-1 and Proto-2, Right: close-up of the control volume that monitors water accumulation in front of the tyre. A display of the partial distance (D) is also shown.

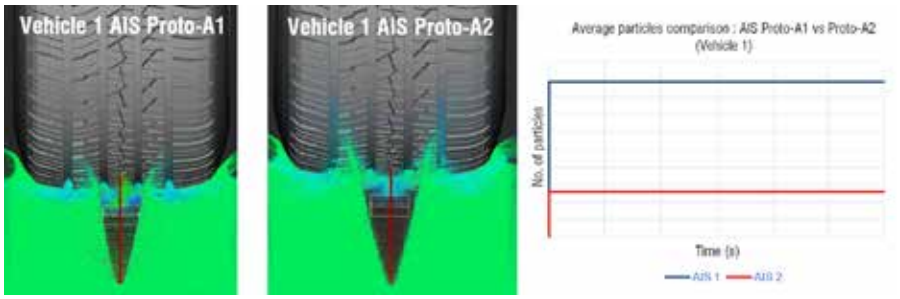

Fig. 6. Left: side-by-side comparison of jet opening capacity for two AIS prototypes, Right: number of particles (related to water volume) in the front of the tyre, with a 25% improvement in water removal.

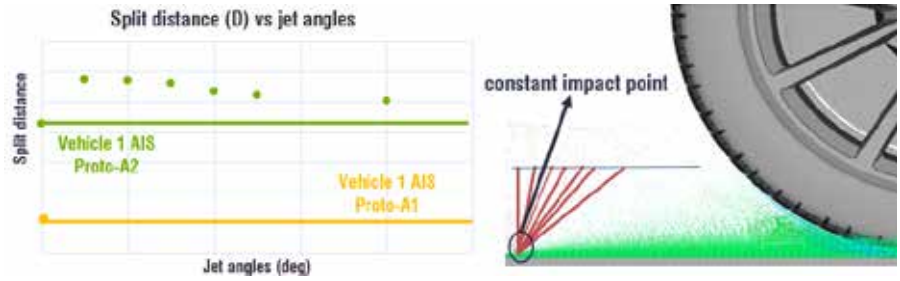

Fig. 7. Split distance at different jet angles (constant jet impact point).

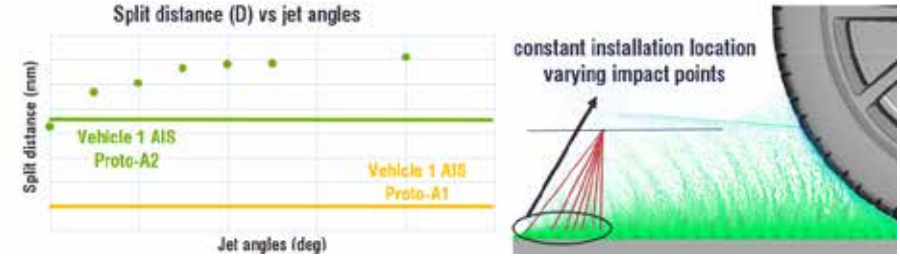

Fig. 8. Split distance at different jet angles (constant installation position for the injector).

As can be seen, compared to AIS Proto-1, the MPS simulation suggests that the second prototype results in a 25% improvement in clearing capabilities. These results have increased EASYRAIN's confidence in the improved efficiency of the system. EASYRAIN intends to use future tests to seek further confirmation of the simulation results with track tests.

Parametric improvement of the AIS Proto-2 system

After validating the methodology with experimental data and evaluating the ability of the post-processing results to discriminate between and compare the performance of AIS based on working conditions (pressure profile), we examined the influence of other parameters such as jet position and inclination. This analysis is crucial not only to gather further insights into the system, but also because some car bodies limit the installation angles or positions of the AIS system. Therefore, in order to adapt the AIS Proto-2 system to vehicles that differ from the initial EASYRAIN reference (vehicle 1), a sensitivity analysis was performed on the position of the AIS nozzle.

One piece of information that could be of interest is the clearing ability while maintaining the same point of impact. As can be seen (Fig. 7) changing the jet angle while maintaining the clearing region at a fixed distance from the tyre can result in better partial clearance, reduced aquaplaning, and improved safety. The trend is non-linear, with a clear optimum jet angle, after which the efficiency decreases.

In other AIS applications, the mounting position of the nozzle may be limited by the car body design. For these cases, changing the impact angles will result in different distances between the clearing region and the tyre. The influence of the jet impact angle for a fixed installation position is shown in Fig. 8. In this case, increasing the jet angle will result in improvements in the clearing capabilities. The methodology is thus promising for the identification of the best combination of mounting positions and jet angles, depending on the car body constraints and other technical requirements.

Conclusions and future work

In this paper we described the analysis of and improvements to the EASYRAIN Aquaplaning Intelligent Solution (AIS) using moving particle simulation (MPS), a mesh-free CFD strategy. We reported the validation of the simulation results by comparing the flat plate force predictions at different injection pressures.

Real-life footage of track tests was also used as confirmation of the MPS results. In addition, we digitally compared two prototypes, allowing an initial estimation of the anti-aquaplaning efficiency of the new prototype for which no track data is currently available. The method also provided information on mounting angle and position, allowing guided design when considering other car bodies with different and unique geometric/hydraulic constraints. Once AIS Proto-A2 track tests further validate the methodology, EASYRAIN will continue to use MPS to further fine-tune the injection parameters.

Article from:
Futurities Year 19 n.3
Autumn 2022

About EASYRAIN

EASYRAIN is an auto-tech company focusing on road safety for human-driven and autonomous vehicles. We have extensive experience in wet road, dangerous wet road, aquaplaning conditions and other grip-related issues. We have built the most complete ecosystem of safety solutions, including AIS (anti-aquaplaning system), the first on-board actuator to counter aquaplaning; EDP (EASYRAIN Digital Platform) on-board virtual sensors for vehicle dynamics; and ERC – EASYRAIN Cloud Platform for off-board analysis of road safety.

References

[1] S. Koshizuka, "Moving particle semi-implicit method for fragmentation of incompressible fluid", *Nuclear Science and Engineering*, 1996.

[2] S. Maruyama, "Prediction of amount of water received for vehicle by using splash simulation", *Mazda Technical Report* n. 38, 2021.

[3] S. Tokura, "Shape optimization of tyre tread pattern to minimize water splashing on vehicle body using particle method CFD simulation", NAFEMS World Conference, 2021.

Comparing cooling methods for e-motors

A simulation methodology developed by TotalEnergies

by Jonathan Raisin[1] and Michele Merelli[2]
1. TotalEnergies - 2. EnginSoft

Electrification of light and heavy-duty vehicles can help reduce global emissions by about 1Gt CO_2-eq. The current automotive market shows a strong acceleration towards electric propulsion (plug-in hybrid and battery), with one million sales in both Europe and China and the global share of electric vehicles exceeding 10% of total sales. The rapid and technically demanding transition poses significant challenges: innovative propulsion systems must be designed quickly, considering complex fluid, electromagnetic and thermal aspects that cannot be easily decoupled or thoroughly analysed with physical prototypes.

As power density increases, standard e-motor cooling methods (based on external air or water-jackets) fail to provide the necessary heat removal performance. Because of all these issues, a direct oil cooling strategy is proposed to directly remove heat from the most critical areas of e-motors, such as the coils and rotor.
In addition, for compact and weight-efficient drive solutions, e-motors are increasingly coupled with transmissions in e-drives, forming a single gearbox, and the same oil used for lubrication is also used in the cooling of the e-motor circuit via pumping systems. Therefore, having a single simulation that can provide information on both e-motor cooling and gear lubrication can be very advantageous.

In this paper, we will present the methodology developed by TotalEnergies and EnginSoft to select, design and improve an e-motor by simulating and predicting electromagnetic losses, fluid flow behaviour and temperature distributions. After establishing the workflow, the main objective of the study is to compare the direct oil-jet strategy with the external water jacket cooling circuit.

This analysis will compare the two approaches by considering various combinations of flow rate and motor speed. In addition, we report on the influence of the oil's physical properties on cooling performance, showing how the established workflow can guide TotalEnergies in the selection and improvement of oil for better e-motor cooling and longer working life.

Mission TotalEnergies: from lubrication to cooling

The thermal properties of electric vehicle fluids are of paramount importance. For decades, the lubricant industry has sought to optimize friction and fuel economy, but today it focuses on improving the thermal properties of the fluids it offers, with thermal management replacing fuel economy as the new leitmotif. Although there are different and sometimes more compact cooling architectures, particularly for the electronic peripherals of the electronic engine, each of these assemblies is subject to

different constraints that directly influence the type of fluid required for them. For example, some fluids must provide flawless lubrication, while others do not, but efficient cooling is always crucial and determines the formulation of the different fluids used.

The architecture of next-generation electric vehicles will require the development of a single type of fluid for their electric drive units (EDUs), combining high-performance lubrication of the transmission and efficient motor cooling.

First-generation electric motors were entirely air-cooled, but the low specific heat capacity of air in relation to its volume required a different approach. Thus, water cooling systems began to appear, but these were soon replaced by the use of dielectric cooling fluids, a much-needed step that was also confirmed by the simulation results reported.

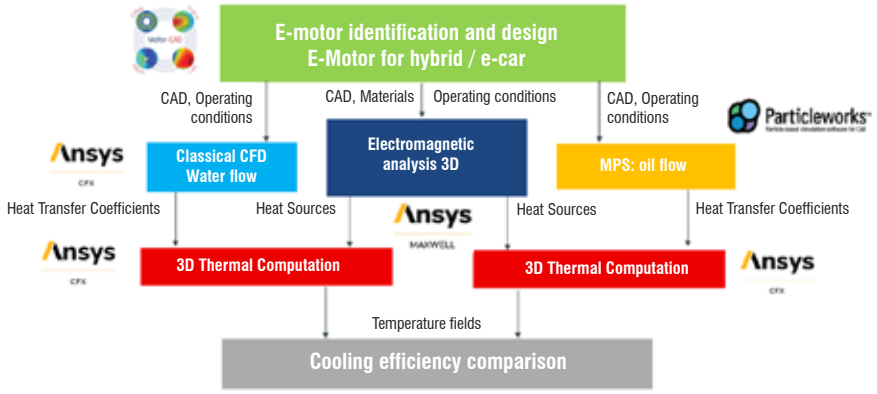

Fig. 1. Overview of the simulation workflow: e-motor identification (Motor-CAD), electromagnetic analysis (Ansys Maxwell), fluid dynamics (Ansys CFX and Particleworks) and thermal model (Ansys CFX). The arrows show the geometry / boundary conditions transferred between the software.

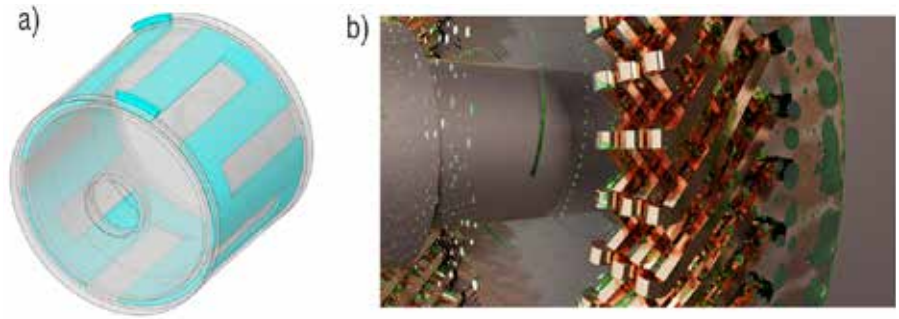

Fig. 2. a) Water jacket for indirect cooling (in blue); b) Oil jets from the rotor shaft and their accumulation on windings and casing (photorealistic rendering of simulation results).

Complete e-motor design and simulation: the advantages of a digital prototype

In collaboration with EnginSoft, TotalEnergies developed a simulation workflow to study the selection, design and improvement of e-motor cooling.

Thanks to the mesh-less nature of the CFD software for oil jet simulation and the Ansys integration between the different simulation tools, the complete simulation (considering geometry preparation and hardware time) took less than two weeks for the first model. Changing operating points or geometric characteristics only resulted in additional simulation time of two to five days.

The reported workflow for the complete e-motor design and analysis includes:

- The selection of electric motors for automotive applications (with Motor-CAD)
- An electromagnetic analysis (with Ansys Maxwell) fluid dynamic analysis (with Particleworks and Ansys CFX, for oil jet and water jacket cooling respectively)
- A thermal analysis (with Ansys CFX)

Articulating the workflow, we first defined a realistic e-motor operating condition (selecting for output torque and rotor speed) and estimated the corresponding efficiency curves with Motor-CAD. Two e-motor operating conditions were identified at 6,000 rpm (representing a car travelling steadily at 70km/h) and 10,000rpm (representing temporary acceleration for overtaking). We then exported the e-motor geometry and material properties of the e-motor digital prototype for a 3D electromagnetic analysis in Maxwell. With this analysis, we calculated the electromagnetic losses and heat generation of the two operating points that we then fed to the CFX thermal model.

Direct (vs indirect) oil-jet cooling: the advantages of a mesh-less approach

We compared two cooling strategies for the e-motor: an indirect water jacket embedded in the stator, and direct oil jets hitting the coils and other critical areas (Fig. 2). Focusing on the simulation of direct oil cooling, we used Particleworks, a mesh-less CFD software based on Moving Particle Simulation (MPS) [1].

This method is suitable for the rapid analysis of free-surface flow phenomena such as jets and sprays. Due to its mesh-less nature, it is easy to manage complex geometries (such as windings) or rotating parts (such as the rotor) [2].

For these same reasons, Particleworks is also widely applied in the analysis of lubrication and cooling in transmissions and gearboxes [3], so using this software enables a complete analysis of both gearbox and e-motor systems.

When applied to e-motor analysis, Particleworks allows the following to be investigated (Fig. 3):

- **Flow split within the rotor.** Since part of the cooling circuit is integrated into the rotor shaft, it is important to investigate the flow split between the different branches at different operating speeds.
- **Windage effects.** Air and windage effects can be simulated in Particleworks with the same digital model, further speeding up and simplifying the simulation workflow.

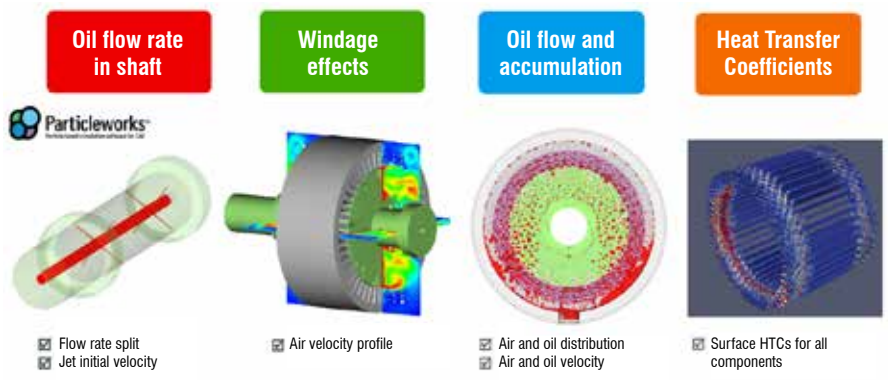

Fig. 3. Simulation steps and observables that can be investigated using Particleworks.

Generally, after the air has been modelled, the airfield is transferred to the oil jet simulation.

- **Oil jet impingement, oil accumulation and wetted surfaces.** The flow of oil jets – influenced by the imported airfield – and its accumulation inside the e-motor is modelled in this final simulation. Wetted surfaces and oil coverage can be also monitored and compared between different configurations.

After the amount of oil had stabilized in the e-motor, we used Particleworks to create maps of the average heat transfer coefficient (HTC) on the most important surfaces. We then transferred the maps to the Ansys thermal solver (Particleworks is also integrated with Ansys Workbench). We then performed a steady-state (6,000rpm) or transient (10,000rpm) thermal analysis on the e-motor, also integrating power losses and thermal loads due to the system's electromagnetism (from Ansys Maxwell). Once the steady-state thermal analysis was complete, we used the CFX model to predict the temperature distribution within each component of the e-motor. This methodology for predicting temperature in the e-motor was previously validated with Ricardo, using experimental data from thermocouples placed around the terminal windings [4].

Results

Comparison of direct and indirect cooling strategies

In order to maintain the same cooling capabilities, we normalized the flow rates for direct and indirect cooling accounting for the different physical properties of oil and water.

A cross-section of the e-motor coloured with the temperature profile is shown in Fig. 4 left for the direct oil cooling setup; right for the indirect water cooling configuration. Although the housing and stator are slightly cooler for the latter system, it is clearly seen that the rotor and winding regions reach higher temperatures in the water-based system. Particularly critical is the rotor, which houses the permanent magnets whose performance can be affected by temperature variations. Overall, the average temperature for direct cooling is 10°C lower.

We tested several flow rate configurations to study the behaviour of the e-motor for the oil jet in the worst case and for indirect cooling in the best case scenarios (2l/min vs 20l/min). The average temperature (Fig. 5) of the windings for oil cooling is at least 14°C lower. This trend is also confirmed at the higher speed

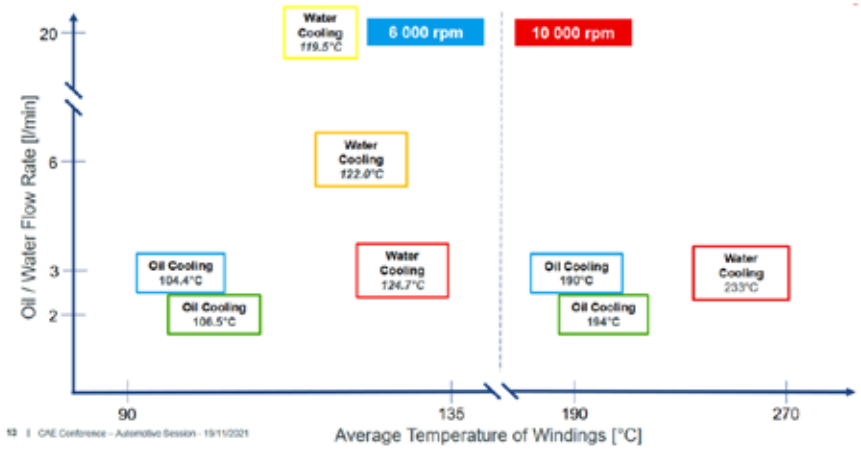

Fig. 5. Average temperature of windings for different flow rate/cooling strategies. Considering different flow rates and rotational speeds, oil cooling proved to be superior to the external water jacket strategy.

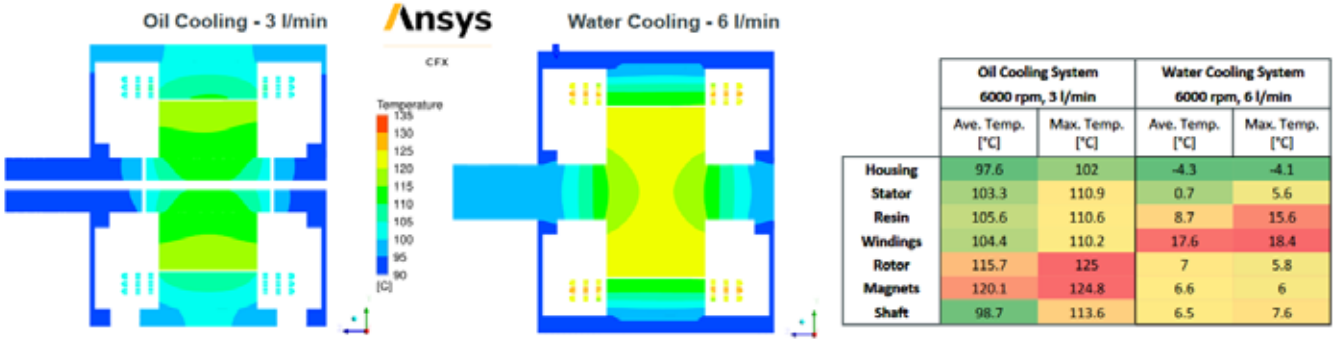

	Oil Cooling System 6000 rpm, 3 l/min		Water Cooling System 6000 rpm, 6 l/min	
	Ave. Temp. [°C]	Max. Temp. [°C]	Ave. Temp. [°C]	Max. Temp. [°C]
Housing	97.6	102	-4.3	-4.1
Stator	103.3	110.9	0.7	5.6
Resin	105.6	110.6	8.7	15.6
Windings	104.4	110.2	17.6	18.4
Rotor	115.7	125	7	5.8
Magnets	120.1	124.8	6.6	6
Shaft	98.7	113.6	6.5	7.6

Fig. 4. Temperature distribution inside the e-motor for direct and indirect cooling. In the table on the right, the average temperatures for the different e-motor regions are highlighted. The direct cooling shows lower temperatures for most of the e-motor elements.

condition, where the temperature can reach higher values.

For this operating point, we report a higher temperature difference (40°C) for the two cooling strategies.

Influence of physical properties

After demonstrating the superiority of the direct oil cooling strategy TotalEnergies wanted to prove the possibility of screening and selecting the physical properties of the oil to achieve better cooling efficiencies.

To do this, we varied four physical properties compared to the reference oil:

- $1/3\times\mu$, the initial viscosity (fluid 1)
- $2\times\lambda$,the initial conductivity (fluid 2)
- $1.5\times C_p$,the initial heat capacity (fluid 3)
- $1.2\times\rho$, the initial density (fluid 4)

The temperature distribution in the e-motor for the four oil variations is shown in Fig.6. As can be seen, all variations show improved cooling at lower temperatures.

This is in line with the trend between heat transfer and each physical property that can be extracted by explicitly isolating all variables in the Nusselt number:

$$h \propto \frac{(\rho u)^{\frac{1}{2}} (C_p)^{\frac{1}{3}}}{\mu^{\frac{1}{6}}} k^{\frac{2}{3}} \quad \textbf{(Eq. 1)}$$

Looking at the results in more detail, the temperatures decrease strongly for fluid 1 and 2 (reaching a reduction of 4% for the magnets). The average temperature decrease is greater than 2.5°C for both configurations.

			Viscosity x 1/3		Conductivity x 2		Heat capacity x 1,5		Density x 1,18	
	Oil Cooling System Reference Oil		Oil Cooling System Fluid 1		Oil Cooling System Fluid 2		Oil Cooling System Fluid 3		Oil Cooling System Fluid 4	
	Ave. Temp. [°C]	Max. Temp. [°C]	Ave. Temp. [°C]	Max. Temp. [°C]	Ave. Temp. [°C]	Max. Temp. [°C]	Ave. Temp. [°C]	Max. Temp. [°C]	Ave. Temp. [°C]	Max. Temp. [°C]
Housing	97.6	102	-2.2	-2.8	-2.5	-2.9	-0.9	-1	-0.1	-0.4
Stator	103.3	110.9	-2.2	-2.7	-2.5	-3.2	-0.5	-1.3	-0.3	-0.3
Resin	105.6	110.6	-2.2	-2.5	-2.8	-3.1	-1.1	-1.3	-0.4	-0.3
Windings	104.4	110.2	-1.9	-2.3	-2.7	-3.2	-1	-1.2	-0.3	-0.5
Rotor	115.7	125	-1.5	-3.5	-2.3	-4.5	-0.8	-3.1	-0.3	0.2
Magnets	120.1	124.8	-5.4	-3.5	-6.8	-4.5	-5.4	-3.1	0.9	0.3
Shaft	98.7	113.6	-5.1	-4.1	-6	-5.6	-4.5	-4.3	0.9	0.8

Fig. 6. The average and maximum temperatures of each electric motor component are shown for the reference oil. The temperature differences found for the four different fluids tested are also shown.

This temperature difference can be considered significant, as it is greater than the sensitivity of the digital model.

It is interesting to note that the thermal capacities and temperature differences do not follow the power dependencies shown by the Nusselt correlation in Eq. 1. For instance, viscosity has a greater effect than density, although the exponential factor should be more favourable.

Overall, the results show that simulation and quantitative CFD analysis are crucial and can be more thorough than the theoretical estimates that currently guide most traditional R&D processes. Complex flow patterns and multiphase interactions may arise, resulting in oil accumulations and surface coverage that cannot be estimated without accurate digital models.

Conclusions

The numerical results obtained in this collaborative project between TotalEnergies and EnginSoft consistently demonstrated the superiority of direct oil cooling over indirect water cooling for e-motor systems. With its high dielectric properties, oil can be sprayed or splashed directly wherever heat is generated, resulting in significantly lower average and maximum temperatures of crucial components such as magnets and coils.

Direct oil cooling thus opens the way to higher power densities for the future generations of e-motors and optimized cooling control strategies.

Finally, the digital approach presented in this paper has shown real potential to serve as a versatile complementary tool to optimize the formulation of dielectric cooling fluids and will join other approaches at the core of TotalEnergies' research and development activities for thermal management of electric vehicles.

Article from:
Futurities Year 19 n.2
Summer 2022

About TotalEnergies

TotalEnergies is a broad energy company that produces and markets energies on a global scale: oil and biofuels, natural gas and green gases, renewables and electricity.

Our 100,000 employees are committed to energy that is ever more affordable, cleaner, more reliable and accessible to as many people as possible.

Active in more than 130 countries, TotalEnergies puts sustainable development in all its dimensions at the heart of its projects and operations to contribute to the well-being of people.

References

[1] S. Koshizuka, "Moving particle semi-implicit method for fragmentation of incompressible fluid", *Nuclear Science and Engineering*, 1996.

[2] D. Ioan, W. Juan and M. Michele, "Optimizing the spray cooling of e-drives", *Futurities* Enginsoft newsletter, Year 19 no. 1, Spring 2022, pp. 23-25, Apr. 2022.

[3] E. Fava, "Oil flow rate optimization of an axle with an integrated input planetary stage for an uphill and downhill path", presented at the 2020 International CAE Conference, Vicenza, Italy, 2020.

[4] B. Martin and M. Michele, "Thermal simulation of an oil-cooled e-motor", presented at the 2020 International CAE Conference, Vicenza, Italy, 2020.

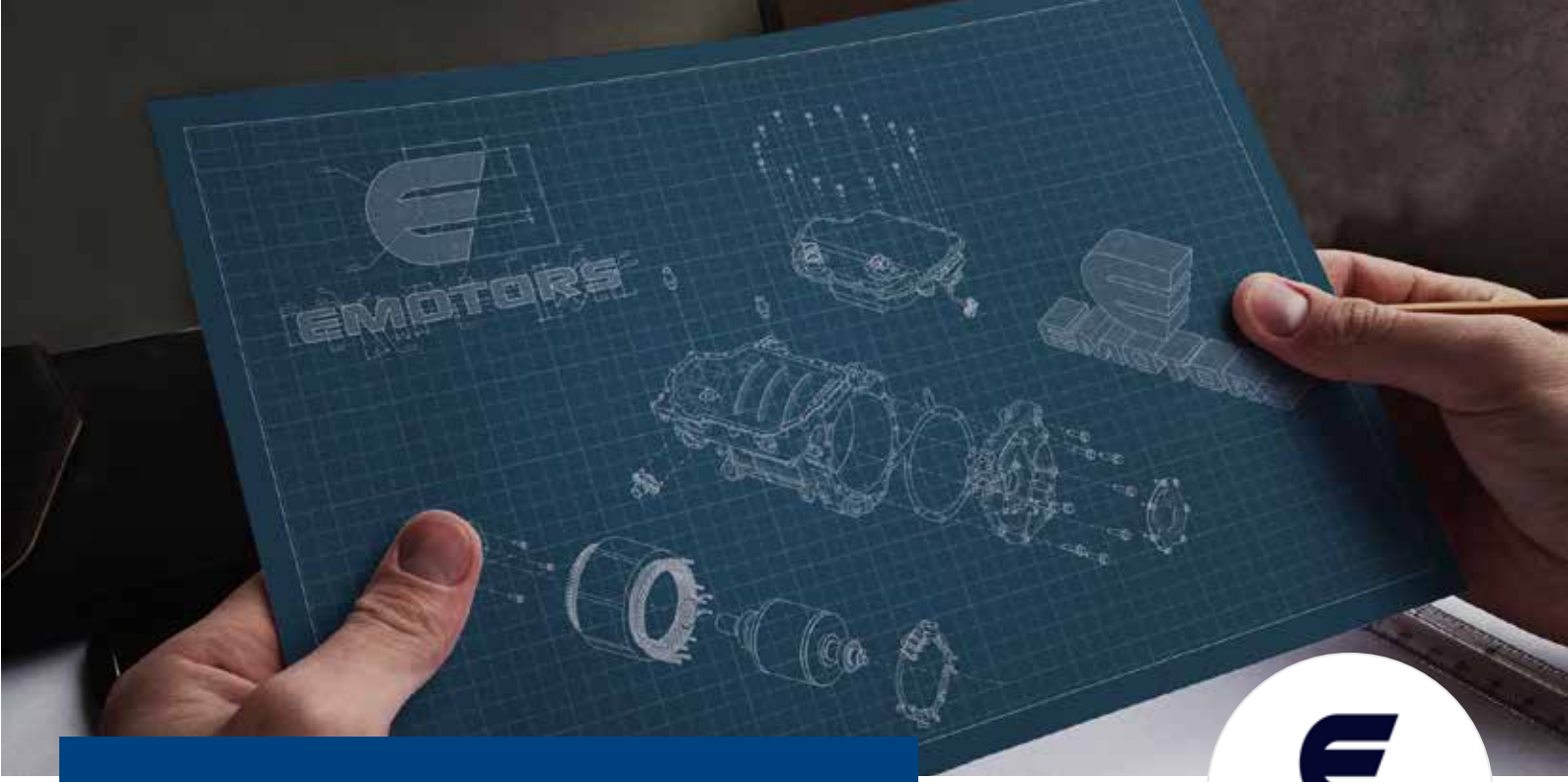

Optimizing the spray cooling of e-drives with moving particle simulation

by Ioan Deac[1], Juan Wang[1] and Michele Merelli[2]
1. EMOTORS - 2. EnginSoft

Moving particle simulation (MPS)

The advances in simulation methods and computing power have resulted in new simulation methods becoming available over the last three to five years. One of the most interesting for powertrain applications is MPS, a meshless CFD approach.

The MPS method is a deterministic Lagrangian particle method for calculating incompressible free-surface flows and non-Newtonian liquids. MPS was proposed by Koshizuka and Oka in 1996 [1]. While its core concept is similar to smooth particle hydrodynamics (SPH), MPS has evolved from a semi-implicit predictor-corrected formulation to fully explicit formulations that are more efficient for large-scale models, reducing simulating time and computing effort.

The use of MPS has grown in popularity within the automotive sector and it is now a well-established approach to free-surface flow and liquid flow analyses. Applications include oil splash and sloshing in gearboxes and transmissions, forced lubrication by oil jet, piston cooling, crankcase sloshing, and jet or spray cooling of wet electric motors.

The simulation process of e-motor cooling

The simulation of oil-cooled e-motors is difficult mainly due to the geometrical complexity of the system (culminating in the winding region), the multiphase nature of the flow dynamics, and the rotational speeds up to 20,000rpm.

Traditional, Eulerian mesh-based fluid dynamics solvers are unable to produce models with affordable setup times and computing requirements. These are critical functions to efficiently integrate CFD codes into the industrial R&D workflow.

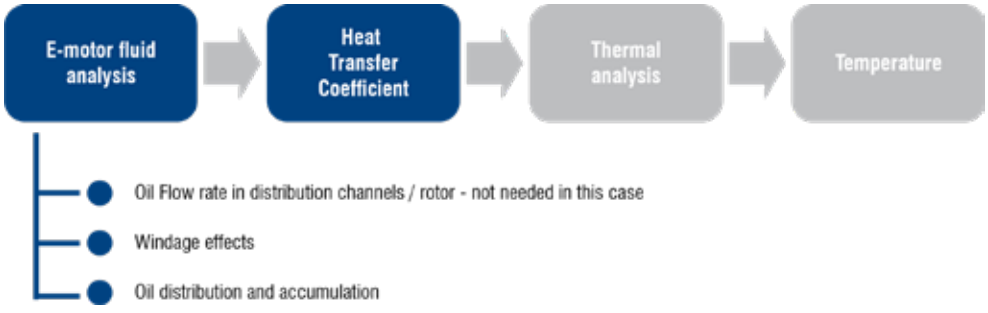

Fig. 1. Diagram of the simulation methodology for e-motor cooling. The CFD related topics analysed with the MPS method are shown in blue.

Engineers from EMOTORS and EnginSoft have developed virtual e-motor prototypes based on different simulation requirements, rarely considering the subsystems of the unit for further analysis.

However, the main objective of e-motor cooling simulations is to evaluate and improve oil distribution for different cooling branches and to maximize heat transfer between the oil and the e-motor components. The process can be summarized into the following steps (Fig. 1):

1. Evaluation of the oil flow distribution in the rotor shaft channels and at the nozzle outlets;
2. Calculation of the windage effects (aerodynamic drag);
3. Visualization of the oil jets and flow in the e-motor, from nozzle outlet to motor outlet;
4. Mapping the heat transfer coefficient and heat fluxes over the critical geometrical element;
5. Transferring the cooling effects to a thermal model for temperature prediction.

More specifically, given the above-mentioned steps, the entire simulation process (from CAD preparation to the configuration of the different simulations and including the hardware simulation times) takes about two weeks.

As for the numerical parameters and the particle size (a concept comparable to the minimum mesh size of traditional Eulerian methods), these may vary from one sub-simulation to another. In general, MPS simulation times are mainly influenced by:

- Volume of fluid/air to initialize
- Total number of resulting particles (calculation nodes)
- Initial delta time (DT) of the simulation and the Courant-Friedrichs-Lewy condition (usually the Courant Number for MPS is 0.2)
- The type of pressure solver (if implicit or explicit)
- The activation of an additional physics model (turbulence, thermal equation, conjugate heat transfer, etc.)

As shown in Fig. 1, the first step in the simulation process is to analyse the flow distribution inside the e-motor circuit. Fig. 2 summarizes the flow pattern with flow distributed in the rotor, winding and stator regions. It is important to study the distribution of the flow across all sub-circuits and to verify it with respect to different conditions of speed and viscosity to avoid unbalanced configurations. In this step, the pressure distribution of the fluid within the channels can be measured and verified against the design requirements or manufacturing specifications.

Considering that the rotor speed can be up to 20,000rpm, windage and air drag effects have to be taken into account. For this purpose, an additional simulation is usually included in the presented methodology. In this step, only the air is simulated, with a discretization size capable of providing results within a few hours of simulation. As a result, the same MPS model can be used to extract the internal air flow without creating any additional numerical model and without mesh/geometry cleaning.

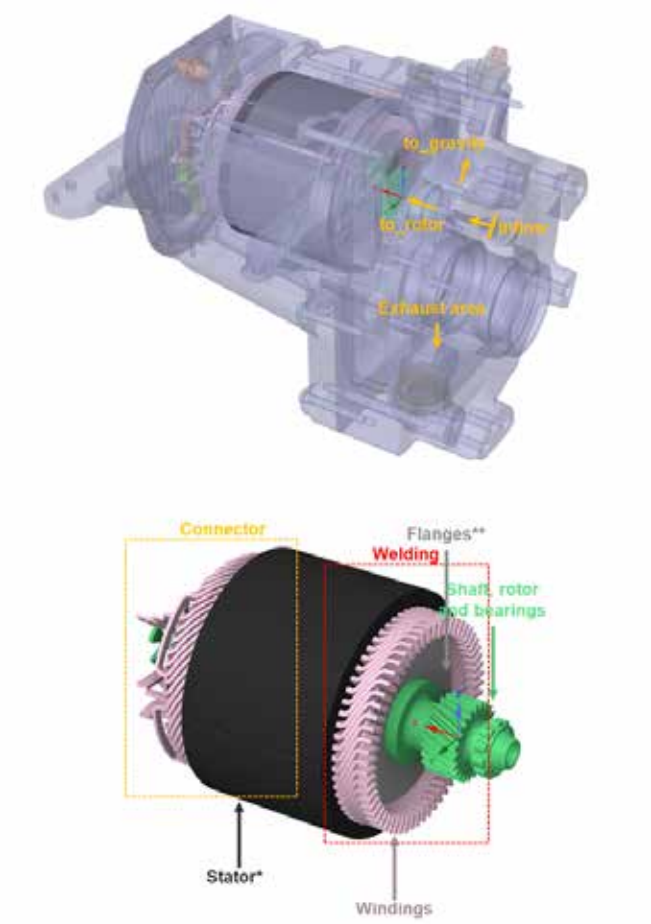

Fig. 2. Isometric view of the e-motor presented. Top: the names of the cooling sub-channels. Bottom: the names of the most important parts of the e-motor.

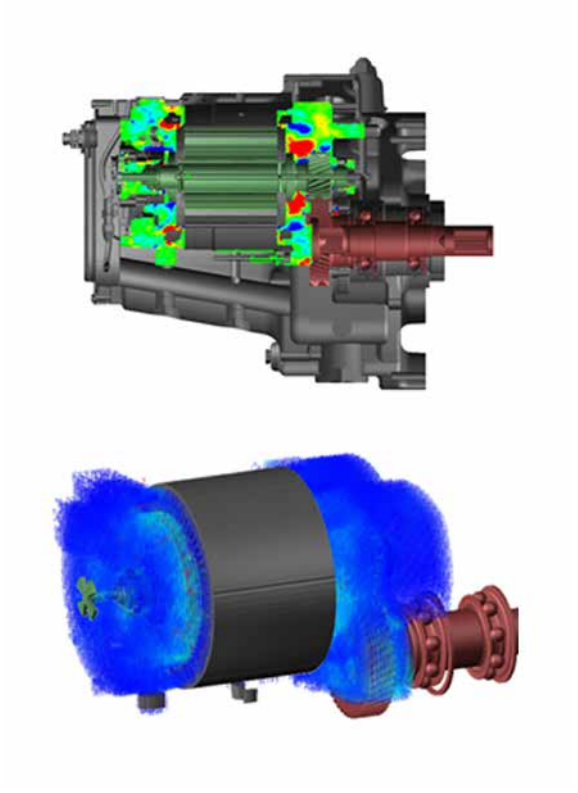

Fig. 3. Overview of the airfield as calculated by the MPS method (top) and the same airflow imported into the oil-only simulation (bottom).

Next, the main simulation is performed, focusing on the extraction of the heat transfer coefficient (HTC) maps which are then used to calculate the temperatures inside the e-motor components. The precalculated airfield is transferred to the oil-only simulation, with a one-way coupling (air influencing oil with a specific drag coefficient). The numerical parameters (particle size, simulation time step, thermal modelling) are adjusted to better capture the jet spray effect and for a more correct thermal assessment.

The convergence of the CFD model is checked by monitoring the oil distribution with control volumes in different areas (end-windings, stator, brackets). Subsequently, HTC maps, usually averaged over the last 0.5-1s of steady-state operation (see Fig. 4) are extracted. In this way, maps as shown in Fig. 4 are obtained for each wetted element inside the e-motor. These maps are also exported as .csv files by the software, ready to be transferred to the finite element analysis (FEA) model for predicting the temperature distribution. For the temperature distribution prediction, the MPS methodology introduced was previously validated by experimental tests [2].

Cooling circuit and validation of the methodology

In the design stage of the prototype, EMOTORS conducted several simulations focusing on different aspects of the e-motor design. The cooling circuit diagram of the analysed prototype is shown in Fig. 5.

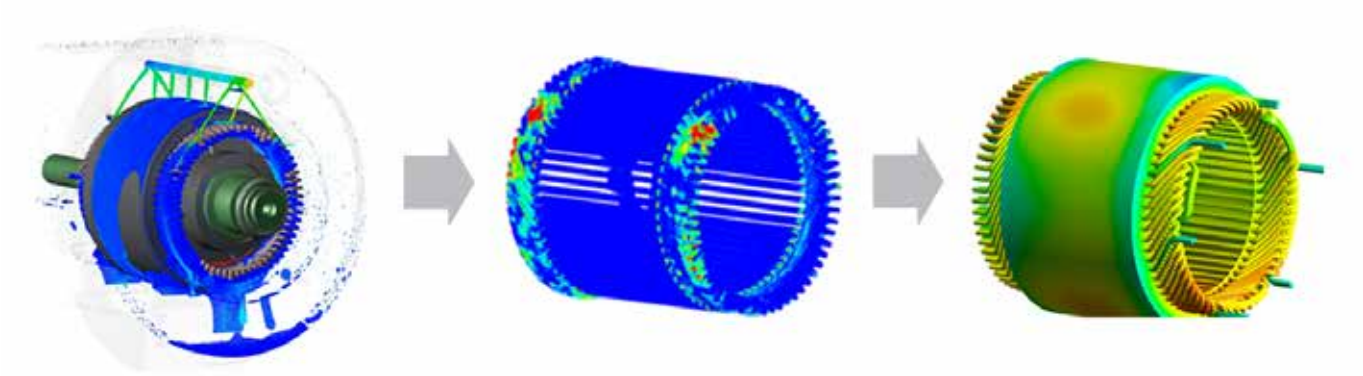

Fig. 4. From oil distribution to temperature distribution. On the left, the oil can be inspected and, once stabilized, an HTC map is extracted. The maps are transferred to the FEA model to obtain the temperature prediction.

The housing contains two oil cooling circuits: one static (gravity cooling) and one rotating inside the shaft and rotor (rotor cooling).

As shown in Fig. 4, the oil enters the housing from a lateral main circuit which then splits and part of the oil passes into the middle channels of the shaft (rotor cooling) while the remaining oil is directed to an additional upper layer above the windings and stator (gravity cooling). The rotor cooling circuit is designed to cool the inner surfaces of the windings, while gravity cooling sprays the outer surface of the end windings and the outer surface of the stator plate. Volume flow rates are measured by probes placed near the inlet and at the inlet of the rotor cooling and gravity cooling passages.

The simulation of this first step and approaching the problem using the RANS VOF (Reynolds-Averaged Navier-Stokes Volume of Fluid) method, proved to be troublesome at first. The challenge of modelling this internal flow is mainly related to the multiphase nature of the flow and the high rotational speed. The MPS method has proven to be more reliable for this purpose. In order to validate this first step of the MPS model we used a dedicated prototype designed to test multiple flow configurations and parameters. Different circuit configurations of the prototype were obtained using nozzles and plugs to limit the internal diameter or even to close off certain portions of the circuit.
We also had control over other parameters: oil temperature, inlet flow rate and rotation speed. In addition, we measured the pressures at the inlet and at some intermediate points of the circuit and the flow rate for an outlet branch of the circuit. In addition, we opted for a Design of Experiment (DOE) approach to testing in order to prepare the results for statistical post-processing. The purpose of statistical post-processing of the results is to help us assess the physics and reliability of the measurements and to remove noise from the readings.

We also decided to verify the statistical model we developed with an out-of-sample control configuration that was not used in the post-processing. As can be seen in Fig. 5, the statistical model correctly predicts the flow rate distribution of the out-of-sample dataset.
Fig. 6 compares the results between the experimental data and the MPS calculations, for a single flow operating condition (8l/min).

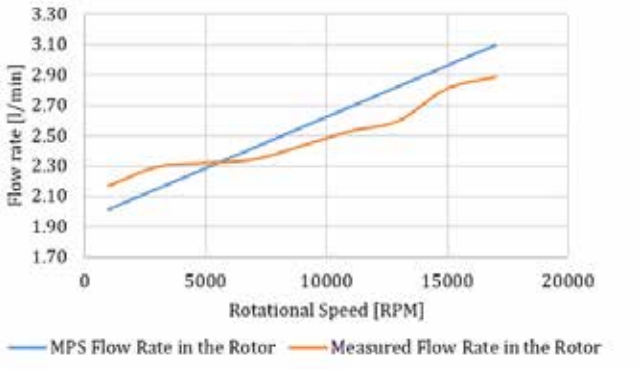

Fig. 5. Flow rate through the rotor cooling circuit of the out-of-sample dataset (orange) and the predicted trend of the statistical model constructed using the DOE (blue).

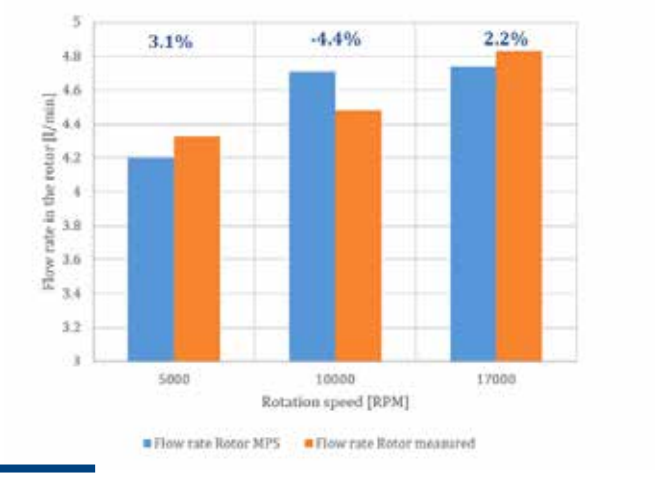

Fig. 6. Flow rate to the rotor cooling system (rotor circuit) for three rotor speeds. The MPS predictions (blue) are compared to the experimental results (orange).

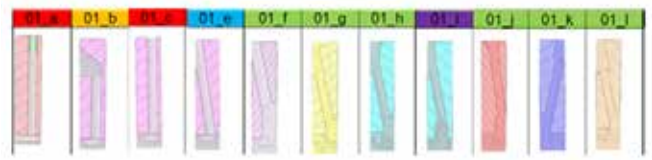

Fig. 7. Cross sections of the flanges considered in the single jet HTC analysis.

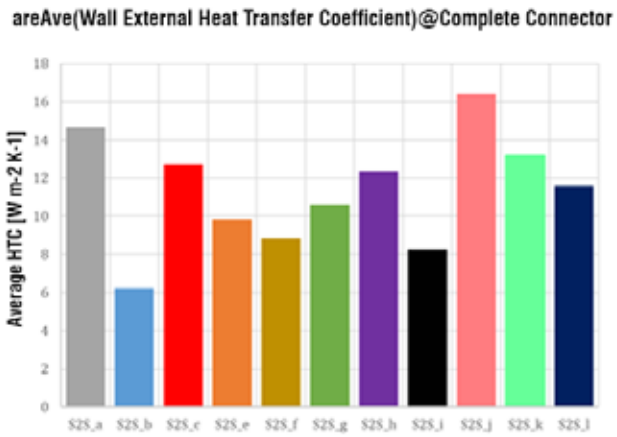

Fig. 8. Area weighted average HTC across the windings for different flanges (contribution of a single oil jet).

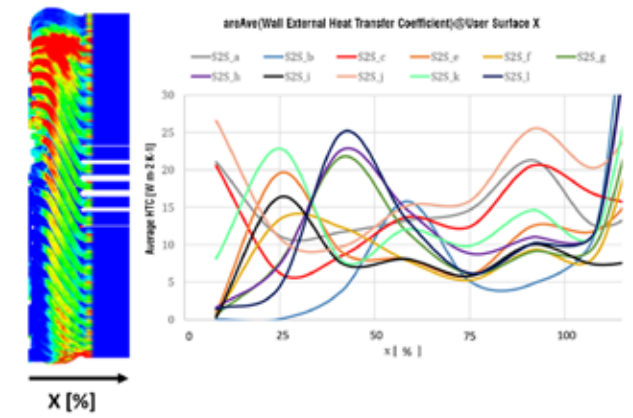

Fig. 9. AreaAveHTC for different x-slices of the windings. This analysis allows the HTC values to be mapped spatially in a quantitative way.

The flow through the rotor cooling system is reported for three different rotor speeds. We obtained an error of ±5% between the simulation results and the post-processed experimental data.

Design improvements: flanges and brackets

After validating the MPS methodology for internal flow analysis, an important element to analyze in the early design phase are the flanges at each side of the rotor laminations. The size of the oil passage in the flange can change the balance of the oil flow between the rotor and the stator. The shape of the passage was found to have a critical influence on the trajectory of the oil particles and on the size of oil jet before it hits the windings.

To reduce calculation time, only the rear of the windings (the side corresponding to the phase connector element) is simulated. Also, only part of the channel (one of the four jets) is modelled to further reduce the quantity of oil simulated.

Several geometrical modifications to the rotor flanges were considered to improve the cooling efficiency of the e-motor. These geometrical details are shown in Fig. 7.

In order to compare the configurations, we computed the area weighted average of the HTC values (AreaAveHTC) across the exposed windings. The following formula averages the n-th HTC value calculated on the n-th triangular surface of the .stl file, weighted for its surface area:

$$AreaAveHTC = \frac{\sum HTC_n \cdot A_n}{\sum A_n} \quad (Equation\ 1)$$

The results for the designs discussed are shown in the chart below (Fig. 8). As can be seen, careful design and direction of the flow in specific areas of the windings can result in a two- to three-fold improvement in the cooling efficiency, compared to the poorest configuration.

In order to evaluate the flow distribution on the windings in more detail, the average HTC was evaluated for different slices (in the axial direction). The results are shown in Fig. 9. The AreaAveHTC for each slice x is reported against the x% (0% end of the windings, 100% inner side of windings, rotor side).
It can be observed that:

- Flanges 01_a, c, and j have the best HTC near the 0 and 100% mark of the length of the end winding;
- Flanges 01_g, h, and l have the higher HTC near the 50% mark of the length of the end winding;
- Flange 01_e has a better HTC near the 25% mark of the length of the end winding;
- A small nozzle (01_k) has the effect of focusing the oil near the 25% mark of the length of the end winding (closer to the stator lamination) compared to 01_g and 01_l.

The stator brackets also help to improve heat transfer inside the e-motor. They are situated between the inner surface of the housing

and the outer surface of the windings. Without the stator bracket, the oil jet from the rotor will mainly spray the inner surface of the housing. The stator bracket's purpose is to redirect the oil from the rotor injection towards the windings. We decided to test the possibility of improving the performance of the baseline bracket design. The geometrical features of the two variations (labelled as Small and Axial) are shown in Fig. 10 below.

One way to monitor the efficiency of a specific design is to measure the amount of oil in the region of the windings by means of a control volume. Fig. 11 shows the oil accumulation trend for the first two seconds. A clear difference can be seen between the proposed designs and the baseline. To examine the efficiency of the system more closely, we focused on the AreaAveHTC on the windings, comparing the two bracket designs with the baseline. The AreaAveHTC result trends follow the oil accumulation, with the baseline design showing better cooling performance.

These simulations enabled us to test and exclude two proposed bracket designs that proved to be less efficient at keeping more oil in the area of the windings.

Conclusions

This paper described the simulation of e-motor cooling using MPS, a mesh-less approach well-suited to impinging jet and free-surface flow analyses. We reported the methodology of the MPS e-motor simulation, the internal flow rate split, the windage effects, the HTC distribution, and the temperature distribution.

At the internal flow distribution step, we validated the MPS methodology using a dedicated prototype and a statistical technique. This validation also demonstrated the range of reliability and confidence of the simulation results, significantly reducing the number of prototypes necessary to move from the initial design to the final product.

Moreover, we showed how MPS simulation can provide insightful design indications for key components of the e-motor, like the rotor flanges and the stator brackets. The EMOTOR engineers were thus able to propose further improvements to the cooling of their e-motors, achieving competitive power densities for the motor while reducing the use of materials and increasing the reliability of key components.

References

[1] S. Koshizuka and Y. Oka (1996), "Moving particle semi-implicit method for fragmentation of incompressible fluid", *Nuclear Science and Engineering*, Vol 123, pp. 421-434.

[2] M. Brada (2020). "Thermal simulation of an oil-cooled e-motor", 36th International CAE Conference and Exhibition.

Article from:
Futurities Year 19 n.1
Spring 2022

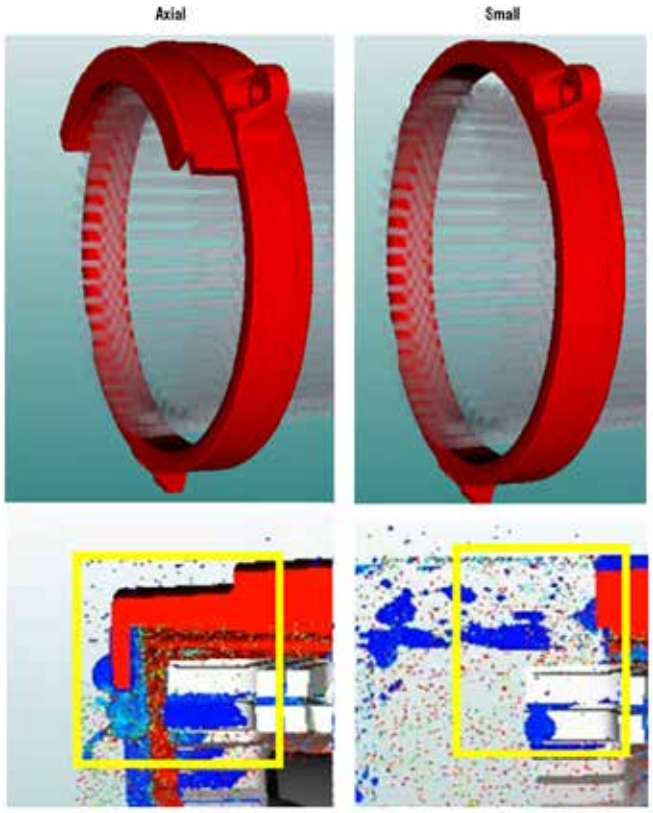

Fig. 10. Overview of the bracket design (top, isometric view) and detail of the modification near the windings (bottom). As can be seen, the Axial bracket design collects the oil (blue) so it does not splash onto the external housing as seen on the bottom right.

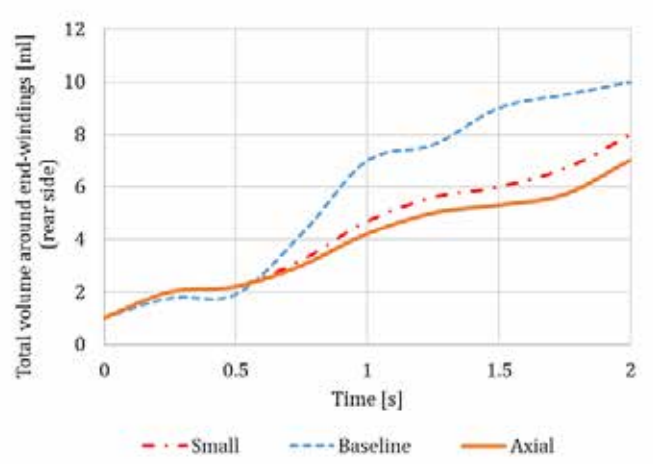

Fig. 11. Total amount of oil in millilitres around the windings (at the rear of the e-motor). Two proposed bracket designs (Small, Axial) are considered as possible improvements of the baseline.

	Area Weighthed Average HTC
Small	68
Baseline	84
Axial	63

Fig. 12. AreaAveHTC for the two proposed brackets (Small, Axial) compared to the baseline design.

Using a combination of Particleworks and Ansys Fluent to simulate snow drift volume and deposition

by Dmitry Stepanov and Denis Khitrykh
CADFEM CIS

In civilian residential area, the formation and distribution of snow cover has a significant impact on people's lives, affecting the movement of vehicles, safety and the maintenance costs of facilities. Two of the most important factors in this regard are heavy snowfalls and the high wind speeds during blizzards. Snow fences are often used to protect larger areas, but the selection of their shape and position are critical for their effectiveness. This study evaluates the combined use of Particleworks and Ansys Fluent to simulate the volume and deposition of snow transported around such snow fences and compares the simulation results with experimental results, showing a strong correspondence.

The formation and distribution of snow cover in places where people live affect their livelihoods: snow drifts negatively affect the movement of vehicles, and the accumulation of drifts determines the safety and maintenance costs of facilities. Heavy snowfall and high wind speed (blizzards) in particular become significant factors for people living in areas with harsh climatic conditions. Residential areas in such regions need to be protected in some way. Snow fences of various configurations are often installed to protect large areas. But in order to choose the right shape of and position for the fence, it is necessary to know the volume of snow that is transported.

At present, there are a number of Russian and foreign methods that allow the volumes of snow to be calculated [1-5]. These methods can be used for the initial estimation of this parameter. However, when solving practical problems, for example, the formation of snow drifts behind a snow-retaining fence, the data obtained using these methods is insufficient.

Furthermore, the snow drifts formed also affect the parameters of the atmospheric boundary layer. This suggests that choosing the correct type of fence and its location is a critical task.

The numerical simulation of these complex processes makes it possible to obtain sufficiently complete information about the nature of the snow drift, taking into account the influence of various factors. To determine the correct placement and the required number of rows of snow fences, it is necessary to create a model that couples the continuous flow and the particle flow, so that the direction, wind speed, and snow properties (particle size, density), as well as the values of the coefficients responsible for interaction with the fence (such as the friction coefficient) become the input variables. This paper illustrates the combined use of Particleworks and Ansys Fluent to simulate the process of snow drifting, while considering the effect of snow fences.

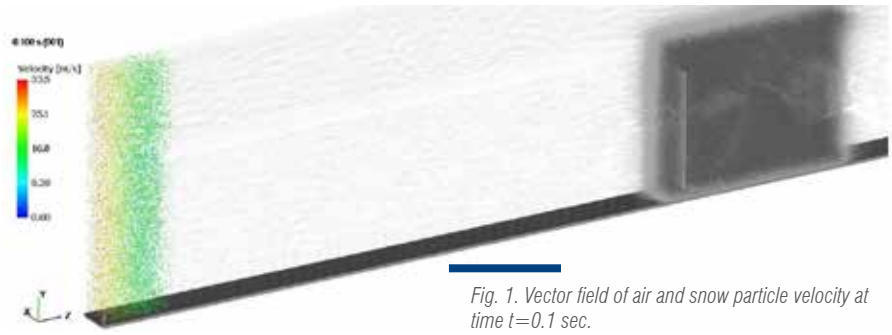

Fig. 1. Vector field of air and snow particle velocity at time t=0.1 sec.

Description of the mathematical model

With respect to the simulated process, the motion of snow in an air flow can be considered as a primary flow of inert particles, where the particle size has no inverse effect on the primary phase.

This problem can be easily solved using a combination of two solvers: Ansys Fluent and Particleworks. Ansys Fluent performs the aerodynamics calculation and the output data should be a csv file containing the values of the velocity components at each node of the mesh. Then, based on the resulting aerodynamic flow field obtained, Particleworks calculates the motion of the discrete particles and simulates their interaction with the downstream objects using the discrete element method. Each calculation is performed independently of the other. It should be noted, however, that the two modules can currently be coupled through the Ansys Workbench platform.

The geometry of simulation domain is a parallelepiped with sides of $1.5 \times 7.1 \times 117.5$m. The mesh size in Ansys Fluent was approximately 4.3 million elements with 28.1 million nodes. Particleworks reads csv-files with up to 40 million lines fairly easily. The velocity profile was set in Ansys Fluent as the boundary condition, and the symmetry at the lateral boundaries was taken into account. In Particleworks, the properties of the snow were specified, and its polydispersity was taken into account: the particle diameter was set to a range of d=10…20mm. The initial moment of time was taken as the distribution of air in

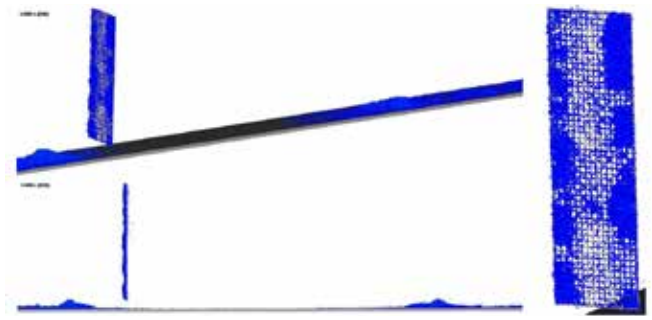

Fig. 2. Distribution of particles deposited on the wall of the fence and on the surface of the ground at the time t=5sec.

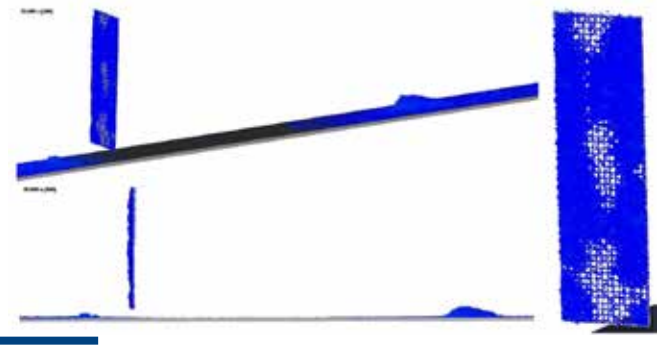

Fig. 3. Distribution of the particles deposited on the wall of the fence and on the surface of the ground at the time t=30sec.

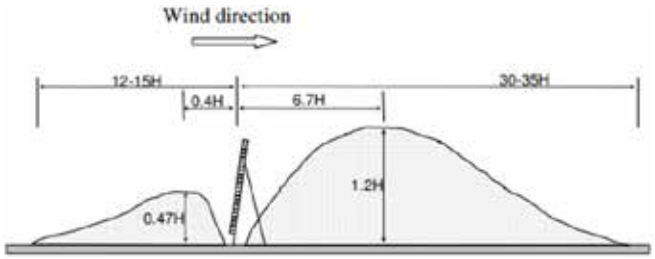

Fig. 4. Dependence of snow drift size on the effective height (H) of the wall [3].

the simulated area (see Fig. 1). The results presented below in Figs. 2-3 characterize the distribution of the snow cover at different points in time.

Concluding observations

The simulation results were compared with the experimental data presented in the reference [3] (see Fig. 4). It can be noted that there is a qualitative agreement between the results of numerical simulation and the results of the experiments: two snow drifts are formed in front of the first fence and behind it. The position of the snow cover did not change during the 30 seconds simulated. In addition, one can note that the snow cover between the first and the second fences, which were spaced 40m apart, had the appearance of small drifts with a regular structure (see Fig. 5). It was observed that snow particles between the drifts moved due to the effect of saltation: in the air flow, moving particles collide with static ones thereby dislodging them and engaging them in further movement. This type of inert particle motion is only inherent to the discrete phase where the particles have a diameter of d=10…40mm. This thesis is confirmed in the references [3,4].

About CADFEM CIS

CADFEM CIS is the largest CAE systems distributor and Ansys, Inc. certified elite channel partner in Russia. CADFEM CIS provides delivery, implementation and technical support for Ansys multidisciplinary solutions and related software products. The company also offers engineering consulting services, including customized calculations, development of methods to resolve specific issues, and software adjustment. CADFEM CIS helps solve all issues, offering an effective computing IT infrastructure for resource-intensive simulation. In the transition to Industry 4.0, the company helps its customers to reduce time and costs and shorten the production cycle. For further information, visit: https://www.cadfem-cis.ru/

Conclusion

The results of this study showed that the Particleworks solver is an effective tool for modelling dispersed flow. The validity of the simulation results was confirmed by comparing them with the results of an experimental study. Therefore, the combined use of Particleworks and Ansys Fluent may be considered as a promising method for solving various types of problems in civilian environments.

Article from:
EnginSoft Newsletter Year 18 n.4 - Winter 2021

References

[1] V. Lobkina, E. Kazakova, Y. Gensiorovsky, "The calculation technique for transport of snow in poorly-studied areas (Sakhalin Island)", *Ice and Snow Journal* 52 (3):58, 2015;

[2] A. Soloviev, O. Lebedev, A. Kalach, "Mathematical Modelling of Behavior of Snow Weight on the Hillside" *Journal of Voronezh State Technical University,* P 116-117, 2011;

[3] R. Tabler, "Snow fence guide", Strategic Highway Research Program, National Research Council, Washington DC, report number, SHRP-W/FR-91-106, pp. 1-61, 1991b;

[4] S. Giangreco, "Validation of Lattice Boltzmann model for snow transport and deposition by wind": Doctoral dissertation. 2010;

[5] M. Matsuzawa, Y. Ito, M. Ueda, "Method of Calculating the Amount of Accumulated Snow Transported during a Single Blizzard", Sirwee 2010. Conference Papers, Presentations and Workshops, abstract n°25. 2010 P.1-7.

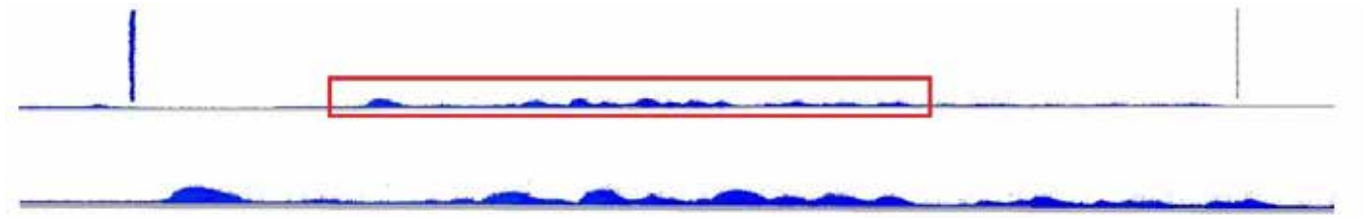

Fig. 5. Distribution of snow between the two fences.

Large bore engine lubrication system: oil flow and pressure analysis using moving particle simulation

by Luciano Perinel[1], Alessio Cherini[1], Irene Gallici[1], Gianluca Parma[2]
1. Wärtsilä Italy - 2. EnginSoft

Lubrication is critical to the efficiency and longevity of the moving parts of an engine, particularly large internal combustion engines.

By definition, a lubrication system is designed to deliver a stable, clean film of oil at the correct temperature and with the correct flow. It must prevent direct contact between the moving parts; reduce friction; reduce wear; cool, seal and clean; absorb shocks, and reduce noise. All of these functions combined contribute to the durability of components and systems, and to the overall operation of the engine.

Predicting and simulating the effectiveness of engine lubrication is particularly challenging, both with respect to oil splash in the sump and forced flow in the oil circulation system. With regard to the latter, a computational fluid dynamics (CFD) model of the oil channels must allow for the inertial effect resulting from the complex motion of the engine parts, and must simultaneously be able to simulate the transient nature of the flow at very different spatial scales. In a large combustion engine with a meter-long crankshaft, the flow within the bearings and leakage through small gaps, strongly affect the oil flow and pressure behavior.

In this study, the focus was on the oil supply system for the big-end-bearings of an 18-cylinder engine, which is one of the largest four-stroke gas engines in existence, ideal for base load applications. Wärtsilä and EnginSoft created a moving-particle simulation model, a meshless method of solving Navier-Stokes equations, which allows complex geometries with moving parts to be simulated. The model of the Wärtsilä engine included all relevant moving parts, such as crankshaft, bearings, connecting rod, pistons, and their motion. Modelling and simulating the engine using finite-volume CFD techniques would be impractical due to the geometric complexity of the oil system, and especially due to the motion of the engine parts, which would make it impractical to manage the mesh movement.

By simulating the flow through the channels, the moving particle simulation model allowed the transient pressure behavior to be calculated in crucial areas. Comparison of two bearing configurations revealed differences in pressure stability, spikes and low-pressure values that could potentially lead to cavitation problems. The results

of the comparative analysis are presented and explained, along with accompanying illustrations.

In this article, the forced lubrication system of an 18-cylinder engine is studied by means of a fluid dynamic model of the lubrication channels. Particular attention is paid to the pressure trend and behavior in the oil channels and in the vicinity of the big-end bearing (BEB). The purpose of the study is to evaluate the effect of a change in the bearing design on the surrounding pressure field.

Due to the nature of the system, a traditional finite volume CFD approach would be unfeasible due to the many moving parts and the complexity of their motion. Therefore, a meshless CFD approach based on the moving particle simulation (MPS) method is used.

Moving particle simulation (MPS) method

The moving particle simulation (MPS) method, originally called moving particle semi-implicit method, was conceived by Prof. Koshizuka of Tokyo University in 1996 [1]. It is a meshless method for resolving fluid motion by solving Navier-Stokes equations in incompressible conditions. It discretizes the fluid domain using particle elements, and each particle becomes a computational node carrying information about position, velocity, temperature, and all variables of interest. Since the core of the computation is the particles, the Navier-Stokes equations are written in a Lagrangian framework, in contrast to traditional mesh-based methods, which use the Eulerian approach. In the Lagrangian approach, particles are tracked and followed during their motion, whereas in the Eulerian approach the viewpoint is fixed to the computational grid (see Fig. 1).

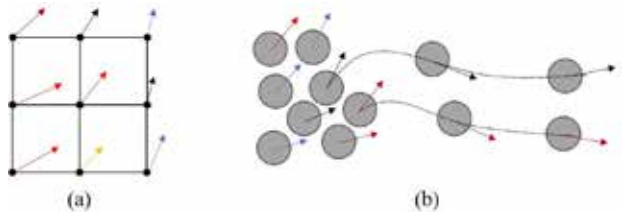

Fig. 1. Difference between the Eulerian approach (a) and the Lagrangian approach (b).

Its meshless nature makes the MPS approach highly flexible and well-suited to applications involving moving parts where mesh generation and deformation using a mesh-based method can be exceedingly difficult.

In this work, the Particleworks MPS solver developed by Prometech Software Inc. is used to analyze the oil flow in the engine lubrication system.

Model description and boundary conditions

The complete engine consists of 18 pistons with connecting rods, mounted on a crankshaft. The crankshaft is supported by ten main bearings (MB) with their respective main bearing caps; internal channels running through the engine components distribute the lubricating oil to all the bearings (see Fig. 2). The bearings are of the hydrodynamic type. The crankshaft rotates at a constant speed,

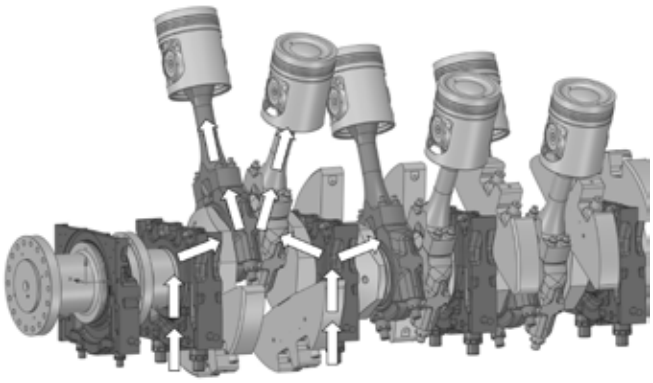

Fig. 2. Diagram of the engine and oil flow path.

converting the reciprocating motion of the pistons into rotary movement.

Oil enters the system through the main bearing caps, lifting the main bearings; then it is delivered to the big-end bearings (BEB) via the crankshaft oil channels. Finally, it reaches the small-end bearings (SEB) through the connecting rod oil channels. Figs. 2 and 3 show the oil path and diagram of the internal lubrication system.

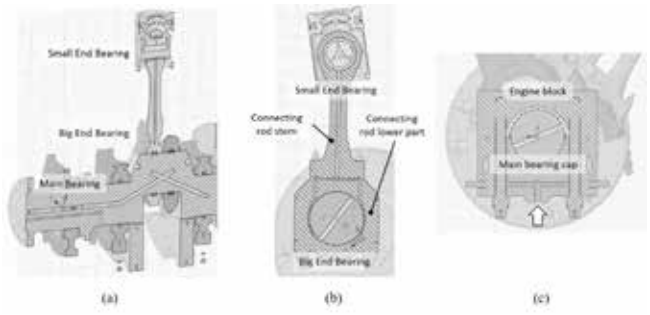

Fig. 3. Internal lubrication channels. Crankshaft (a), connecting rod (b) main bearing cap, main bearing channel and engine block (c).

Fig. 4 shows a cross-section of the crankpin and its oil channel, the lower part and stem of the connecting rod, and the BEB that is interposed between.

The lubricating oil from the crankpin oil channel reaches the SEB by flowing through the clearance between the pin and BEB, its groove, and then the oil channels inside the connecting rod. The rotation of the

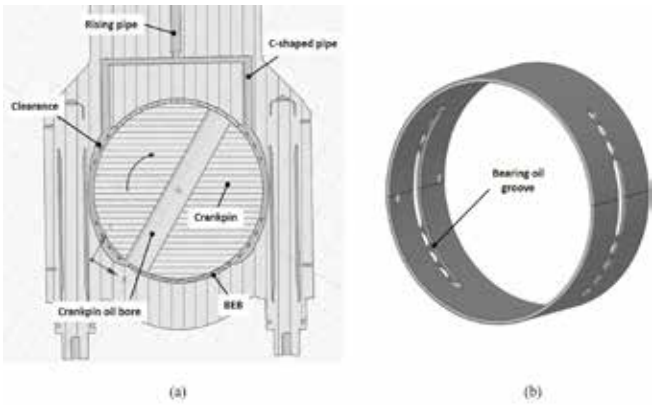

Fig. 4. (a) Section of crankpin, BEB, connecting rod and C-shaped pipe. (b) BEB geometry.

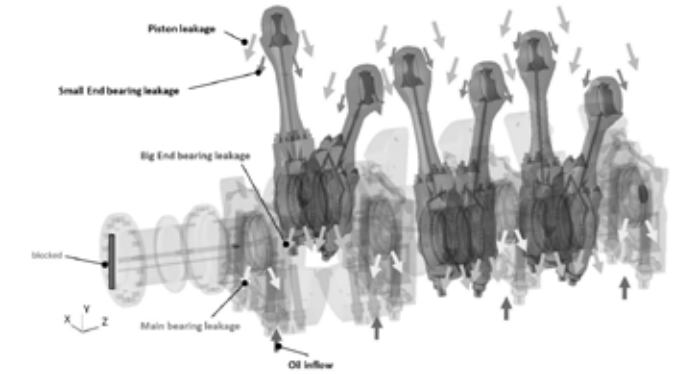

Fig. 5. Distribution of inflow and outflow boundary conditions.

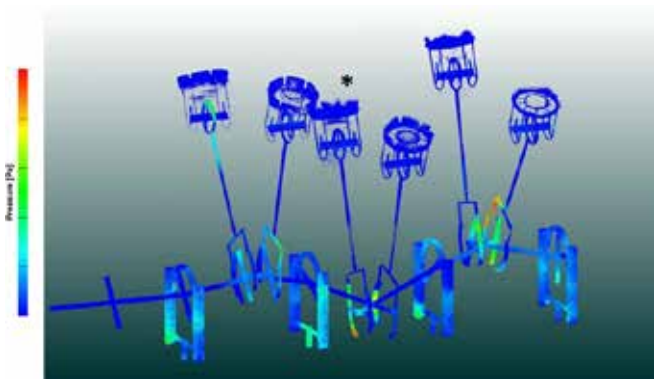

Fig. 6. Pressure distribution in the simulated domain.

crankshaft, together with the alternating movement of the connecting rod and the engine oil pump, ensure sufficient oil flow through the channels that feed all the bearings.

The moving particle simulation only takes into account the first three turns of the crank, six pistons, and four main bearing caps. An inflow with the prescribed volumetric flow rate is applied to the base of each main bearing caps, and outflow rate conditions are applied in the bearing regions to simulate oil leakages that will then be collected in the oil sump. Fig. 5 summarizes the oil sources and leaks.

Analysis conditions

The same simulation method is applied to two different BEB geometries. The crankshaft rotation speed, inlet and outflow rates are kept constant throughout the simulation.

The particle size and the integration time step are the two main parameters that play a key role in the simulation. The particle size must be small enough to address the smallest gap of interest in the geometry. A 2mm particle size is chosen in the MPS model to capture the smallest passages in the channels and grooves. The film of lubricating oil between the bearings and crankshaft pins is not the scope of the current work. Particle size affects solution accuracy and simulation time (smaller particles increase solution accuracy and computation time).

The second key parameter is the integration time step, which must be set to ensure the numerical stability of the simulation. Its value depends on the maximum velocity in the system, and simulation of the two geometries was in the range of 8E-6s. An adaptive time-step is used to allow the solver to adjust according to the solution.

An implicit pressure solver is used to improve the accuracy of the pressure field calculation. The simulation was performed on two CPU cores (Intel Xeon Silver 4114) along with an NVIDIA V100 GPU. The benefit of using a graphic processing unit (GPU) is the remarkably high performance-to-cost ratio due to the large number of computing cores in the GPU card. For example, an NVIDIA V100 has 5120 CUDA cores and is capable of 15.7TFLOPS in single precision, with performance comparable to 48-64 CPU cores.

MPS Results

The goal of the activity is to compare two BEB designs, with attention to the pressure distribution in the oil channels and the pressure behavior in the vicinity of the bearings in question. During the transient simulation, the pressure values in different areas of the channels are monitored, focusing on the two central connecting rods to avoid boundary effects.
An overview view of the oil flow in the full domain shows that the highest pressure values are found in the lower part of the connecting rod (see Fig. 6).

Due to the motion of the power system parts, pressure waves generated in the system are periodic and are continuously reflected from the thrust side and the anti-thrust side of the BEB.

Fig. 7 shows the evolution of the pressure field around the BEB of the central pair of pistons (marked with an asterisk in Fig. 6). The pressure field is smooth and the pressure waves are well captured by the solver. The left corner of the C-shaped channel is reached periodically by a pressure peak (red values in frames 4 and 6), which is followed by low pressure values.

Low-pressure values are predicted near the corners of the C-shaped tube and other areas of the BEB. This may result in an improper lubrication. The predicted pressure trends were confirmed by experimental investigations.

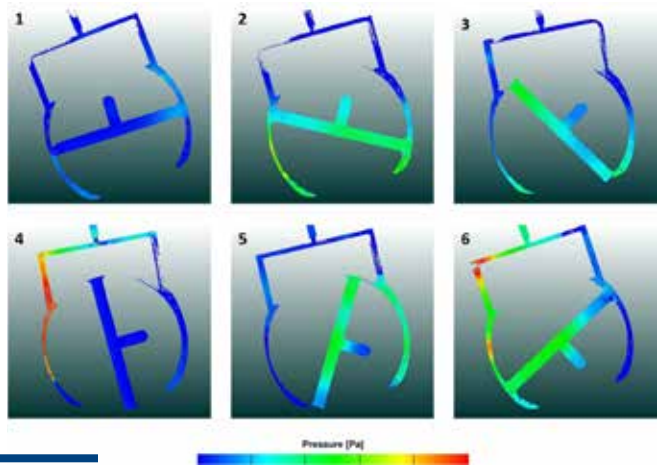

Fig. 7. Pressure evolution in the connecting rod oil channels.

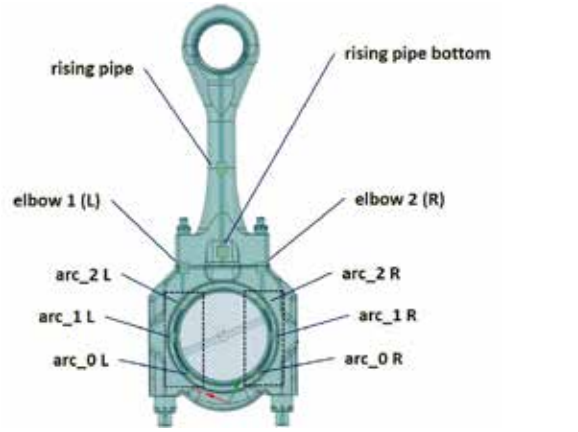

Fig. 8. Locations of control regions used to monitor pressure within the lubrication channel.

To measure the magnitude of the pressure shocks, ten control regions are defined in the connecting rod channels: three on the thrust side of the connecting rod; three on the anti-thrust side of the connecting rod; one in each corner of the C-shaped tube; and two in the rising pipe of the connecting rod. Fig. 8 highlights the locations of these control regions.

Along with the pressure measurement, quantitative indices are defined to compare the different BEB design configurations. Specifically, the following quantities are monitored: average pressure and standard deviation, peak pressure, time at low pressure, and pressure derivative at peak occurrence.
A high average pressure with a low standard deviation is desirable; it means that the flow is uniform and the risk of inadequate lubrication is low. Pressure peaks, time at low pressure, and pressure derivative should be as low as possible to ensure longevity of the engine components.

Fig. 9 shows an example of the pressure signal measured in the control regions described above. These signals reveal spikes, and some control regions have long intervals at extremely low pressure followed by sudden spikes. This behavior can be observed in particular in control regions arc0_L, arc1_L, and elbow_1(L).

A thorough analysis of the previous indices over the entire domain shows that the most critical regions are the lower regions of the

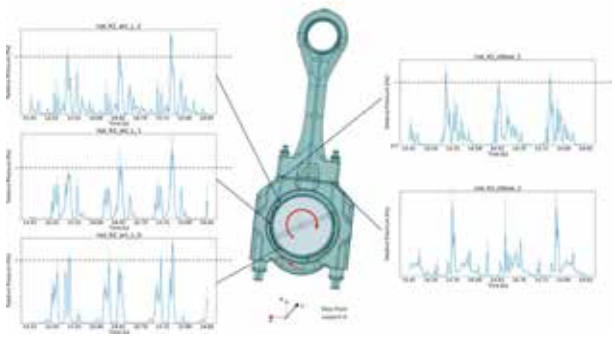

Fig. 9. Example of pressure signals measured in the control regions. The horizontal dashed line corresponds to the average peak values.

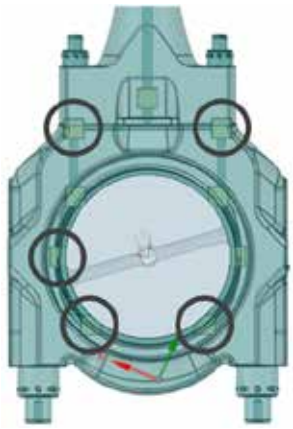

Fig. 10. The most critical regions in the big-end bearing.

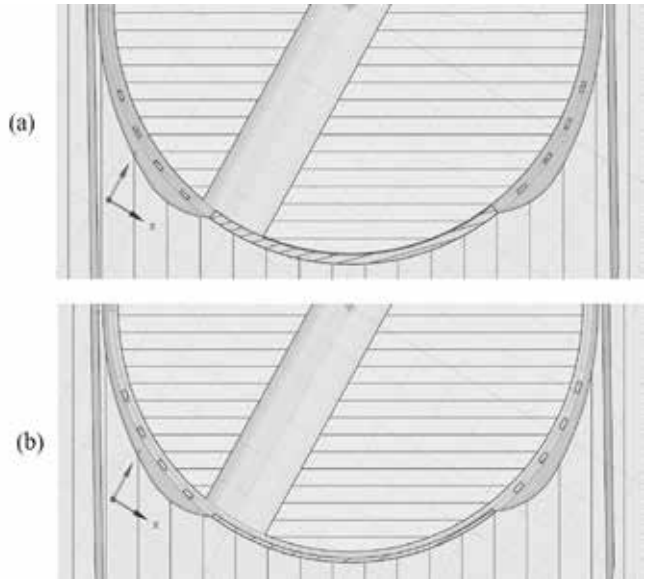

Fig. 11. Detail of the lower passage joining the two sides of the bearing. Original bearing (a) compared to the improved design (b).

bearing (arc0_L, arc0_R), the left middle section (arc1_L), and both corners of the C-shaped channel (Fig. 10).

These regions all feature long periods at low pressure followed by steep spikes with high pressure derivatives.

The locations of the most critical regions suggest a potential improvement in the bearing design. From the simulation data, it is clear that the new bearing design (see Fig. 11b) has two substantial advantages: it reduces pressure spikes and provides pressure continuity on both sides of the bearing.

Comparing the simulation results for the two configurations shows an overall improvement in all quality indices. The oil has a higher average pressure overall and a lower standard deviation; pressure peaks and pressure derivatives are reduced by 20-30%. As a result, the internal channels are more filled and the oil flow is smoother.

Fig. 12 shows the comparison of pressure distribution between the original (a) and improved (b) designs. The new bearing design helps

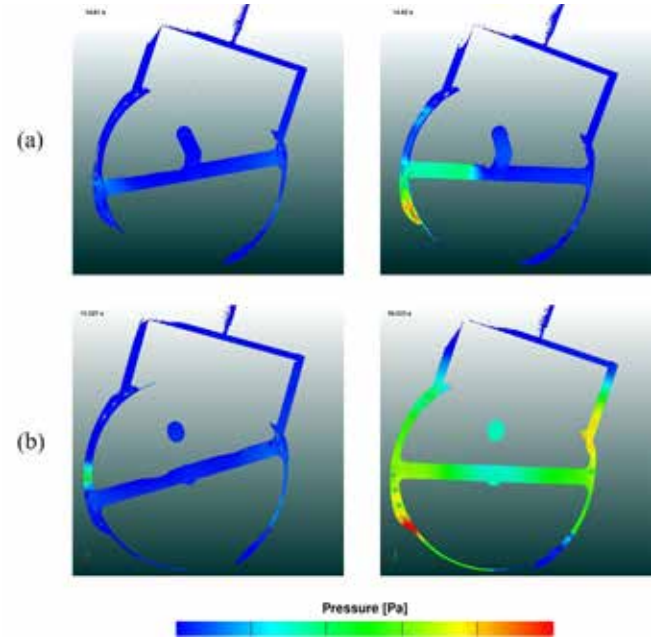

Fig. 12. Pressure comparison in big-end bearing. Row (a) refers to the original bearing, row (b) to the new design.

balance the pressure in the system, which is more uniform overall than the original design.

Figs. 13 and 14 show the comparison of the pressure spikes and derivative signals measured for the two configurations. The grey lines represent the peak values of the original design, while the black lines refer to the improved design.

The blue and orange signal lines refer to the new geometry. Most regions depicted in the images show good improvement (lower pressure peaks and lower pressure derivatives).

Conclusions

The lubrication system of a large bore engine was analysed using Particleworks moving particle simulation (MPS) software. MPS is a meshless method of solving the Navier-Stokes equations which easily accommodates complex moving geometries, such as crankshafts, connecting rods, and pistons.

The simulation method was applied to two different big-end bearing geometries. The pressure behavior for both designs was compared in terms of pressure peaks, average values, and minimum values. The first big-end bearing design showed higher pressure peaks, higher pressure derivatives, and longer periods at low pressure. This combination is associated with higher pressure shocks and potentially inadequate lubrication.

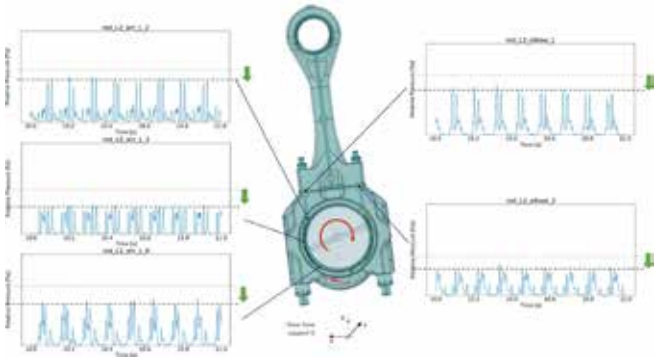

Fig. 13. Pressure measurement comparison between the original and improved designs. The black dashed line represents the peak values of the improved design; the grey line indicates the peak values of the original design. The blue signal line is for the improved BEB configuration.

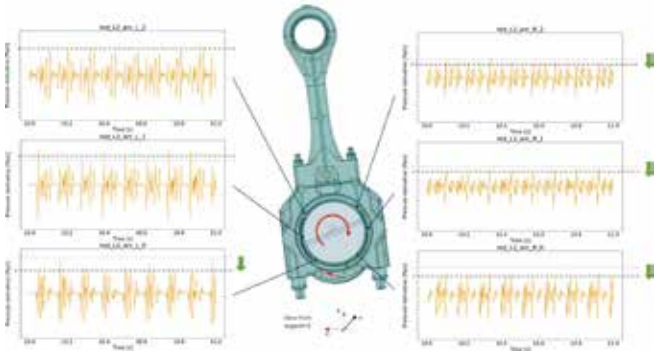

Fig. 14. Pressure derivative comparison between the original and improved designs. The black dashed line represents the derivative values of the improved design; the pink line indicates the derivative values of the original design. The orange signal line refers to the improved BEB configuration.

The modified big-end bearing design allows pressure waves to propagate between the thrust and anti-thrust sides of the connecting rod, helps reduce spikes and stabilizes overall oil pressure behavior.

The predicted pressure trends and behavior of both designs were confirmed by experimental investigations.

Article from:
EnginSoft Newsletter Year 18 n.4 - Winter 2021

References

[1] S. Koshizuka, Y. Oka. Moving-particle semi-implicit method for fragmentation of incompressible fluid. *Nuclear Science and Engineering*, 123. Pp. 421-434

About Wärtsilä

Wärtsilä is a global leader in innovative technologies and lifecycle solutions for the marine and energy markets. We emphasise innovation in sustainable technology and services to help our customers continuously improve their environmental and economic performance.

Our dedicated and passionate team of 17,500 professionals in 200 locations in more than 70 countries shape the decarbonisation transformation of our industries across the globe. In 2020 Wärtsilä's net sales totalled EUR 4.6 billion. Wärtsilä is listed on Nasdaq Helsinki.

Analysing the process of filling a flexible pouch by coupling multi-flexible-body dynamics and particle-based CFD simulation

Investigating the effects of the parameters to select the optimal machine configuration

by Matteo Berlato[1], Davide Marini[2], Michele Merelli[2]
1. Department of Industrial Engineering, University of Trento - 2. EnginSoft

Packaging companies are always striving to stay one step ahead of their competitors in providing the best solutions for product capacity. Furthermore, in most cases, significant effort is devoted to the design of flexible machines: performance is expected to be high and consistent even if the packaged goods, packaging format, or packaging material are changed. Materials, in particular, are heading for a revolution driven by the regulatory restrictions that will take effect over the next few years.

Coesia partnered with EnginSoft and the University of Trento's Department of Industrial Engineering to simulate a stand-up pouch packaging machine (Doypack®). The stages analysed were opening, filling with detergent, and closing (Fig. 1). The scope was to develop a digital model to perform the two-way coupling between the flexible package structure and the fluid content.

The problem was addressed using two commercial tools: Particleworks and RecurDyn. The former represents the fluid behavior using particle-based computational fluid dynamics (CFD) while the latter efficiently calculates the deformation and dynamics of the flexible pouch by performing a Multi-Flexible-Body Dynamics simulation. We first demonstrated the feasibility of the analysis and then verified the results using the experience of Coesia's engineers with the Doypack machine.

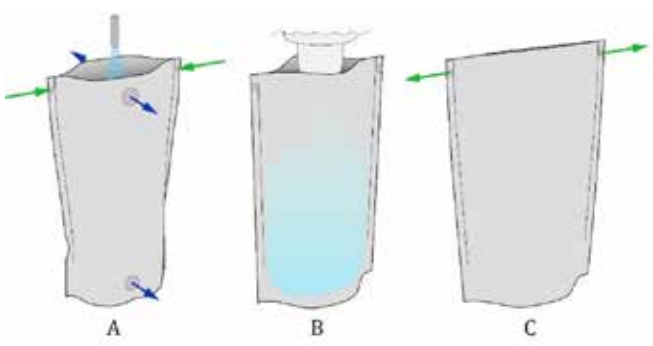

Fig. 1. Schematic representation of the operations analysed.

Three different simulations were performed to understand the influence of the material properties, pouch thickness, machine velocity, and opening span of the pouch on the process of preparing and filling it.

Description of the stations

The machine operates cyclically, alternating between pack feeding movements and stationary operations in which each process is executed. The movement is implemented by a set of upper and lower clamps that support the pouch. Each station is equipped with two pairs of upper clamps that restrain the pouch during stationary operations.

Forward movement of the pouch to consecutive stations is provided by the lower clamps, which are moved back and forth by a four-bar linkage mechanism. The stations can be widened to accommodate up to three packages per stage (triplex), increasing the capacity of the machine.

The automatic process begins with the unwinding and forming of the film. The film is then trimmed and laterally sealed to obtain each individual flat package.

The focus of the simulation project was to model the subsequent stations (and the lateral movement of the pouch between them). The machine workflow includes:

- opening the flat pouch,
- filling it with a liquid detergent,
- closing the filled pouch.

At the beginning of the opening stage (A), the upper clamps and the lateral suction cups engage (Fig. 2). The suction cups open the pouch by pulling apart and the upper clamps accommodate the opening. Simultaneously, pressurized air is forced into the pouch from above, inflating it to ensure the correct shape. The suction cups

are released and the air turns off when the process is complete. The upper clamps release as soon as the lower clamps, responsible for forward movement, pinch the pouch.
As the open pouch nears the filling station (B), the nozzle moves downward, partially entering the package. A second exchange of the support clamps occurs. Once the upper clamps are engaged, the nozzle's shutter is pneumatically moved upward, allowing fluid to flow through the nozzle into the pouch (Fig. 3). Once the pouch is full, the shutter moves downward again.

The lower clamps then move the filled package toward the closing station. Here the clamping switch is repeated. The upper clamps then pull apart, stretching the pouch and restoring the flat configuration at the top, closing the pouch (C). The remaining machine operations are then performed. The top-sealing stage follows the closing phase. The

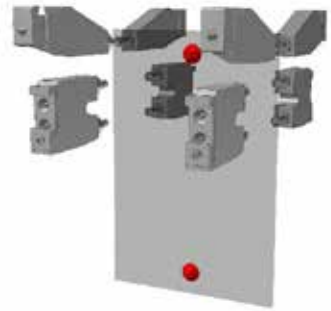

Fig. 2. Initial configuration at the beginning of the opening process.

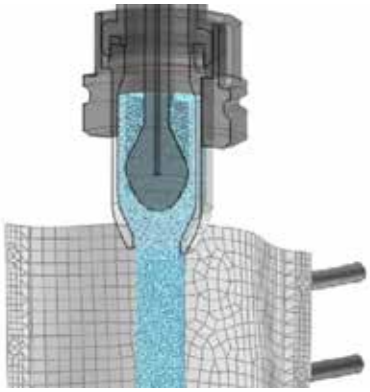

Fig. 3. Flow of the fluid particles through the nozzle.

final operation of the machine is performed at the rejection station (quality check), and the full pouches that conform are distributed through the discharge belt.

Analyses performed

An in-depth knowledge of the processes in a high-capacity automatic machine is essential when the goal is to achieve fast, high-quality production. For this reason, several analyses were prepared to study the operations, focusing on different configurations and parameters.

Three sets of simulations were performed:

1. Pouch opening, filling and movement; analysis of the influence of pouch aperture and of the material properties (coupling of Particleworks and RecurDyn)

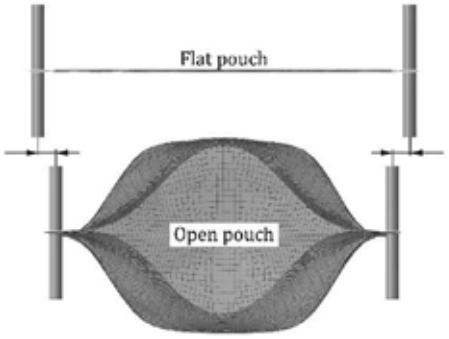

Fig. 4. Description of the opening configuration (top view).

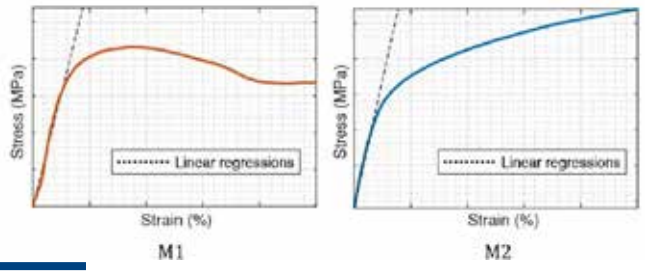

Fig. 5. Experimental stress-strain results of the analysed materials.

2. DOE of the pouch; analysis of the Young's Modulus and pouch thickness (RedurDyn)
3. Sloshing analysis; analysis of the velocity of the machine and pouch aperture (Particleworks)

The first analysis was performed on the entire process (opening, filling, and closing) to study the influence of two parameters:

- the span of aperture during opening (Fig. 4), defining two configurations in which the pouch is less (A1) or more (A2) open,
- the physical properties of the pouch material (Fig. 5), by selecting two different types of film (M1 and M2).

The second analysis focused on the sensitivity to variations in the physical properties of the packaging film (thickness and Young's modulus), compared to a reference configuration.
The stability and shape of the package were studied, evaluating the influence of percentual variations to the pouch properties (-10%, -5%, +5%, +10%).
The final study was conducted focusing on the phenomenon of sloshing, which occurs when the pouch moves from the filling to the closing station. This was analysed by considering two configurations of opening and varying the speed of the machine. The fluid level cannot exceed a predefined limit to ensure that the sealing area remains clean. Higher machine speeds tend to increase the internal sloshing and an upper limit for the velocity can be identified based on the minimum distance required from the top of the pouch.

Modelling of the problem

The multi-body and structural parts of the model were developed in RecurDyn. The rigid components (i.e. upper and lower clamps, suction cups, nozzle, and shutter) were inserted into the RecurDyn model using their CAD designs and assigning them their specific laws of motion.

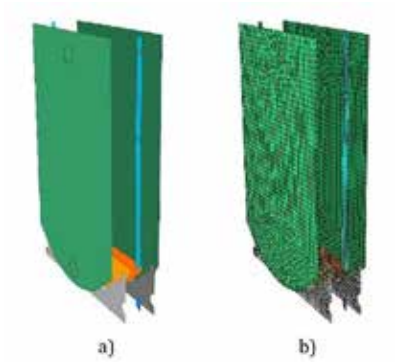

Fig. 6. Development of the Full Flex structure of the pouch.

The structure of the pouch was modelled using the Full Flex approach: a series of flat geometries was created (Fig.6a), meshed with 4-node 6-DOFs shell elements (Fig.6b), and merged to obtain a single Finite Element (FE) flat structure. The shell elements are well suited to representing thin films. RecurDyn's Full Flex method also enables efficient and effective simulation of nonlinearities related to large displacements and contacts.

To accelerate and automate the calibration of the pouch model, a script was developed (using the integrated PNet environment) to easily repeat the steps of structure definition and meshing. By varying a few parameters in the code, an iterative procedure was accomplished to correctly define the properties of the FE structure.
Once each component was correctly defined, the interaction of the package with the tips of the clamps and the suction cups was configured.

Particleworks is a mesh-less CFD software based on the Moving Particle Simulation (MPS) Method. The underlying Lagrangian approach is ideal for analyzing free-surface flows, such as the injection of the fluid into the pouch (jet flow and splashing phenomena). An annular surface was defined and positioned above the shutter. From this surface, fluid particles are generated with a constant flow rate. Among the physical properties of fluids, the most influential is the rheological law.
Detergents and foods injected into pouches frequently exhibit non-Newtonian behavior, with viscosity that varies according to the local shear rate. In this analysis, the liquid detergent displays a shear-thinning behavior (with viscosity decreasing at higher shear rates). The experimental data was fitted and applied to the fluid settings. The particle size and numerical settings were selected by evaluating the desired sensitivity of the simulation results, while also considering the computational cost.

The co-simulation configuration is assisted by a communication strategy already implemented between the two tools, RecurDyn and Particleworks. A two-way Fluid-Structure Interaction (FSI) can therefore be used to simulate these tightly coupled physical domains.

Results

The results of the complete analysis at different frames are depicted in Figs. 7-9. During the first process (Fig.7), the progressive unfolding and opening of the pouch can be observed. The structure is represented displaying the von-Mises stress. Fig. 8 shows a cross-sectional view of the gradual filling of the package. The velocity and pressure distribution of the particles can be seen, allowing a detailed analysis of the detergent flow into the pouch and its interaction with the lateral film and the bottom gusset. Fig. 9 illustrates the closing process.

One of the most interesting results with respect to the analysed configurations concerns the lateral deformation of the filled pouch as it exits the filling station. The deformation is defined by the difference between the nominal and the actual mean position of the bottom gusset (Fig.10). The deformation of the pouch is more strongly influenced by a less (A1) or more (A2) open package, rather than by a less (M1) or more (M2) rigid material.
A summary of the results of the variational analysis is shown in Fig 11. The stability of the bottom gusset during the opening operation is the aspect that is most sensitive to changes in the physical properties of the film. A collapse of this part tends to refold the entire package,

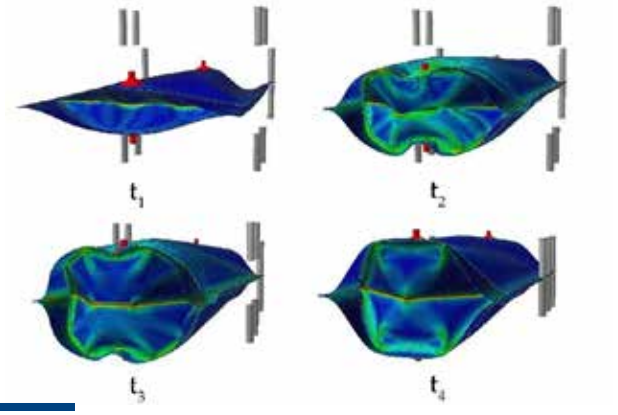

Fig. 7. Progression of the opening process showing the von-Mises stress (bottom view).

Fig. 8. Progressive filling of the pouch with the liquid detergent.

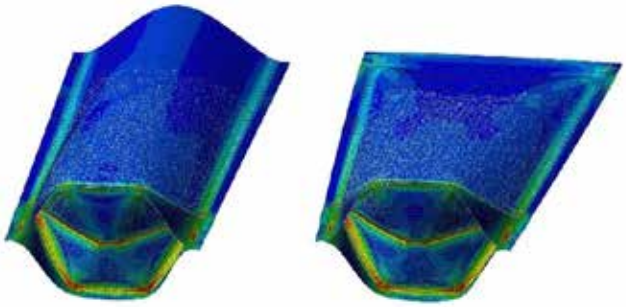

Fig. 9. Von-Mises stress of the filled pouch before (left) and after (right) the closing process.

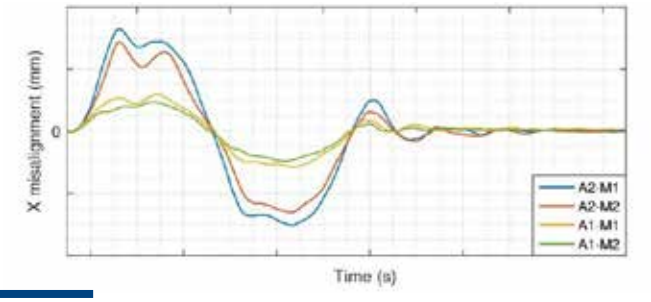

Fig. 10. Pouch deformation for four different combinations of the pouch aperture (A1 less open than A2) and the pouch stiffness (M1 more flexible than M2).

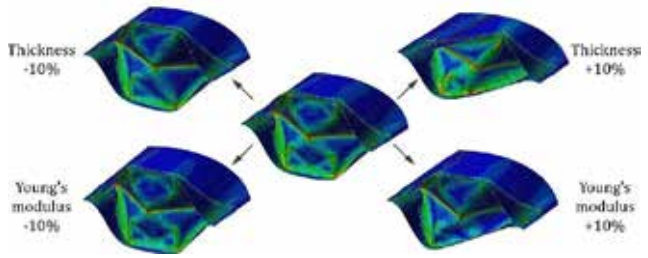

Fig. 11. Results of the parametric analysis of the effects on the structure of the bottom gusset.

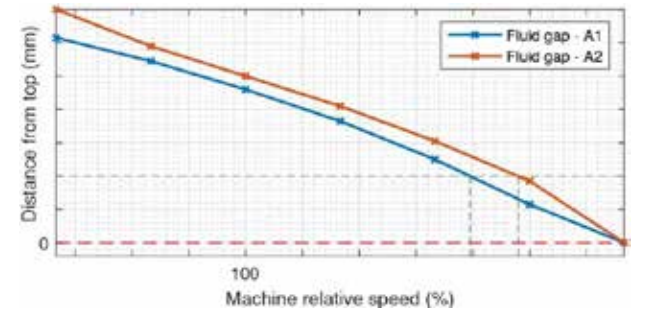

Fig. 12. Gap between the fluid and the top of the pouch at different machine speeds, for a less (A1) or more (A2) open pouch.

blocking the execution of the subsequent operations. The results show that a stiffer film increases the possibility of the gusset collapsing. The variations analysed in the properties help define the boundaries for a successful filling process.

Fig. 12 presents the results of the sloshing analysis. The gap between the maximum fluid level and the upper bond of the pouch is shown for different machine speeds and two apertures of the pouch. The waves in the fluid, caused by the acceleration and deceleration of the package, reach a greater height (smaller gap) when a faster machine speed is selected. At the same machine speed, the more closed pouch has a higher fluid level. If limiting the maximum fluid height is the primary design requirement, then A2 allows higher machine speeds than the A1 version.

Conclusions

This study demonstrated the powerful capabilities of the tools that were used to address a complex two-way FSI simulation. The results are promising: they can be used to select the best combination of parameters and to predict performance as the machine configuration or package characteristics change. Both structural and fluid behavior can be analysed in detail, providing key information that cannot be retrieved experimentally.

All simulations were performed using a standard workstation with an entry-level graphics processing unit (GPU) card. Despite this, the entire simulation was performed in 10 hours allowing it to be run overnight without the need for a high performance computing (HPC) facility. Furthermore, the use of mid-range or high-end GPU cards can easily reduce this time.

The simulation results can be used to identify an ideal combination of parameters. When the rigidity of the package must be ensured throughout the line, the less open configuration is preferable (Fig.10). The stiffness of the material has a visible, though less significant, effect than the opening configuration.

These results are useful as we move to recyclable, less rigid materials since they can be used to study the effect on the process in advance. It is possible to select certain ad hoc opening configurations to compensate for dissimilar behaviors when different package formats or materials are used.

The sloshing results led to an opposing conclusion. When the machine speed is high and must be maximized, a greater aperture of the pouch should be selected to reduce the height of the waves in the fluid in the pouch. While these results show opposing directions for improvement, by relaxing some constraints (such as selecting a constant opening configuration), insightful simulations can be performed to identify the best compromise combination for each specific operation.

The results obtained for the first operation (opening and lateral motion of the empty pouch) and the final operation (lateral movement of the full pouch) show opposing positive correlations with the span of aperture. This hint at possible improvements, such as varying the span of aperture across the stages of the machine.

Article from:
EnginSoft Newsletter Year 18 n.3 - Autumn 2021

About Coesia

Coesia is a group of companies specialised in highly innovative industrial and packaging solutions, headquartered in Bologna, Italy. Isabella Seràgnoli is the sole shareholder.
Coesia companies are leaders in the sectors of:

- Advanced automated machinery and packaging materials
- Industrial process solutions
- Precision gears

Coesia's customers are leaders in a wide range of market sectors, including Aerospace, Ceramics, Consumer goods, Electronics, Healthcare, Luxury Goods, Pharmaceuticals, Racing & Automotive and Tobacco. coesia.com

Application of Particleworks to the design and performance evaluation of waterproofing for automotive air conditioning systems

by Kosuke Masuzawa[1], Shun Fujimoto[2] and Akiko Kondoh[2]
1. akf, Inc - 2. Prometech Software, Inc.

When it comes to cars, people tend to focus on driving performance and safety. However, one should not forget about the air conditioning system, which plays a crucial role in enabling a comfortable ride over long periods, even in extremely hot or cold weather conditions or in heavy rain. There was a time when air conditioning in cars, which we now take for granted, was a luxury only found in expensive cars. After years of development and innovation, all vehicles today are equipped with air conditioning systems. However, the design of such systems is not simple since they operate at full capacity in all weather conditions. As with the vehicle body and various other automotive parts, it is necessary to evaluate the system's performance through experiments that assume driving under real weather conditions and through simulations using CAE. This article introduces a case study on the waterproofing of an automotive air conditioning system for rainy conditions using Particleworks, a particle method CFD software.

Air conditioning in cars inevitably requires ventilation inlets to introduce external air. A waterproof design is necessary since rainwater is likely to enter with the exterior air. To evaluate the impermeability of an air conditioning system, a simulation tool that considers water droplets and free surfaces is required. Using these tools usually requires a high degree of skill. However, Particleworks, which uses the particle method, is a simple tool that non-professionals can use to study waterproofing.

In many modern cars, the air conditioning system, commonly referred to as an HVAC, provides integrated air conditioning control with heaters (heating), ventilation, and air conditioning (air conditioning and cooling). The heater heats the interior air of the vehicle with a radiator using hot coolant from the engine, while the ventilation function controls between recirculating internal air and introducing external air. In addition, air conditioning sends cool air into the car through a refrigeration cycle that uses a compressor and a condenser. This simulation using Particleworks, focused on the ventilation portion of the system.

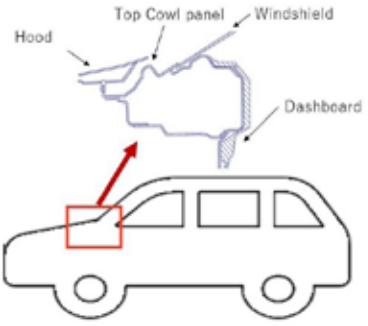

Fig. 1. Cross-section of top cowl panel.

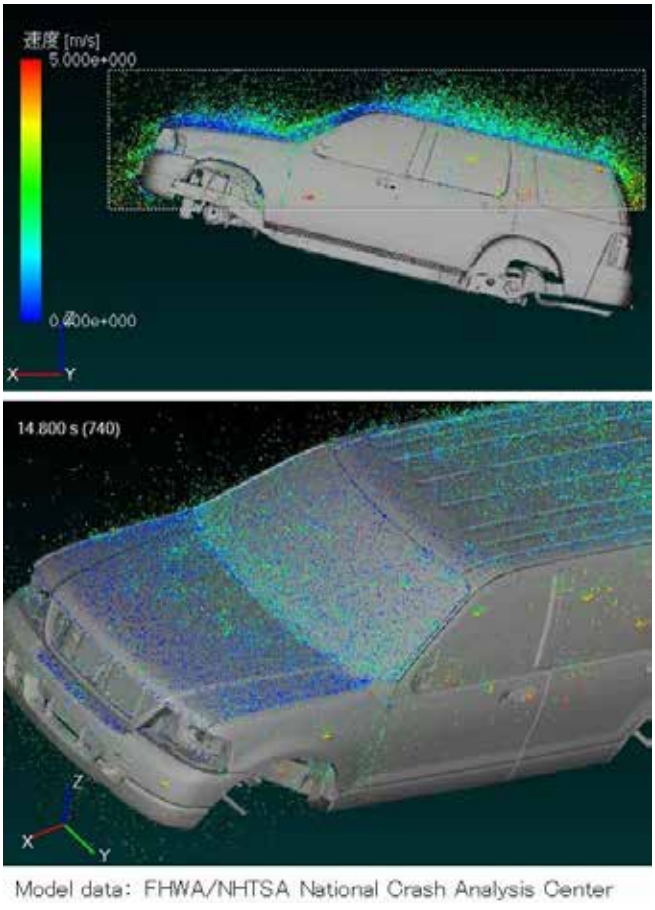

Fig.2. Rainfall simulation of the whole vehicle body inclined uphill at a 15-degree angle.

Internal air recirculation, which is one of the ventilation functions, only enables the recirculation of air inside the car without any incoming air from outside. It is used to improve the cooling capacity in scorching weather. It operates when the user deliberately blocks polluted external air from entering, such as when driving behind a large vehicle. However, there are some disadvantages, including the tendency for windows to fog up due to increased humidity in the cabin. There is also the possibility that the driver's concentration may fall due to the lack of oxygen because of decreased air freshness.

On the other hand, external air induction is a function that delivers fresh air from outside the car into the cabin.

By drawing external air from the front of the vehicle and expelling it from vents in the rear of the vehicle, the air inside the car cabin is refreshed. Most modern cars are equipped with automatic air conditioners. In setting up their control, it is common to essentially set the air conditioner to introduce external air, except in scorching weather.

So, what do we need to pay attention to when introducing external air? Since the HVAC system is located in the front of the vehicle, external air is introduced from the front of the vehicle. However, the front of the vehicle is also home to the engine compartment that generates heat due to the combustion from the engine itself, and is also the site of the heat dissipation from heat exchangers such as the air conditioning condenser and radiator. This means that it is essential to introduce fresh air that avoids these high temperatures.

Therefore, as shown in Fig. 1, it is common to introduce external air from the upper cowl vents between the windshield and the hood. However, the problem arises that water enters through these vents during rain. It is therefore necessary to design a waterproofing system that separates the air from the liquid, allowing only the air to enter the HVAC system and preventing water from entering the passenger compartment.

In the Particleworks simulation, we first analysed the rain patterns for the full vehicle when parked to reproduce the overall rain situation. Here, assuming that the car was parked on a flat surface, we were able to confirm that the rainwater falling on the vehicle body flowed to the top of the cowl across the windshield. Next, to evaluate the results in more severe conditions, a rainfall analysis was performed with the vehicle body inclined uphill at a 15-degree angle. This confirmed that a large amount of rainwater flowed back to the car cabin from the hood area, and mainly from the windshield when stopping the car (Fig. 2). In other words, it was apparent that it was necessary to design the top section of the cowl to allow fresh air to flow in and to enable waterproofing of the cabin.

To evaluate the water flow into the top of the cowl in greater detail, a simplified model as shown in Fig. 3 was used. The area enclosed by the black dotted frame and surrounded by the windshield, hood, and fenders, and including the exterior air inlet, is the subject of this analysis. This model is well separated from the engine compartment when viewed from the side and has holes on both ends for drainage. The red frame seen on the inside of the model is the air intake for the HVAC unit and we will study its design to prevent rainwater from entering here.

Fig. 4 shows the results of the water flow analysis at the top of the cowl top with a 15-degree inclination. In this case, based on the results of the whole car rain analysis, the mass flow rate conditions were set to

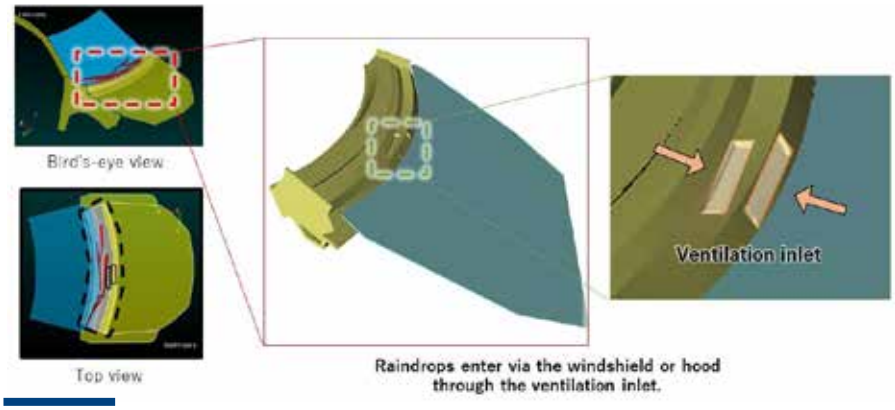

Fig. 3. Simplified simulation model.

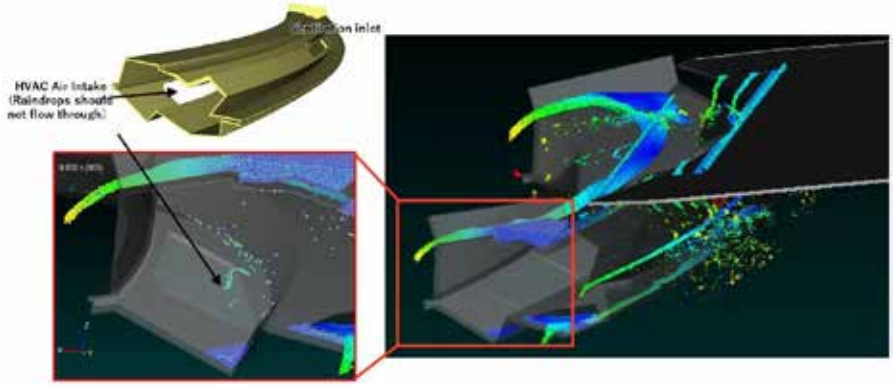

Fig. 4. Water flow simulation of top section of cowl at a 15- degree uphill incline.

reproduce the flow from the windshield and hood areas, and the other conditions were analysed using the Particleworks default settings. We were checking to see if water was entering the exterior air inlet. At this 15-degree inclination, it was confirmed that the water flow from the hood was the inflow path to the top of the cowl. We also found that the water that had accumulated due to the slope was overflowing into the vicinity of the external air inlet.

Having confirmed the above, it was found that there are two possible routes for water to enter the external air inlet: one being the path where raindrops that have entered and dripped down enter as droplets, the other being the water that has accumulated near the opening overflows and enters when the car inclines. Various countermeasures can be considered here, and the design plan will be discussed while factoring in the cost.

In this study, we considered two countermeasures for the original cowl top and conducted simulations. Countermeasure 1 adds a simple wall to the bottom edge. Although it is basically necessary to prevent all splashes, and a simple wall would not be sufficient, we decided to only add a wall in countermeasure 1 to see what improvement could be achieved at the lowest cost. In countermeasure 2, we examined the shape of a cover to simultaneously prevent splashing and water overflow. We modelled a part that inverted a typical range hood or duct cover (see Fig. 5).

Fig. 6 shows a comparison of the initial shapes, countermeasure 1 and 2 and the simulation results, and Fig. 7 shows a graphical comparison of the number of particles (the amount of water) entering into the air inlet with the initial shape, with countermeasure 1, and with countermeasure 2. We found that countermeasure 1 prevented the water from overflowing, but was not sufficient to prevent droplets. In contrast, countermeasure 2, a design proposal that adds a duct cover, reduced water infiltration by about 90% compared to the initial shape.

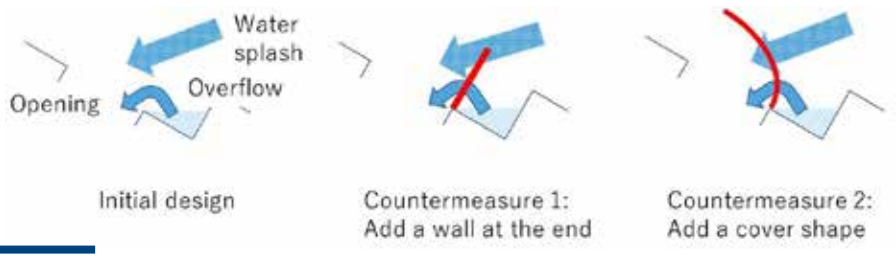

Fig. 5. Considerations of countermeasure design ideas.

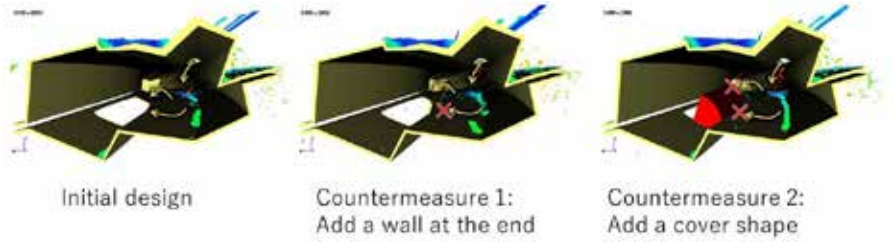

Fig. 6. Comparison of simulation results for each countermeasure design proposal.

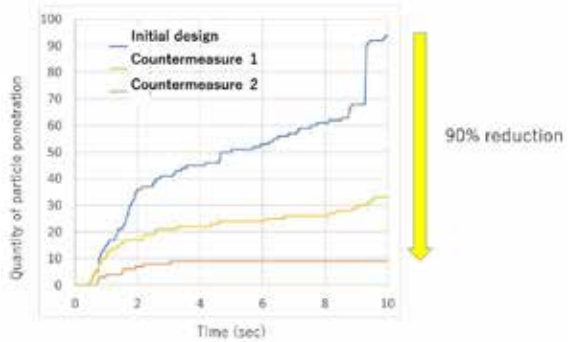

Fig.7. Comparison of water inflow for each countermeasure design idea.

Using Particleworks to study the waterproofing design of the external air intake of a car air conditioning system, it is possible to visualize the event itself by simulation, to clarify the problems and causes generated by the initial shape, and study the countermeasures and their effectiveness. As you can see from the simulation results, we were successfully able to use Particleworks to improve the waterproofing performance by preventing drops from entering the cabin.
The advantage of using Particleworks in this project was that it was easy to model and simulate without any meshes. In particular, we were able to quickly compare multiple design proposals, reflecting simple countermeasure shapes.

Particleworks is expected to be used more widely in the future as a tool that can quickly and stably simulate such various fluid behaviours.

Article from:
EnginSoft Newsletter Year 18 n.3
Autumn 2021

Lubrication and heat dissipation in transmissions and bearings

Lubrication and heat dissipation in transmissions and bearings are critical to both the performance and the life of these systems

by Elisabetta Fava[1] and Massimo Galbiati[2]
1. Comer Industries S.p.A - 2. EnginSoft

Transmission design is mainly based on the mechanical aspects of the transmission and lubrication is an aspect that is verified, and eventually corrected, based on bench testing, i.e. once the design phase has been completed and a physical prototype is available.

The use of transparent prototypes or windows in specific regions of the transmission makes it possible to visualize, at least partially, the flows and distribution of the lubricant within the transmission, and to understand whether it reaches the various components.

Similarly, by means of a physical prototype and bench tests, it is possible to verify the correct positioning of the breather ducts, which must be adequately protected in order to prevent the escape of the lubricant, and the functioning of the transmission under different operating conditions, for example by changing inclination, number of revolutions, or direction of rotation.

These are some of the issues faced daily by those who design and build transmissions of all kinds, from the automotive and industrial sectors to the aeronautical sector; from small transmissions to those for the naval and wind-power sectors.

However, waiting for an advanced stage of the project (i.e. once you have a prototype on the bench) to address the issue of lubrication can present surprises that can significantly impact both the development time of the transmission and its cost.

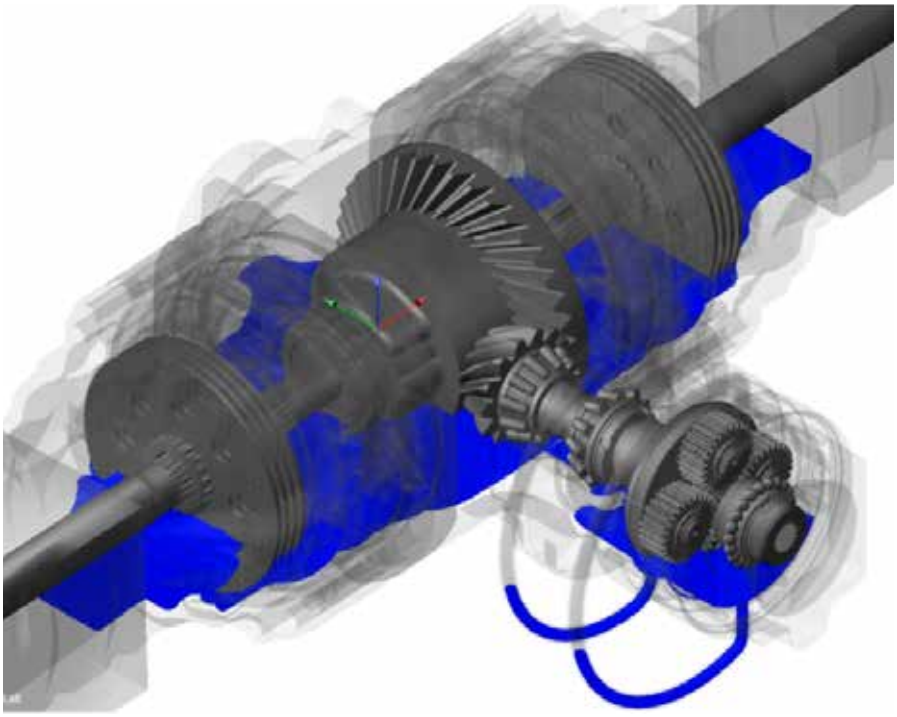

Discovering that some vital components, such as bearings, are not properly lubricated, or that there are oil leaks from the vents may require design changes, which can be costly at this late stage. In addition, there are some machine operating conditions that cannot be or are difficult to test on the bench, such asdynamic braking, acceleration, or particular temperature conditions.

To address these issues and to reduce the risks, costs and development times of transmissions, more and more companies are shifting the issue of "good lubrication" from the experimental verification phase to the actual design phase.

This has come about thanks to the availability of new numerical simulation technologies that enable the use of a virtual bench to test different operating and lubrication conditions quickly, and especially before building a physical prototype.

Models of this type complement and complete experimentation and, if used in the preliminary stages of the design, allow the project to be directed correctly and prevent lubrication or overheating problems.

One of the companies that has adopted these numerical simulation methods is Comer Industries.

Comer Industries, based in Reggiolo in the province of Reggio Emilia, is the leading global player in the design and production of advanced engineering systems and mechatronics solutions for power transmission. The company operates in the fields of agricultural machinery, construction and forestry equipment, energy and industry.

Founded in 1970 by the Storchi family, today the company is led by the second generation. The president and CEO is Matteo Storchi.

Comer Industries has 1400 employees, exports to all five continents and has seven offices in Europe, one in the United States, one in Brazil, two in China and one in India, including production plants and commercial branches it reaches 54 countries with its products and in 2020 it registered has a net turnover of 396 million euros. In March 2019, the company opened to external investors by listing on the Milan Stock Exchange's AIM market.

Comer Industries is one of most important suppliers of the most relevant world players in the construction of agricultural, industrial and renewable energy machinery. The mechanical components made by Comer Industries represent crucial elements for the correct functioning of combine harvesters, tractors, plows, mowers, round balers, excavators, bulldozers and wind generators.

The market on which Comer Industries works is perfectly globalized and competition has imposed the ability to ensure customers products and assistance services with unique standards of excellence in every part of the world.

One of Comer Industries' numerical simulations for lubrication concerned predicting the path of the oil in an axle with an integrated planetary gear system input stage for a compactor.

During its operations, the compactor frequently travels uphill and downhill. The lubrication of the planetary gears is critical in these phases and must be guaranteed, as must the correct exchange of oil between the planetary gears and the axle to avoid dangerous increases in temperature.

Since the planetary gear system and the axle communicate via two oil passages, the analysis aimed to optimize the geometry of these two passages by recreating a meaningful operating condition in a single simulation consisting consecutively of a horizontal machine path phase, an uphill, a downhill, and a horizontal phase to return to the starting point.

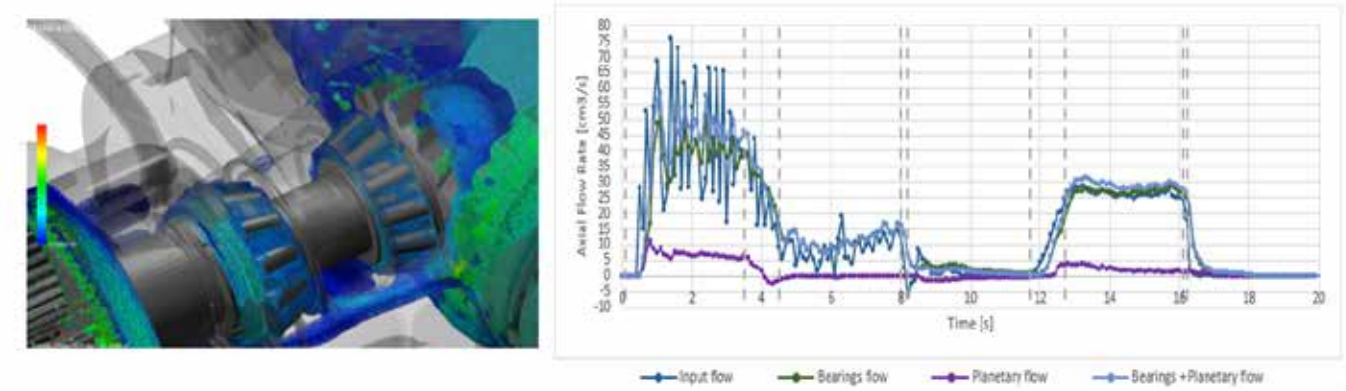

All internal components of the axle and planetary gear system were included in the model along with two variants of the housing: the first with the existing oil passage geometry and the second with some proposed optimized oil passages. Finally, the oil was modelled at its working temperature properties: the model consisted of about six million particles.

The results obtained were very interesting and made it possible to evaluate:

- the oil redistribution between the two oil passages both qualitatively and quantitatively in terms of oil flow rates
- how this redistribution changes in the various phases - horizontal, uphill and downhill
- how the previous stage of the path affects the next stages, and how the oil behaves during transitions

It was found that, with the same oil quantity, the geometry of the current passages does not allow the oil to reach the planetary gears in all the configurations, thereby the oil exchange between the two environments is insufficient.

On the other hand, by enlarging and shaping the passages differently, it was possible to guarantee a greater flow of oil to the planetary gears and to ensure an adequate exchange of oil between the axle and the planetary gears that can avoid temperature raise.

This analysis was validated experimentally with some specific tests on a test bench: a high correspondence was obtained during the same work cycle (with the same inclinations) when comparing the simulated dynamic oil level with the experimental one.

This made it possible to implement the modifications to the oil passages without carrying out multiple experimental iterations which, since they affect the casting models, would have resulted in excessive time and costs related to potentially numerous remakes of equipment and components. In addition, there was no need to increase the oil level, so efficiency could be preserved.

Article from:
EnginSoft Newsletter Year 18 n.2 - Summer 2021

About Comer Industries

Comer Industries, based in Reggiolo in the province of Reggio Emilia, is the leading global player in the design and production of advanced engineering systems and mechatronics solutions for power transmission. The company operates in the fields of agricultural machinery, construction and forestry equipment, energy and industry.

Founded in 1970 by the Storchi family, today the company is led by the second generation. The president and CEO is Matteo Storchi. Comer Industries has 1400 employees, exports to all 5 continents and has 7 offices in Europe, 1 in the United States, 1 in Brazil, 2 in China and 1 in India, including production plants and commercial branches it reaches 54 countries with its products and in 2020 it registered has a net turnover of 396 million euros. In March 2019, the company opened to external investors by listing on the Milan Stock Exchange's AIM market.

Comer Industries is one of most important suppliers of the most relevant world players in the construction of agricultural, industrial and renewable energy machinery.

The mechanical components made by Comer Industries represent crucial elements for the correct functioning of combine harvesters, tractors, plows, mowers, round balers, excavators, bulldozers and wind generators. The market on which Comer Industries works is perfectly globalized and competition has imposed the ability to ensure customers products and assistance services with unique standards of excellence in every part of the world.

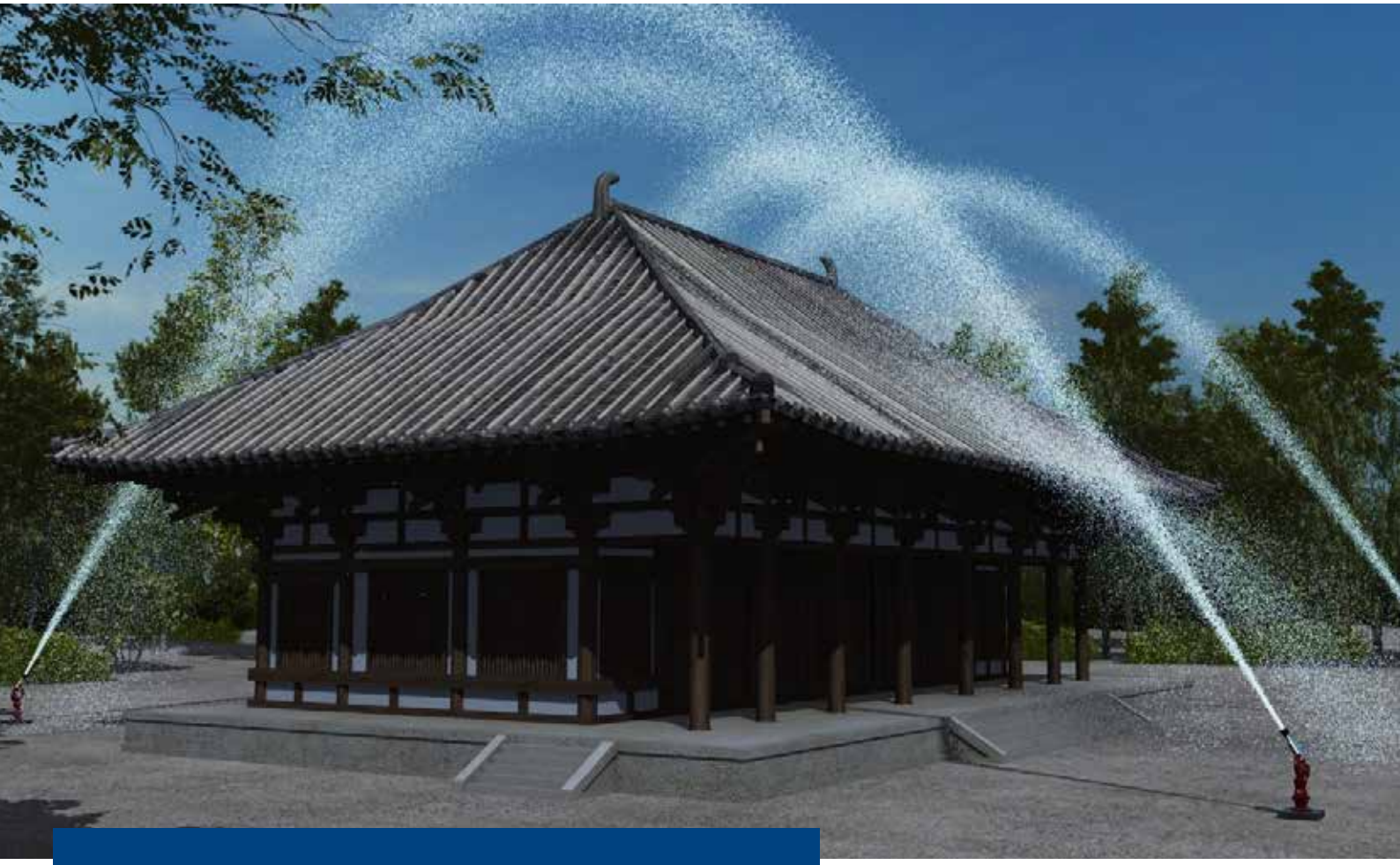

Simulating fire extinguishing equipment for historical buildings with Particleworks and Granuleworks

Studies of three methods: a water discharge gun, a drencher, and a firefighting drone

by Sunao Tokura, Shun Fujimoto and Akiko Kondoh
Prometech Software, Inc.

This article presents simulation examples for three types of firefighting equipment for cultural heritage buildings using Particleworks, a CFD software based on the Moving Particle Simulation (MPS) method: a water discharge gun, a drencher, and a firefighting drone.

Such firefighting equipment is generally verified by means of installation standards and on-site water discharge tests, however, field tests that include all realistic fire conditions are impractical due to the cost and the physical risk to valuable buildings. Numerical simulation is therefore beneficial for the first evaluation of the firefighting equipment's effectiveness.

In recent years, some valuable cultural heritage sites, such as the Notre Dame de Paris cathedral and Shuri Castle in Okinawa, have been destroyed by fire (both in 2019). These tragic accidents and the sense of loss they provoked are still fresh in our memories. We have a mission to protect these symbols of history, tradition, and culture, and to pass them on to future generations by preventing such accidents from happening again.

In East Asia, including Japan, many historical buildings are made of wood and so there is an impelling need to prevent such fires. As a result, many facilities today are equipped with fixed and mobile water guns and drenchers that do not affect the surrounding landscape, while research and development of firefighting drones to extinguish fires in high-rise buildings continues.

The effectiveness of such firefighting equipment is generally verified by means of installation standards and on-site water discharge tests. However, conducting field tests that include all realistic fire conditions are impractical due to the cost and the physical damage to valuable buildings. It is, therefore, beneficial to evaluate the firefighting equipment's effectiveness first by using numerical simulation. The simulation considers the total amount of water applied to the building from the water discharge, the trajectory of the water discharge, and the direction of flow. Particle method computational fluid dynamics (CFD) is well-suited to effectively handle the large number of droplets and the free surface of the water as it flows over the building's exterior in these simulations.

This article presents simulation examples for three types of firefighting equipment using Particleworks, a CFD software based on the Moving Particle Simulation (MPS) method: a water discharge gun, a drencher, and a firefighting drone. Water guns and drenchers are designed to extinguish and prevent fires by spraying water, while firefighting drones use powdered extinguishing agents, which requires the powder model to be defined. Particleworks includes Granuleworks software which uses the discrete element method (DEM). By either coupling the functionality of MPS and DEM for liquid and powder interactions, or by using them individually depending on the target materials, the operation of firefighting equipment can be evaluated realistically.

Modelling airflow in the MPS method

MPS uses a formula that reproduces the incompressible flow of water and other substances and this formula is applied to the representation of water being released. During an actual fire, strong winds may be blowing which would affect the flow of the water discharged from the gun, so that the water doesn't flow in the direction of the target.

Moreover, even in the absence of wind, water droplets and powder flying through the air are subject to air resistance, which gradually reduces their momentum and shortens their flight distance. To simulate a water discharge gun while taking air into account, we performed calculations using an air resistance model. One way to analyze two-phase gas-liquid flow is to use the finite volume method (FVM), also available in Particleworks, and perform the simulation using FVM-MPS coupling. However, in this case, we chose to use the air resistance model to reduce the amount of computation.

Simulation of a water discharge gun in high wind conditions

We chose a wooden structure called a Yosemunezukuri, as the target building for the water gun simulation. A Yosemunezukuri has a roof that slopes in four directions and is one of the representative architectural styles of historical buildings in Japan where there were used in many national treasures such as the Great Buddha Hall of Todaiji Temple. The main shape and dimensions of the simulation model are shown in Fig. 1. Four water discharge guns are placed diagonally across the building, and the discharge angle is set at 60 degrees from horizontal so that the water can reach the top of the roof. Note that Particleworks uses CAD data in STL format to define the shape of the structure, so meshing is not required.

For the analysis conditions, the flow rate from each water discharge gun was set to 0.15m^3/s (150l/s), and the physical properties of water and air were defined as general values. We set the particle diameter, which is an index of resolution when fluid is modelled as particles, to 20mm in consideration of the calculation time, and used the pressure explicit method to calculate the pressure explicitly.

Fig. 2 shows the result of a simulation of water discharge in windless conditions. Even in such conditions, the flying water droplets are subject to air resistance and the distance varies. Fig. 3 is a contour plot showing the total amount of water on the roof. The wet area can be seen, and the water discharge gun's angle and position can be evaluated in relation to the extent of the area covered by water.

Next, we simulated the water discharge gun with a strong, 25m/s wind blowing around the building. The airflow velocity field that combines spatial coordinates and airflow vectors is imported into Particleworks in .csv format. The air resistance is given by a 3D interpolation of the air velocity at each particle position.
The result is shown in Fig. 4. Since the wind is blowing to the right in the figure, we can see that the water flow is pushed away and only a part of the roof becomes covered with water. As such, it is difficult to change the direction of the water discharge with a fixed water discharge gun according to changes in wind speed and direction. It is necessary to change the direction manually at the fire site, but this is not safe.

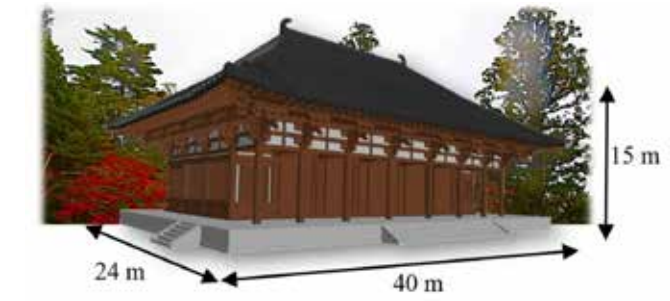

Fig. 1. Simulation model and dimensions.

Fig. 2. Visualization of firefighting simulation using a water discharge gun in windless conditions.

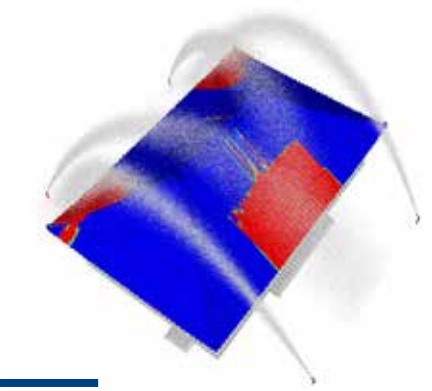

Fig. 3. Contour plot of the total amount of water applied to the roof in windless conditions.

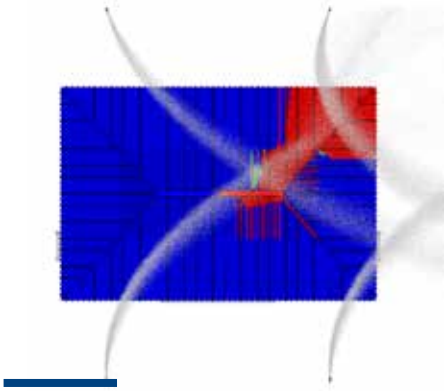

Fig. 4. Contour plot of the total amount of water applied to the roof from a fixed water discharge gun in a 25m/s wind.

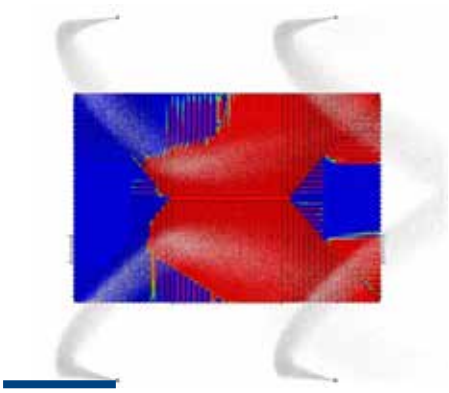

Fig. 5. Contour plot of the total amount of water applied to the roof from a rotary water discharge gun (60° rotation) in a 25m/s wind.

The next step was to simulate whether the firefighting capability could be improved by using a movable water discharge gun, using a remote control to adjust the direction of the water gun according to the situation.

Fig. 5 shows the area of water coverage when the gun is rotated by 60 degrees around the vertical axis in the same 25m/s wind. We can see that the area covered by water is wider with the movable type of water discharge gun than with the fixed type. The final number of particles was approximately 350,000 and the calculation time was 30 hours using NVIDIA's GeForce GTX TITAN X GPU. If a faster GPU is dedicated to the numerical calculation, the calculation time is estimated to be several hours.

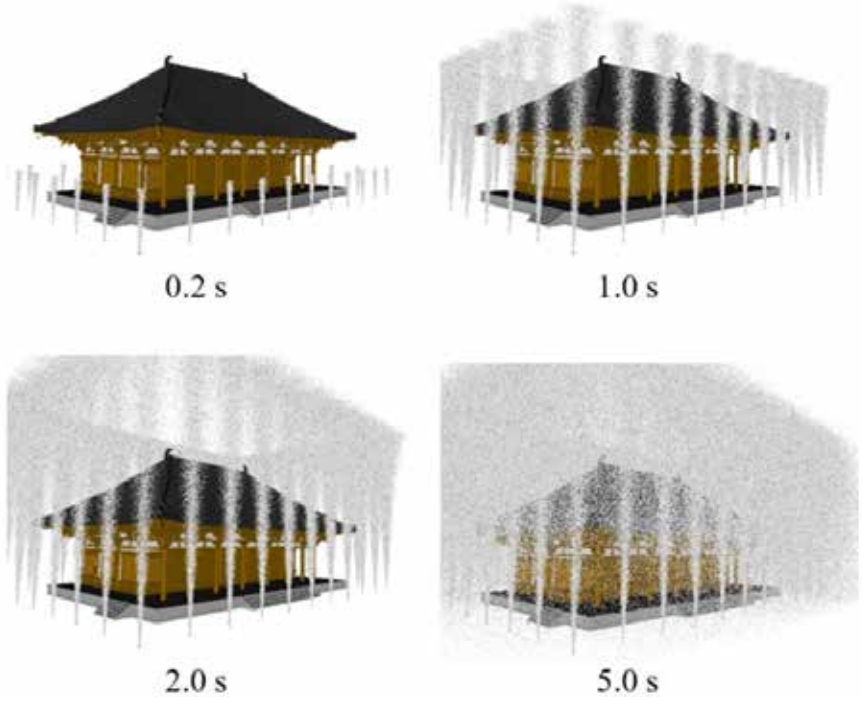

Fig. 7. The drencher's process of forming the curtain of water.

Simulation of fire prevention using a drencher

A drencher is a fire extinguishing device in which pipes are installed on the roof or exterior walls of a building, and the sprayed water forms a curtain to prevent the spread of the fire from the surrounding area. Water is also sprayed from pipes embedded in the ground surrounding the building to wrap the building in a curtain of water. Since it does not spoil the landscape, it is often used as fire-fighting equipment for cultural heritage properties.

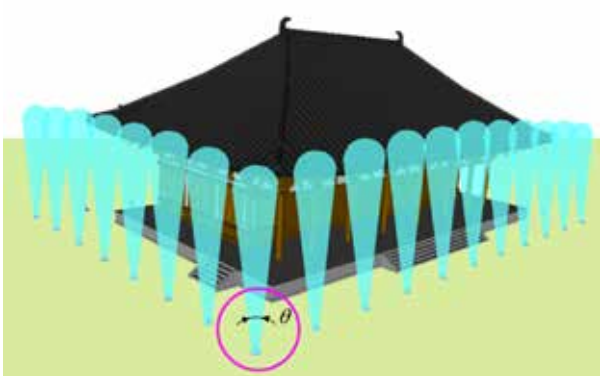

Fig. 6. Drencher simulation model: spray nozzle angle was set at $\theta=6°$.

The same building model was used for the drencher simulation. Water spray nozzles with a diameter of 100mm were configured at intervals of 5m, with a flow rate of 0.2m^3/s per nozzle and a spray angle of 6° (as shown in Fig. 6) so that the water sprayed by the nozzles would spread radially. Particle diameter was set to 25mm. To verify the drencher's effectiveness in preventing the spread of the fire, we created a situation where debris from a fire that had broken out near the building would fly in. The fire debris was modelled using DEM particles and the simulation was performed using MPS and DEM coupling. A coarse-grained DEM model was used to avoid excessive computational load, and the particle diameter was set to 50mm.

Fig. 8. The drencher's method of preventing fire debris from reaching the building (right: CG rendering).

Fig. 7 shows the drencher's process of forming the curtain of water. The water spray reaches a height of around 27m above the ground about two seconds after the water is discharged. It then descends and, about five seconds later, the curtain of water is formed, and a dynamic steady state is reached. We tracked the behavior of the moving fire debris in this state. The simulation result showed that five seconds after the fire debris reached the curtain of water, almost all of it was blocked by the curtain of water and did not reach the building. Fig. 8 shows the results of the MPS-DEM coupling analysis of the fire debris. In the simulation, some debris from the fire reached the vicinity of the building. But the actual fire was extinguished by the water flow, so the drencher's fire extinguishing effect is deemed to be good enough. The final number of particles in this calculation was about 2 million and it took about 230 hours using an NVIDIA GV100 GPU board. In fact, further reduction of calculation time is possible by using the multi-GPU calculation capability in Particleworks.

Simulation of a firefighting drone

Research and development of firefighting drones for high-rise buildings is currently underway, some of which have reached the practical stage. This drone firefighting activity also considers the effects of wind, whether the drone can be guided to its desired destination without damaging valuable buildings, and whether a limited amount of firefighting agent can accurately reach the target. Here, we used a five-story pagoda as the model of a high-rise building, simulating the process of a drone approaching the top floor and spraying the fire extinguishing agent.

The five-story pagoda is about 31m high, and the drone has a diameter of about 1.5m. An inlet with a diameter of 60mm was defined for the nozzle at the tip from which the extinguishing agent was sprayed. The simulation assumed that the drone would rise from the ground to the height of the top floor (18m) in ten seconds, and that the fire extinguishing agent would be sprayed at rate of 30m/s immediately after the drone rose. When a liquid fire extinguishing agent is used, the drone reaches the top floor (18m) in ten seconds. However, since the use of liquid fire extinguishing agents can damage wooden structures, we used DEM to model a powder-based fire extinguishing agent that is believed to cause less damage to wooden structures. A coarse-grained model was used to reduce the computational load, and the particle diameter was set to 6mm.

Fig. 9 shows the result of the simulation and the reach of the extinguishing agent from the drone. It was evaluated in windless conditions, but the extinguishing agent's trajectory in the presence of wind can be tracked like that of the water in the example described above. Furthermore, by linking to the motion dynamics simulation, it is possible to configure more realistic conditions in which the drone flies and fights fire under the influence of wind. In this simulation, the number of DEM particles was about 90,000, and the calculation time using GeForce TITAN X was 46 hours.

This article discussed the use of Particleworks and Granuleworks to simulate fire extinguishing activities to protect important architectural buildings from fire. MPS and DEM can handle not only industrial products such as the water discharge equipment and drones discussed here, but also those used for disaster prevention in floods, tsunamis, and landslides, and in a wide range of environmental issues such as clean energy fields, which are of increasing concern in the world today. I hope that simulation technology will be used wherever possible to help protect our heritage, traditions, and culture and to realize a safe and comfortable future for everyone.

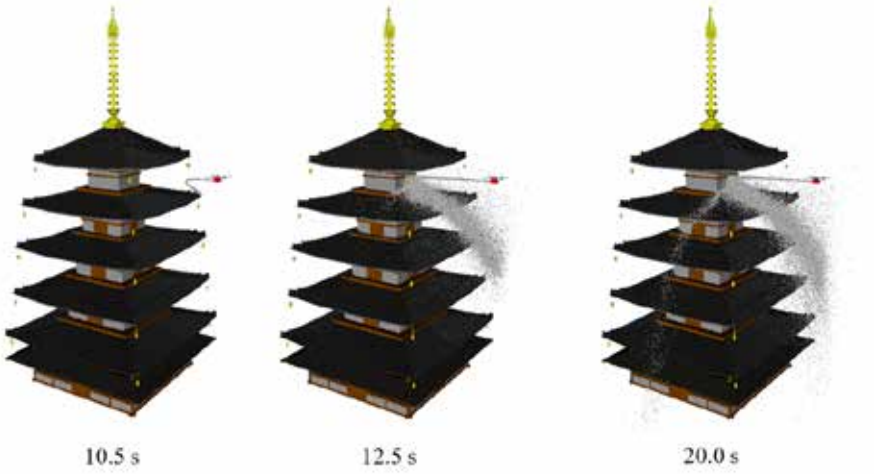

Fig. 9. Simulation of fighting a fire on the upper floors of a wooden high-rise building with a drone.

References

[1] S. Koshizuka, K. Shibata, M. Kondo, T. Matsunaga, "Moving particle Semi-implicit Method", Academic Press, ELSEVIER, 2018

[2] P.A. Cundall, O.D.L. Strack, "A discrete numerical model for granular assemblies", *Geotechnique* 29, No.1, 1979, 47-65

[3] The conference proceedings of the Japanese Society of Computational Engineering and Science, 2021

Article from:
EnginSoft Newsletter Year 18 n.2
Summer 2021

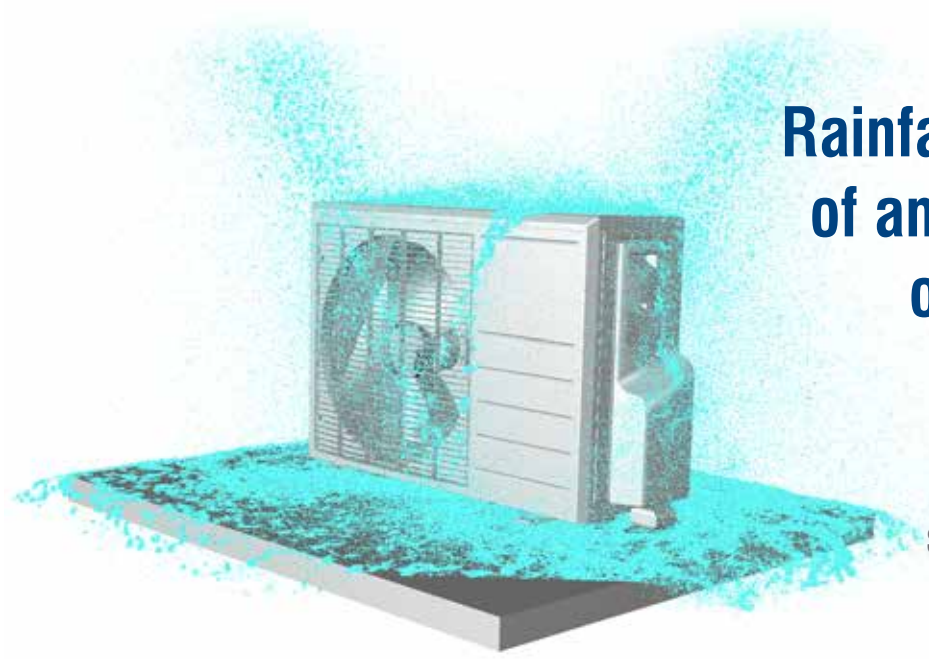

Rainfall test simulation of an air conditioner's outdoor unit using Particleworks

By Indraneel Samanta[1], Sunao Tokura[2] and Akiko Kondoh[2]
1. R&D, BlueStar Ltd.
2. Prometech Software, Inc.

Today, many outdoor installations of electrical appliances are increasingly exposed to extreme weather patterns, particularly torrential rainfall, resulting from climate change. Typically, these appliances undergo a rain test during design to determine the potential for water penetration and damage to important internal components. However, these tests usually do not reveal where the water penetration occurs. Numerical simulation can predict rainwater penetration and its penetration path to inform relevant design changes and waterproofing measures for improved product performance. Such studies represent complex free-surface phenomenon simulations for which Particleworks is particularly well-suited. This article presents the simulation of rainfall on the outdoor unit of an air conditioner as a concrete example of this approach.

Many electrical appliances around the world are installed outdoors where they are continuously exposed to the elements. In designing these appliances, a rain test is performed in a shower to evaluate the effectiveness of the waterproofing and to examine the possibility of water penetration and damage to important internal components.

However, while these tests can determine whether water has penetrated the product, it is not easy to determine where it entered. In order to develop these products more efficiently, numerical simulation can be used to predict the intrusion of rainwater and its path into the product so that appropriate design changes can be made and waterproofing measures can be taken before prototyping to improve product performance.

Rainfall or the flow of agglomerated raindrops on a product represent a complex free-surface phenomenon. Particleworks, a particle-based computational fluid dynamics (CFD) software that can efficiently process water droplet behavior and free-surfaces, is well suited to simulating such problems.

In this article, we will introduce a simulation of precipitation on the outdoor unit of an air conditioner as a concrete example of dealing with such a problem. Initially, the problem was posed as a challenge by the manufacturer, Blue Star Limited in India, where it often rains heavily. In recent years, torrential rains, which are considered to be an abnormal weather condition resulting from climate change, have occurred every year in many parts of the world. As a result, appliances installed outdoors need to be more waterproof than ever before.

These waterproofing measures extend the life of the product by preventing critical electronic components from being exposed to water, compromising product functionality and also prevent corrosion of internal components if they are exposed to water. For outdoor units, this includes reducing the ingress of water through the large front grille openings used to control airflow as much as possible. Numerical simulations play an important role in detailing the behavior of these raindrops, identifying the path of water penetration into the product, and using this information for waterproofing measures.

Fig. 1. Rainfall test.

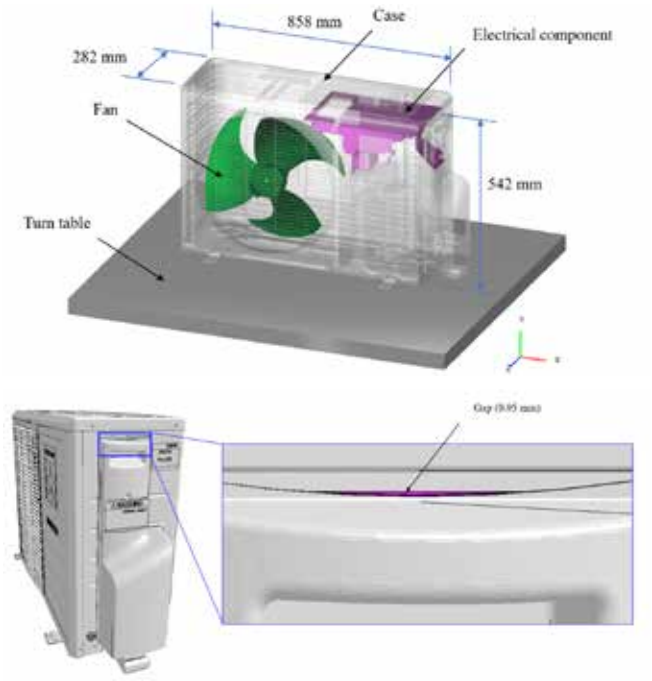

Fig. 2. Geometry of the simulation model.

Fig. 1 shows the actual precipitation test. Assuming torrential rain, the amount of rainfall is set to 80mm per hour. The turntable on which the product is placed rotates slowly, allowing raindrops to hit the product from all directions, while two blowers behind the test chamber constantly blow strongly. Fig. 2 shows the model geometry prepared to evaluate the product by simulation under these conditions.

Overall, the dimensions of the product are approximately 860mm wide, 540mm high, and 280mm deep. Although the actual product is composed of many components, the simulation models only the major components that affect raindrop behavior: enclosure, fans, turntables, and electronic components to be assessed for water damage.

Particleworks does not require meshing and the CAD data itself can be used directly for simulation, so there is no need to spend a lot of time on pre-processing. Importantly, the product has a small gap above the handle through which raindrops may enter. The width of the opening is only 0.95mm, but since it is close to the electronic components, the possibility of raindrops entering from here cannot be ignored.

The water sprinkling from the shower was set as an analysis condition. In the test, three rows of showerheads were installed at a height of about 2 meters from the product. However, only the water from two rows of showerheads had an effect, so eight showerheads were modelled for the two rows that would be needed for the simulation.

In Particleworks, we created an inlet above the showerheads and set a flow rate of 80mm per hour, similar to the test. Considering the precipitation and the area of the sprinkler holes, we defined the flow velocity as 2,000mm/s. As boundary conditions, the fan speed inside the outdoor unit was set to 3,600rpm, and the turntable speed was set to 2.3rpm, estimated from the test video.

We also had to consider the effect of airflow. In order to reproduce the actual rainfall test, we had to consider the effects of the airflow generated by the fan and its rotation on the trajectory of the raindrops inside the outdoor unit. Such an airflow field can be obtained by modelling the air around the outdoor unit with particles, but this is not efficient in practice due to the large number of particles.

In this study, the results of the airflow field calculated by general CFD software were imported into Particleworks as a set of spatial coordinates and velocity vectors in .csv format, and the airflow field was examined as shown in Fig. 3. This airflow field can be used to calculate the state of the raindrops under the influence of wind as a so-called one-way coupling simulation.

The water falling on the entire outdoor unit of the air conditioner was modelled with 2mm diameter particles for practical reasons of calculation time. However, this model geometry has a 0.95mm gap above the handle, so a smaller particle size had to be set to model the particles passing through this gap.

Particleworks provides a feature called “zooming” that allows the spatial resolution, or particle size, of certain areas within the analysis space to be fine-tuned. The zooming function is also intended to reduce the computational load. As shown in Fig. 4, in this simulation,

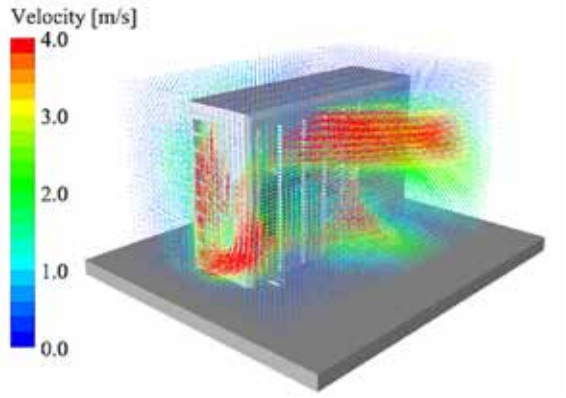

Fig. 3. Air-flow field inside and outside the outdoor unit.

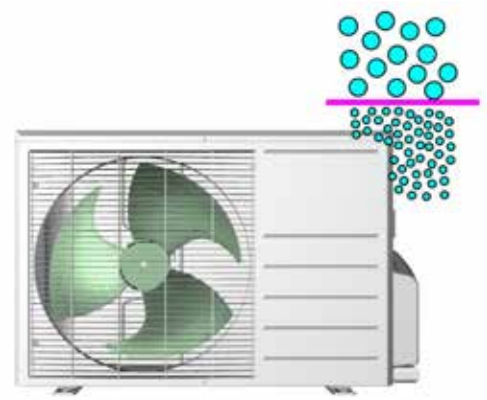

Fig. 4. Zooming function to fine-tune the particle size.

Fig. 5. Comparison between the test and simulation results.

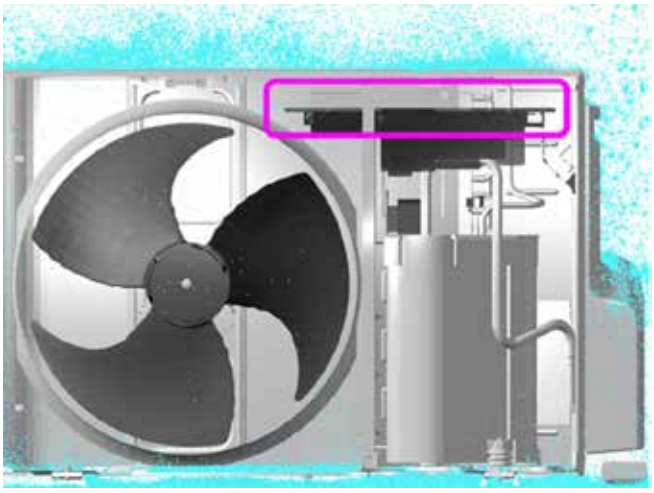

Fig. 6. Raindrops in the outdoor unit.

a single particle with a diameter of 2mm that reaches the vicinity of the gap is replaced with approximately 500 particles with a diameter of 0.25mm, and a high-resolution calculation without partial increase in the number of particles in the entire analysis space is performed.

Fig. 5 shows the simulation results. Water was sprinkled from the eight showerheads and fell onto the outdoor unit. The test confirmed that the surface of the electronic component box was covered with water. The simulation also shows that water droplets adhere to the box.

As shown in Fig. 6, the raindrops that penetrated the outdoor unit reached the top of the electronic component box and flowed through. Using the post-processing function, it is possible to visualize the infiltration path of the raindrops more clearly by plotting the streamlines of the raindrop particles that reached the top of the electronic component box (Fig. 7).

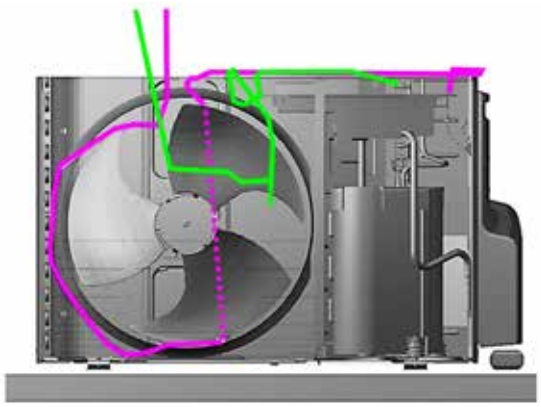

Fig. 7. Plotting the streamlines of the main paths of the raindrop particles entering the unit.

Here, we plotted the streamlines of several particles and found that there are two major infiltration paths. One is the path shown by the green line, where particles entering the enclosure through the front grille hit the rotating fan blades and are blown away towards the top of the electronics box. The other is the path indicated by the pink line, where the fan's airflow also blows particles entering through the grille up towards the electronics.

Next, we focused on the behavior of the raindrops around the small gap. As mentioned earlier, we used the zooming function here to create particles with a 0.25mm diameter. Looking at the aperture from the inside, we could see that raindrops were entering through the gap, as shown in Fig. 8.

Therefore, the ability to visualize the ingress path of the raindrops, which is difficult to observe in the actual test, is a great advantage of simulation.

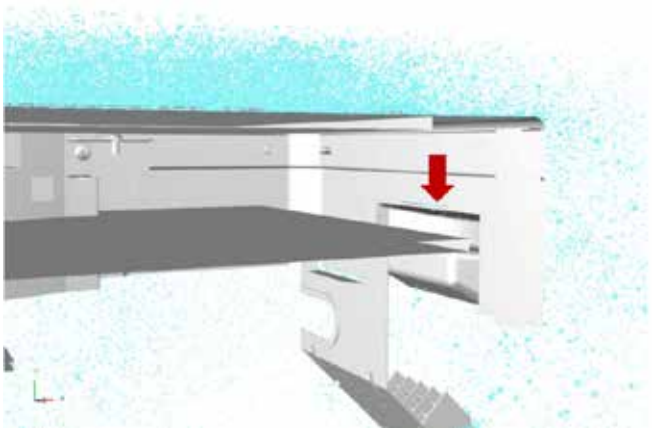

Fig. 8. Raindrops entering through the gap.

As mentioned earlier, it is not easy to identify the path of water penetration into the product simply by testing the actual product and then applying waterproofing and water damage countermeasures in the early stages of design.

Fluid simulation with Particleworks can be applied to the design and development of various home appliances to apply waterproofing and water damage countermeasures more accurately and efficiently.

The simulation presented in this paper uses the 3D CAD data of the outdoor unit of an air conditioner, actual test results, and photographs provided by Blue Star (India). This study was also presented at the International CAE Conference held in November 2020.

Article from:
EnginSoft Newsletter Year 18 n.1 - Spring 2021

Reference: Presentation material of Particleworks topics seminar2019 organized by Prometech Software, Inc.

Testing Particleworks coupled with RecurDyn to simulate water behaviour in water technology products

By Chiaki Miyazawa[1] and Akiko Kondoh[2]
1. LIXIL Corporation - 2. Prometech Software

One of the important lines of business for LIXIL Corporation, Japan's largest building and equipment manufacturer, are water technology products, such as baths, kitchens and toilets. LIXIL is trying to introduce Particleworks, a meshless multiparticle simulation (MPS) computational fluid dynamics (CFD) tool into the research and development of these products.

Dr. Miyazawa of LIXIL's Advanced Core Technology Division explains: "I am mainly in charge of digital technology fields such as CFD simulation and virtual reality (VR). Previously, we largely focused on airflow analysis using a finite volume method (FVM) simulation tool that was effective for airflow evaluation even when toilet water flow analysis was necessary. However, since FVM requires a lot of computational resources, when it became necessary to evaluate many small droplets, such as for showers, I started looking for a suitable tool. This was when I found Particleworks, which was introduced with the keywords "liquid splashing" and "mixing".
So, I started a trial of Particleworks. Currently, we are verifying the reproducibility of shower toilets and showerheads, water splashing phenomena in kitchens, and kitchen sink flow behaviour and have already begun using prototypes for research."

Simulation of a shower head

First example of RecurDyn-Particleworks coupling

LIXIL's "Ecoful Shower" shower head product (Fig. 1) consists of a structure in which the impeller incorporated in the shower head rotates at high speed and blocks half of the shower holes. This mechanism increases the pressure inside the shower head, producing a regular shower sensation for the user, however the water consumption is 48% lower than that of the conventional water volume (10L/minute).

Besides conserving water, it is also important to optimize the water pressure and the size of the water drops to improve comfort. Particleworks was used for these evaluations.

In this shower head mechanism, the impeller rotates due to the water flow, and the number of rotations changes according to the flow velocity. Since Particleworks itself only provides a constant rotation speed regardless of the water flow, we used a coupled simulation with the multi-body dynamics simulation software RecurDyn to confirm the effects of both stable rotation speed and rotation changes.

The results of the fluid behaviour simulation were generally good because they met LIXIL's guidelines compared to the measured values. The rotation speed of the impeller gradually increased at first, decreased gradually after reaching the peak, and finally stabilized. The transition states obtained by simulation were roughly consistent with the measured values.

Regarding the internal pressure of the shower head, we verified that the results almost matched the measured values. The size of the particles was measured with a high-speed camera, and the difference from the calculated value was also within the company's guidelines. Overall, it was evaluated as a good result for a shower head simulation.

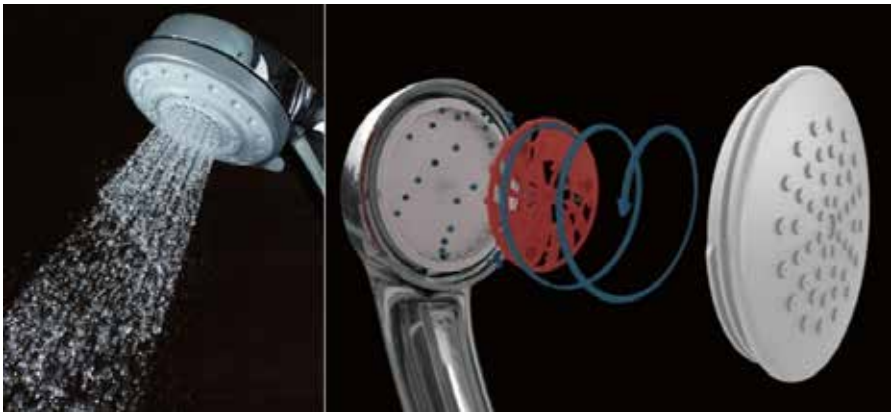

Fig. 1. Ecoful Shower – The red impeller rotates at high speed blocking half the shower holes.

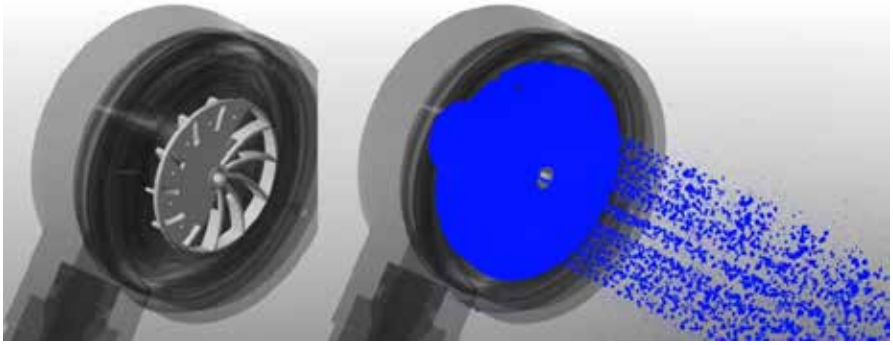

Fig. 2. Simulation of the shower head.

Simulation of waste flushing from kitchen sink

Second example of RecurDyn-Particleworks coupling

Kitchens are easier to use if they are easier to clean. To achieve this, it must be easier to flush dirt and waste to the bottom of the sink and to clean it away efficiently.

LIXIL's new product introduced the "Niagara Flow Type", where the bottom of the sink slopes more from the left and right edges, preventing water from spreading and flowing smoothly towards down.

This allows for efficient drainage from anywhere in the sink. Particleworks was used to evaluate how effective the new shape is. The kitchen sink design was evaluated in tests based on a very large number of assumptions, including how to flush waste.

In the Particleworks simulation, we first tried to reproduce how easily it was for regularly spaced waste to flow. The analysis currently being performed checks how the waste placed at equal intervals flows. Instead of performing detailed settings by coupling Particleworks with RecurDyn, as was done in the shower head simulation, the water supply conditions were set using the Particleworks function.

Initial simulations showed that the water flowed faster, slipped more, and spread less compared to the test. The waste was also flowing unnaturally. Therefore, a test was conducted on a simple shape to obtain

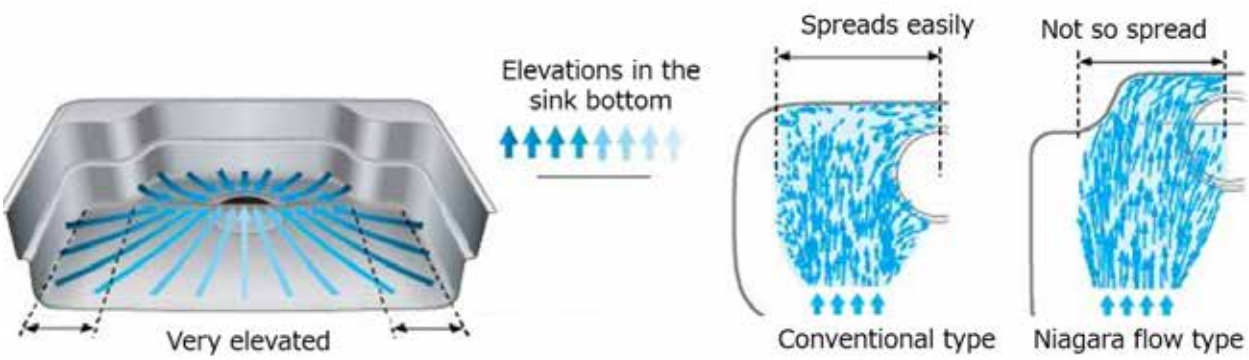

Fig. 3. Difference between a Niagara Flow Type and a conventional type of sink shape.

parameters by associating the test results with the simulation results. In actual phenomena, a film of water penetrates under the waste and surrounds it making the waste slippery.

In the Particleworks calculations, particles didn't penetrate below the waste as easily in the first trial. This was solved by making the particles smaller. However, this required a lot of computational resources.

To reduce the computational load and shorten the simulation times to less than a day, it was necessary to enlarge the particles to some extent. However, this caused some differences from the actual phenomenon. Therefore, several attempts were made to adjust the frictional force parameters to approximate the behaviour of the particles.

Regarding the definition of the frictional force, it was found that it was easier to adjust the parameters by setting the waste with polygons in RecurDyn, so a simulation was performed coupling Particleworks with RecurDyn.

Next, the frictional force and particle shape were defined to prevent the waste from moving before the water supply. A correlation was made by adjusting the frictional force and the transition speed.

Through trial and error, the reproduction of water spread and the behaviour of the waste were improved compared to the first simulation, and could also be improved compared to the actual test.

Although the final result for this simulation has not been obtained, LIXIL continues to try to simulate through trial and error.

Dr. Miyazawa said, "The Particleworks features are a great advantage because they allowed the behaviour of the shower and the internal impellers to be easily reproduced."

Article from:
EnginSoft Newsletter Year 17 n.2
Summer 2020

Fig. 4. Water flow simulation for conventional type (left) and Niagara Flow Type (right) holes.

About LIXIL Corporation

LIXIL Corporation is the largest building materials and equipment manufacturer in Japan, offering a wide range of high-quality products that support people's lives and living with world-leading technologies and innovations based on the Japanese manufacturing tradition. LIXIL's products are used by over 1 billion people in more than 150 countries around the world. One of LIXIL's main businesses is water technology. It provides water-related products such as baths, kitchens, and toilets.

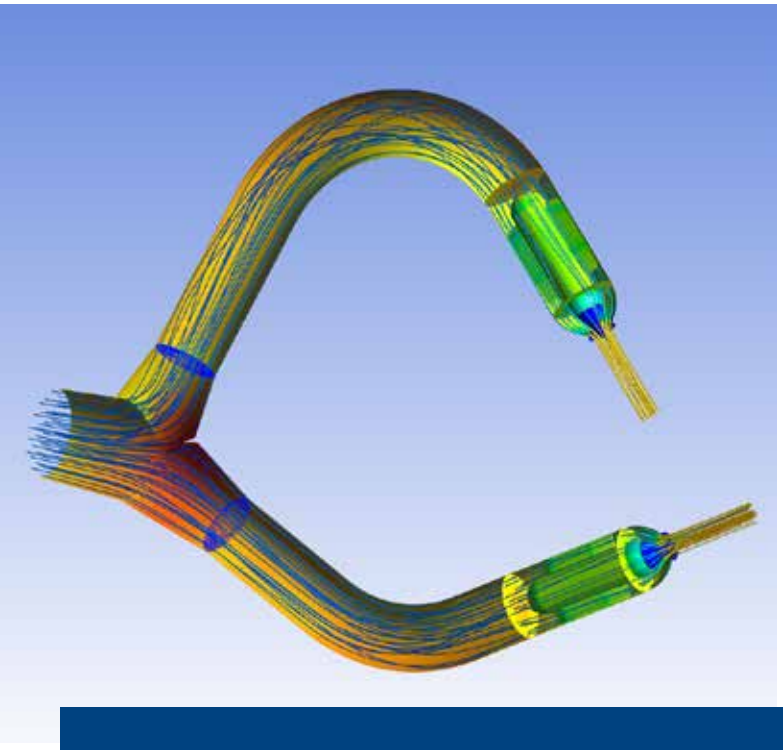

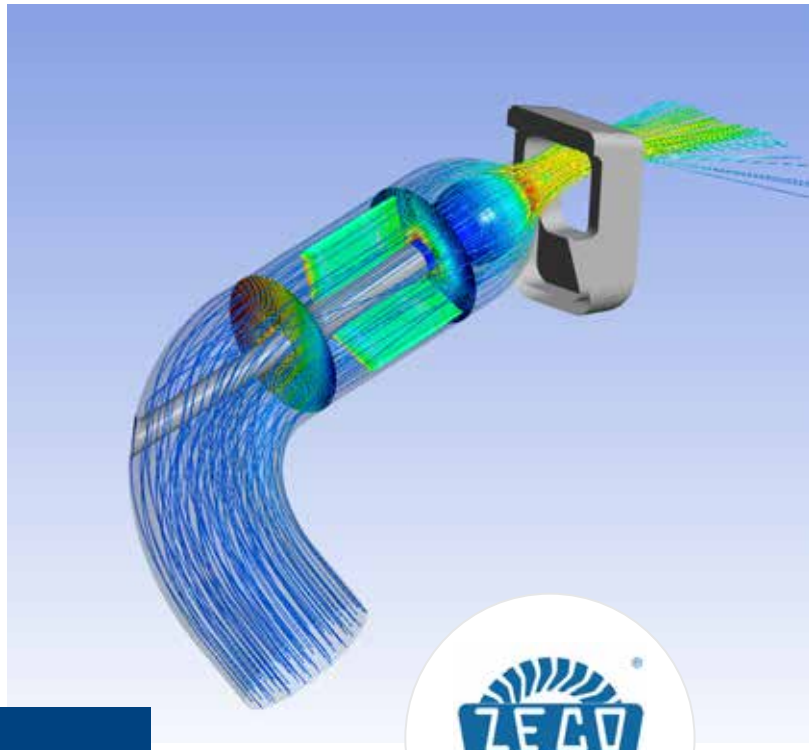

CFD study of a Pelton turbine runner

Comparison between traditional Eulerian and novel Lagrangian approaches

By M. Minozzo[1], R. Bergamin[1], M. Merelli[2], M. Galbiati[2]
1. ZECO - 2. EnginSoft

Hydroelectric power generation is currently the predominant source for low-carbon power generation and to support grid stability in the face of the growing use of other unpredictable, renewable energy sources. This means that water turbines are becoming the focus of increased study and optimization. This technical article, a collaboration between EnginSoft and ZECO, compares two different methodologies for the study and optimization of impulse turbines, specifically Pelton turbines, in order to evaluate which is the quicker and more reliable method. Pelton impulse turbines are more difficult and challenging to analyze than reaction turbines due to the complexity of their fluid dynamics and the resulting computational resources required for the necessary transient multiphase simulation. The unsustainably high time and computing requirements mean that there are some technical deficiencies in sector knowledge about specific elements of these turbines and their functioning, such as the inside of the water jet. Two methods were evaluated: the traditional Eulerian approach and a novel Lagrangian approach using Moving Particle Simulation (MPS). The novel MPS approach proved to save considerable time and revealed information not discovered before, opening up new possibilities for optimizing these turbines.

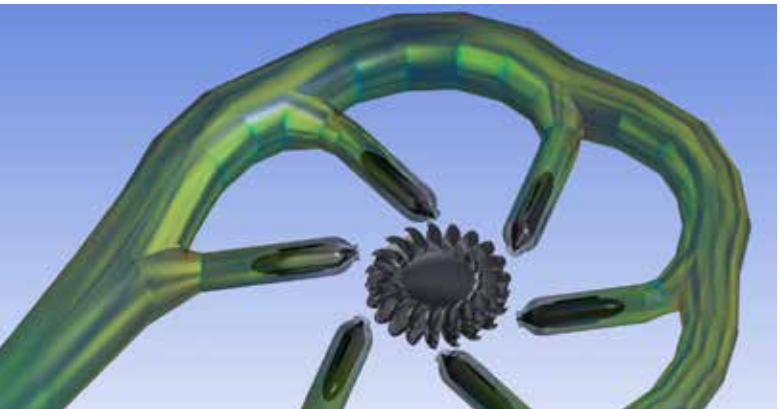

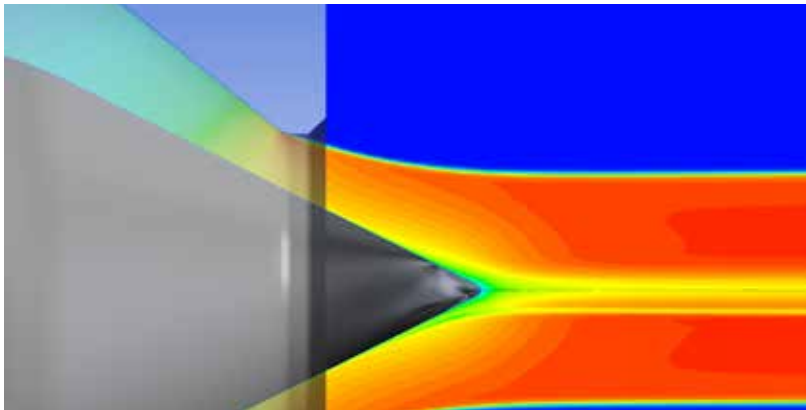

Hydroelectric power generation is a crucial source of electricity, accounting for 44% (IEA, 2020) of global low-carbon power generation. Its leading role is expected to be consolidated, as it becomes reinforced by developing countries and by the growing awareness of climate change. In addition, the renovation or repowering of old power plants is crucial for greener power production and to support grid stability, considering the growing use of unpredictable renewable energy sources, such as wind and solar.

The combination of these factors will increase the need to study and optimize water turbines under different conditions, not only at nominal design points. The standard Eulerian computational fluid dynamics (CFD) approach has been extensively tested and validated for reaction turbines such as Kaplan and Francis turbines.

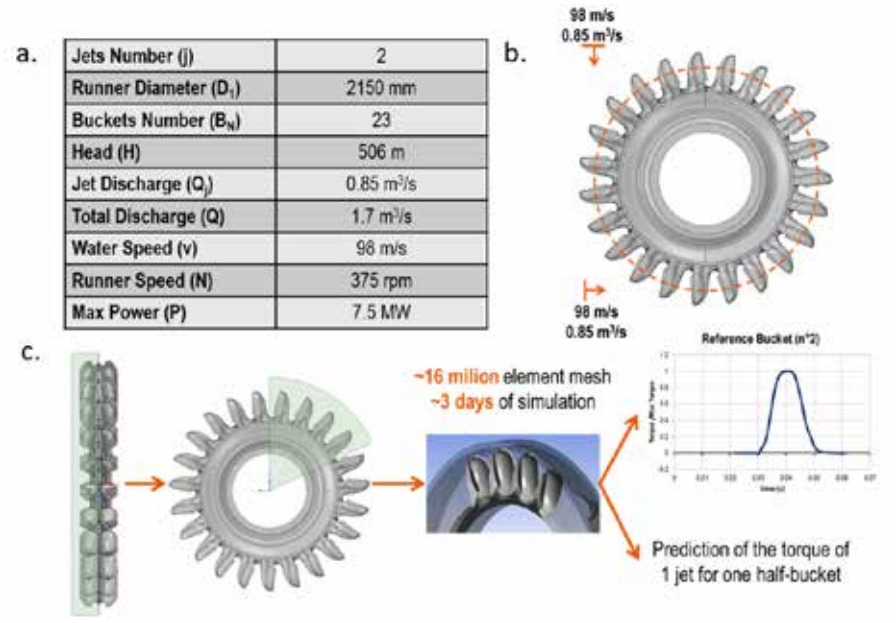

Jets Number (j)	2
Runner Diameter (D_1)	2150 mm
Buckets Number (B_N)	23
Head (H)	506 m
Jet Discharge (Q_j)	0.85 m³/s
Total Discharge (Q)	1.7 m³/s
Water Speed (v)	98 m/s
Runner Speed (N)	375 rpm
Max Power (P)	7.5 MW

Fig. 1 - a) Summary table with details on the presented benchmark; b) Boundary conditions and geometry included in Particleworks (Lagrangian model), where no geometry modification was performed; c) Diagram of the geometry simplification necessary in CFX (Eulerian model) – the turbine is reduced using symmetry (sectors in green), the simulation is run, and the half-bucket profile is extracted.

It is already standard practice to optimize their hydraulic design due to the limited computing resources required. Impulse turbines, such as Pelton turbines, have also been continuously studied using CFD [1], [2], [3], [4].

These studies usually focus on predicting the efficiency of the buckets and on the fluid behaviour of the water entering and leaving the individual buckets, in order to understand how the bucket geometry influences the performance of the machine.
However, compared to reaction turbines, Pelton analysis is much more complex and demanding, both because of the fluid-dynamic complexity of the jet diffusion, and the computational resources required for transient multiphase simulation.

The lack of knowledge about the inside of the water jet – as a result of the unsustainable time and computing resources required – is a technical deficiency that needs to be addressed. For these reasons, ZECO partnered with EnginSoft to investigate a new methodology to quickly and reliably conduct CFD simulations for Pelton turbines.

This article discusses the differences between a turbine runner simulation using a classic CFD (Eulerian) approach and a Moving Particle Simulation (MPS) (Lagrangian) approach. The test case presented is the analysis of a two jets horizontal shaft Pelton turbine. The project data is shown in Fig. 1b.

Conventional CFX (Eulerian) approach

From a hydraulic point of view, the Pelton turbine consists of a water inlet pipe or penstock, from 1 to 6 nozzles, and a runner. The manifold is a pipe, branched into up to six deviations, that leads water to the injector nozzle. The nozzle consists of a needle, which acts as an opening valve, and a water flow regulator that releases the flow in a free jet that impinges on the runner.
From a fluid-dynamic point of view, manifolds and nozzles are quite simple to study as they are either channeled flows or two-phase flows with a jet in the air in a limited and static portion of the volume [5], [3]. Instead, studies of runners involve greater challenges, due to the complex nature of the free-surface flow to be modelled. A Eulerian multiphase analysis of a complete turbine is time consuming and limited by the computational power requirements due to the complexity of the geometry and the simulation. To conduct a feasible Eulerian CFD analysis, the following assumptions establish the best practice for a traditional CFD simulation (see Fig. 1a):

- Reduction of the geometry using symmetry
- Reduction in the number of buckets analysed, down to a minimum of three
- Creation of a domain (a statoric-rotoric for the inlet boundary condition and the rotating runner).

This enables the torque of a half bucket to be simulated and calculated for the full duration of the action of a single jet.

From there, it is necessary to work backwards to reconstruct the torque for the entire turbine. In other words, starting from the torque produced by a single jet in a half bucket, the torque must be doubled to calculate the torque of the whole bucket. The complete time history of the turbine runner's action is reconstructed manually to yield the total torque and its average value (see Fig. 3).

Using the planes of symmetry, it is possible to visually reconstruct the interaction of the jet with the bucket to better visualize the interaction between the two. This approach accurately estimates the power and therefore the performance of the machine and the hydraulic behaviour of a bucket. However, it is obvious that some issues remain unresolved because some hypotheses do not always apply. In addition, jet-jet and jet-casing interactions are totally excluded

from this CFD approach, as the simulations required to analyze these phenomena are unfeasible in an industrial R&D workflow.

Advantages of the MPS methodology

Particleworks uses a Moving Particle Simulation (MPS), a CFD approach in which the fluid is discretized into particles (computational fluid volumes). The Navier-Stokes equations are solved on these particles using a Lagrangian approach which does not require the mesh-generation step, as the fluid has already been discretized. This allows for rapid model preparation and poses no additional problems when moving/rotating domains or wall boundaries are considered.

Typically, software based on this methodology is widely used in the automotive industry, where gearboxes, electronic axles and transmissions are simulated in whole-simulation systems. Other types of applications are soiling, mixing tanks and cleaning-jet analysis. In fact, thanks to its Lagrangian approach, Particleworks is ideal for the study of complex, free-surface flows. In this article, we present another interesting possible application: using MPS to improve product properties and design.

As mentioned, preparing and reducing the geometry slows the simulation time and limits the amount of information that can be extracted from the simulation. On the contrary, thanks to the characteristics of the MPS method, the preparation phases and times are considerably reduced. In fact, the geometry provided by ZECO only needed to be converted to a compatible format for Particleworks (Fig. 1c). It was possible to import the entire turbine without the splitting or meshing steps. After setting the numerical and boundary conditions, the simulation was ready to run. The simulation process was further accelerated by the possibility of parallel processing, enabled by the graphics processing unit (GPU) solver. In addition, it can be seen that the extraction of the torque prediction was easier and did not require the time-consuming profile reconstruction steps.

Just like in conventional CFD, computed results improve with smaller mesh features, at the cost of longer simulation times. In general, you can observe a convergence for better, theoretically expected results. In Particleworks, this type of analysis is performed by changing the particle size, i.e. the dimension of the computational volume. In this way, a solution can be found independent of the simulation settings and the discretization of the fluid volume.

We performed several simulations with particle sizes of 10, 5, and 2mm. To quantitatively analyze the results, we extracted the torque on the turbine and plotted it over time. As can be seen, the torque prediction graph becomes smoother and converges into values closer to the theoretical value (Fig. 2).

To further validate the simulation results obtained using Particleworks, we compared them to the CFX simulation results. As can be seen from Fig. 3, both software packages overestimated the overall efficiency of the Pelton runner by the same percentage. The difference between the two approaches is negligible and simulations within a 1% error margin can be considered an excellent result considering the literature in this field ([2], [6], [7]).

MPS not only achieves qualitatively comparable results to traditional CFD, it does so in less time. Because it can simulate the entire turbine, it also provides design information about long-range runner-water interactions. This makes it possible to analyze the effect of residual water in otherwise active buckets, or other undesirable interactions between the water and the turbine. In addition, the optimization of the casing can be accomplished with the same simulation.

Another type of analysis that is usually performed in this sector is the evaluation of the static mechanical stresses on the turbine

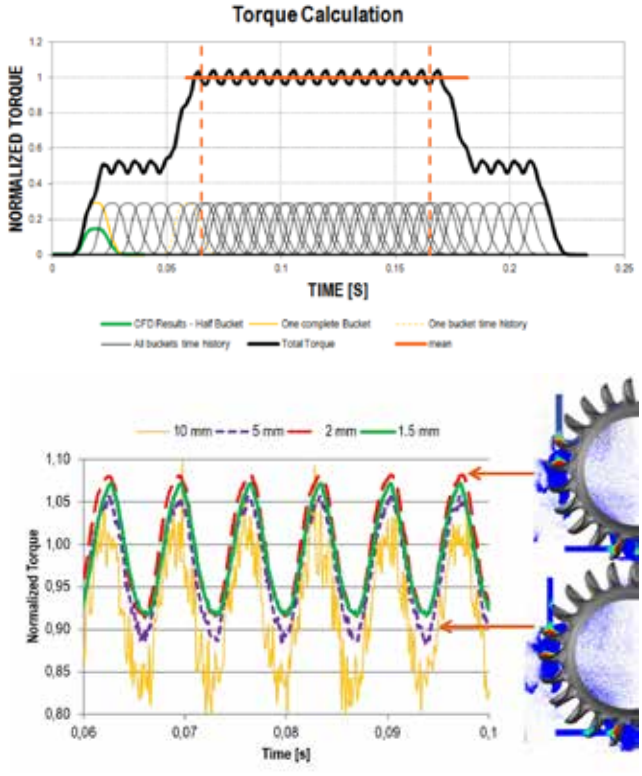

Fig. 2. Top: Normalized torque predicted by CFX – the average value is obtained after reconstruction of the turbine profile from an initial half-bucket profile; Bottom: Normalized torque based on the configuration of the entire turbine – the minima and maxima can be related to specific jet-turbine interactions (on the right).

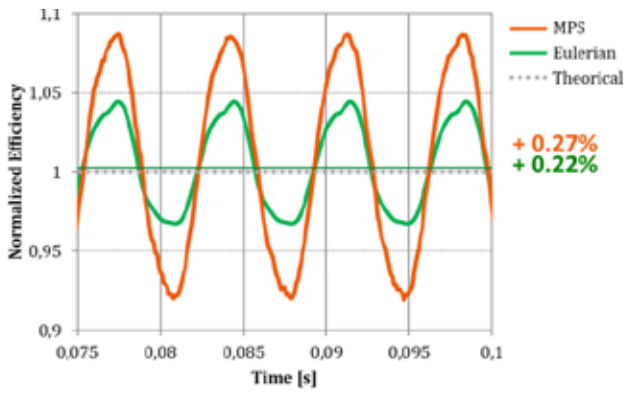

Fig. 3. Normalized efficiency prediction for Particleworks (in orange) and CFX (in green). The percentage of error is reported at the side. The theoretical mean values are also reported (dashed, black line).

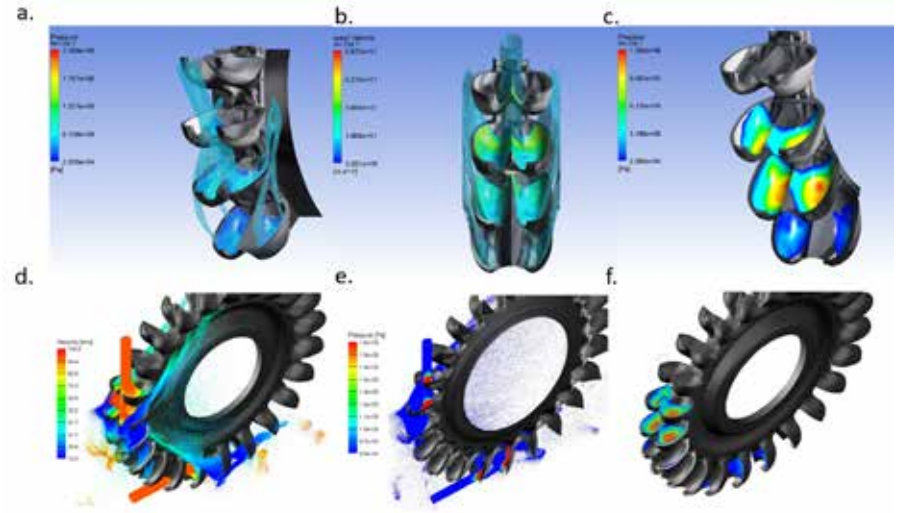

Fig. 4. a) and b) Images of the reconstructed surface (using the mirror plane) of the water jet for CFX (Eulerian method) – the velocity and pressure profiles are mapped on the Pelton bucket; c) Reconstruction of the pressure profile on the runner bucket (Eulerian method); d) and e) Images of the two water jets simulated with Particleworks (Lagrangian method) – the colour map represents the predicted velocity and pressure; f) Mapping of the turbine pressure profile – Ansys Workbench allows direct data transfer of the profile to the finite element method (FEM) solver.

buckets. In CFX, due to the division of the simulated domain, remapping the pressure from the data of only the half bucket is time consuming. On the other hand, due to Particleworks' integration with Ansys Workbench, data transfer to an FEM solver is simple(see Fig. 4c).

To summarize the comparison between the Particleworks (Lagrangian) and the CFX (Eulerian) approaches, the simulation steps and their related time-costs are presented in Table 1.

As can be seen, Particleworks enables a significantly faster and easier simulation procedure. Since time is crucial in industrial applications, simulation times can be the bottle neck that block the development and investigation of new products. Various applications are not studied with CFD because of the complexity of the simulation steps. Particleworks can both accelerate the development of products that have already been studied, and pave the way for new studies and optimizations.

Conclusions

This article has analysed the outstanding issues with and the possibilities of simulating a Pelton turbine runner using CFD. The traditional Eulerian, mesh-based approach was compared to the MPS method.

We found that the qualitative results obtained are comparable and in good agreement with the theoretical values. The Eulerian approach, however, obtained this result through a complex definition and simplification of the model, requiring a considerable amount of simulation and working time.

On the contrary, MPS can easily simulate the entire runner and the estimated workflow should only take 2-3 days. Moreover, the MPS method, from the same simulation, provides additional information never before investigated.

For instance, it provides insights into the jet-jet influence and the long-term jet-runner interactions. Those observables, together with the considerable acceleration in simulation time, open up new product optimization possibilities in the field of Pelton turbines.

	CFX	PARTICLEWORKS
Pre / Post Processing	3 working days / 4h	2h / 1h
Simulation time	70h	2h
Simulated rotation (°)	138°	225°
Geometry	4 half buckets	Complete turbine
Complete runner simulation (multi jet, casing…)	Not feasible	Possible
Mesh elements/particles	16M	4M
Hardware	12 CPU (Intel Xeon X5650 @2.67GHz 96GB RAM)	1 CPU + 1 GPU (NVIDIA V100)
Calculated vs model efficiency (absolute)	+0.22%	+0.27%

Table 1. Summary comparison between the two approaches analysed, highlighting working and simulation times, geometrical assumptions and hardware settings.

References

[1] K Patel, B Patel, M Yadav, and T Foggia. Development of Pelton turbine using numerical simulation. In IOP conference series: *Earth and Environmental Science*, volume 12, page 012048. IOP Publishing, 2010.

[2] Zh. Zhang. *Pelton Turbines*. 2016.

[3] D. Jo˘st, P. Me˘znar, and A. Lipej. "Numerical prediction of Pelton turbine efficiency. 25th IAHR Symposium on Hydraulic Machinery and Systems", 2010.

[4] V. Gupta, V. Prasad, and R. Khare. "Numerical simulation of six jet Pelton turbine model". *Energy*, 104:24–32, 2016.

[5] J. Zhang, Y. X. Xiao, J. Q. Wang, X. J. Zhou, M. Xia, C. J. Zeng, S. H. Wang, and Z. W. Wang. "Optimal design of a Pelton turbine nozzle via 3D numerical simulation". Asian Working Group - IAHR's Symposium on Hydraulic Machinery and Systems, 2018.

[6] T. Kumashiro, H. Fukuhara, and K. Tani. "Unsteady CFD simulation for bucket design optimization of Pelton turbine runner". 28th IAHR symposium on Hydraulic Machinery and Systems, 2016.

Article from:
EnginSoft Newsletter Year 17 n.1
Spring 2020

Refining the design of a spout for a laundry detergent

Particleworks enables fluid flow simulation combined with human-like behavior to improve product performance

By Nobuhito Nakagawa[1], Taishi Nakamura[1] and Akiko Kondoh[2]
1. Lion Corporation - 2. Prometech Software, Inc.

LION Corporation produces health care products such as toothpaste, detergent, soap, etc. The company, which has a long 120-year history, faces a rapidly-changing business environment due to the recent phenomena of an aging society, rising health awareness, and technological demands that affect the planning and development of products and services using digital engineering.

LION's Container and Packaging Engineering Research Laboratories is responsible for designing and developing containers and packaging for all LION products and has used CAE simulation for over 30 years. Their use of CAE is increasing year by year due to business acceleration and diversification. In the past, during conventional product development, the company used a 3D printer to make nearly 100 prototypes of a spout cap design, from which they chose the most suitable design.

This time, with the desire to more scientifically verify the designs, with Prometech's cooperation, the company decided to use fluid dynamics simulation with Particleworks, in addition to the 3D printer experiments, for the design of the cap for the new HARETA brand, launched in 2018.

The concept of HARETA is that it always leaves clothing feeling like it has been air dried on a clear day. The detergent has a non-Newtonian viscosity meaning that the liquid tends to be less viscous during the pouring process. Generally, users want to pour the measured dose as quickly as possible, so they unconsciously raise their elbows and tilt the bottle to pour the detergent more quickly. This tendency becomes stronger with high viscosity liquids. This results in the spout becoming

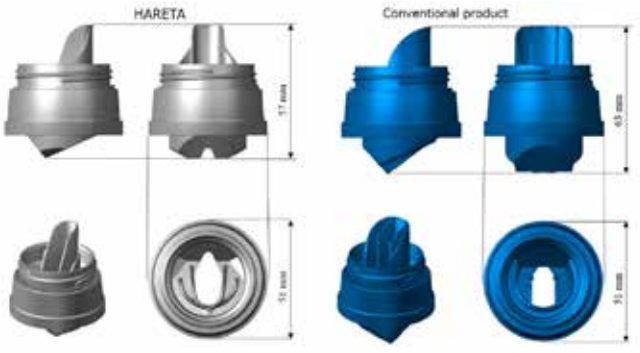

Fig. 1. Comparison of spout cap design for HARETA and a conventional product.

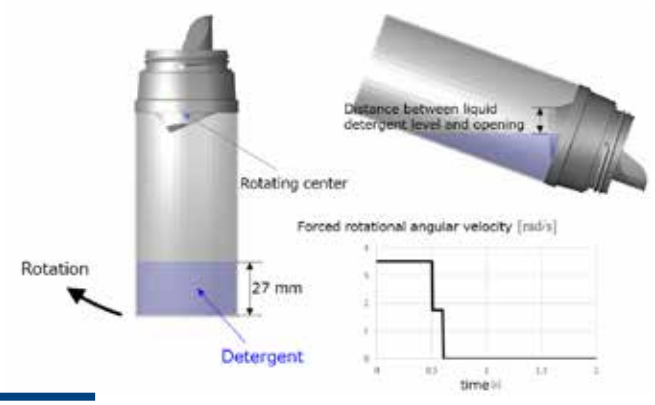

Fig. 2. Settings of detergent amount and definition of the forced rotation.

blocked by the liquid, so the flow isn't constant. In addition, because the measuring cap is small and the liquid's viscosity is high, the detergent may spill and splash the surroundings. To avoid this, the designers wanted to ensure that the flow-down of the detergent could be measured in a comfortable time. Therefore, they changed the design of the spout cap to improve the detergent's flow-down velocity. Fluid dynamics simulation was performed with the objective of improving the measuring process.

During the Particleworks simulations, a conventional cap model was used to calculate the relationship between the spout cap's configuration and the flow-down velocity in order to have a reference point to compare the flow behaviour of the new HARETA designs. The liquid flows from the hole of the cap, moves down through the wall of the spout and falls into the measure. The simulation confirmed that the flow velocity was low as a result of flow resistance near the spout wall, and that the flow velocity increased further away from the wall. Therefore, the designers predicted that the flow-down velocity would be improved by expanding this inner area. Fig. 1 compares the geometry models of the newly developed spout cap for HARETA and a conventional spout cap. Fig. 2 shows the conditions of the flow-down simulation performed using each of these caps. When the detergent is poured, one cannot ignore the air entering the bottle when the liquid surface of the detergent is higher than the opening. This simulation did not specifically consider the influence of air but it defined the detergent amount to not completely fill the opening. In addition, the tilting motion was calculated by applying a forced rotation so that the bottle

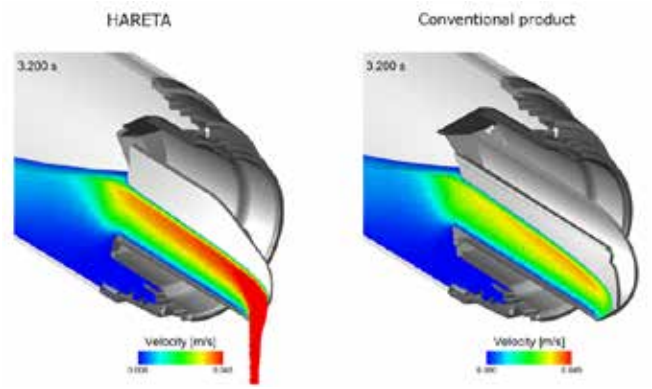

Fig. 3. Comparison of outflow velocity distribution of detergent in longitudinal section of the HARETA spout cap and the conventional product spout cap.

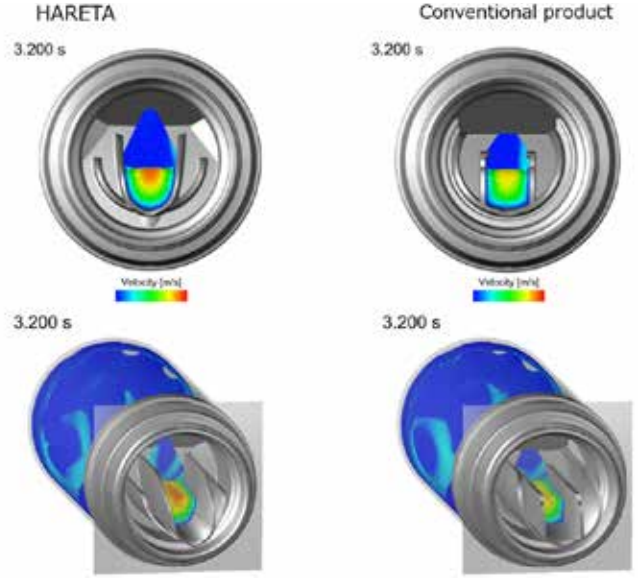

Fig. 4. Comparison of outflow velocity distribution of detergent in a transverse section of the HARETA spout cap and the conventional product spout cap.

gradually tilts to 110° between 0 and 0.6 seconds after the start of the pouring motion. As can be seen from the graph in Fig.2, the simulation divided the bottle tilting operation into two steps to reproduce so-called ordinary human movement on the bottle movement as closely as possible. The machine used in LION's experiments can only tilt the bottle at a constant speed, while simulation allows them to reproduce human-like behaviour more flexibly. The flow-down simulation was performed to compare the spout cap models of HARETA and the conventional product, using these conditions. Fig. 3 compares the velocity distribution of the longitudinal section of the bottle cap while Fig. 4 compares the velocity distribution of the transverse section of the bottle cap. This demonstrates that the HARETA cap design has a larger area with high flow velocity. Moreover, experiments on the flow-down velocity using the combination of the newly developed cap for HARETA showed that the HARETA composition was improved by 140%.

Particleworks allowed the CAE engineers to calculate the velocity gradient and the simulation made it possible to observe how much it affected the whole flow-down phenomenon. When the detergent flows down, its velocity is not uniform, slowing near the spout and increasing further away. In future, the engineers hope to use simulation to visualize the differences in velocity gradients due to design changes, feed back the simulation results to the design values, and study the optimal design. In addition, they believe that they can use simulation as a tool for design inspiration because such understanding would often be the origin of new ideas in the design process. The development of this new spout cap was selected for excellence at the Japan Packaging Technology Research Conference in 2018.

Article from:
EnginSoft Newsletter Year 16 n.3 Autumn 2019

New MPS-based method to design and analyse the cooling systems of engine pistons is faster and more accurate

By Sami Ojala
Wärtsilä Finland Oy

This paper presents a method for calculating the temperature field of a medium-speed engine piston. The method combines simple empirical formulas for calculating the heat load of the piston, the Moving Particle Simulation (MPS) method in Particleworks' software for solving the cooling effect of the oil, and finite element analysis (FEA) for calculating the temperature field of the piston. This method makes it possible to quickly evaluate several different piston cooling designs in the early stage of the piston design process. The paper shows the validation results and compares the simulation times between the MPS method and the Volume of Fluid (VOF) method.

To keep up with the competition in internal combustion engine manufacturing, all the key components of an engine must be designed and optimized very precisely. During last 50–60 years, the brake mean effective pressure (BMEP) of Wärtsilä engines has increased from around the 5bar level of naturally aspirated engines to the over-30 bar level of the recent W31 engine. Higher BMEP (i.e. more work per cycle) also means more mechanical and thermal load to the piston and the other components in the combustion process.

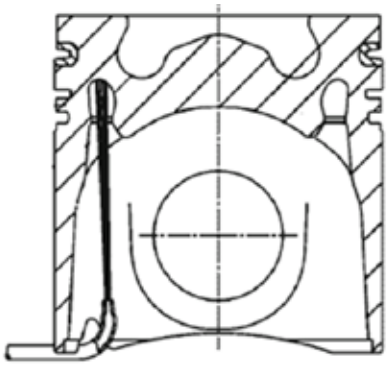

Fig. 1. Piston jet cooling principle [1].

High thermal load generates a need for effective piston cooling. Piston temperature must not exceed a certain level in order to maintain the steel material properties, to prevent hot corrosion and the build-up of carbon deposits. Too high a piston temperature causes thermal expansion which can lead to seizure between the piston and the cylinder liner. Fig. 1 demonstrates the principle of piston cooling by oil jet, which is one method used for controlling piston temperature. Oil is sprayed from below through an inlet hole in the piston. The oil then splashes inside the cooling gallery of the piston, cooling it by means of the so-called shaker effect. The hot oil finally exits the piston and flows back to the oil sump.

When a new piston is developed, the main focus of the computer-assisted engineering (CAE) work is usually on how to calculate the mechanical stresses and dimension the piston against fatigue. Nowadays, mechanical stresses can be calculated very accurately with sophisticated simulation tools. An aspect that often receives less attention than the solid mechanics is the thermal analysis of the piston. The heat transfer-related boundary conditions that are being used might be very inaccurate, which means that the temperature field of the piston is likely to be far from real. The ability to simulate the temperature field of the piston realistically is important as the starting point of the stress calculation. Uneven temperature distribution causes thermal stresses. High temperatures affect the materials' mechanical properties, as mentioned earlier. All these elements have a direct effect on the outcome of the structural analysis. The reason for this

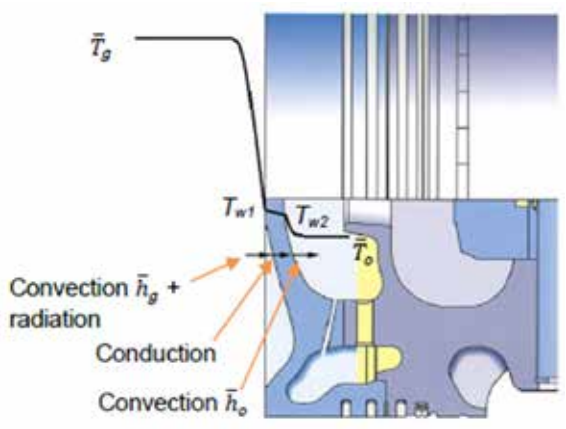

Fig. 2. Combined heat transfer in a piston.

inaccuracy in thermal boundary conditions is that they are often quite difficult to determine.

The objective of the work was to create a reliable and flexible tool that can be used to evaluate many designs which are different in their piston geometry and their cooling arrangements. Thermal analysis must be undertaken in the early stage of the design process to ensure that temperatures will not exceed general limits.

The philosophy was to keep the process quick by avoiding a time-consuming and detailed computational fluid dynamics (CFD) combustion analysis. Instead, simpler experimental formulas to determine the thermal load were chosen. The most difficult part of the problem was how to calculate the cooling effect of the oil splashing inside the piston cooling gallery. Convective heat transfer is always coupled to fluid flow; the existing flow scenario consists of a two-phase free surface flow, which is extremely difficult to handle. As said, to keep the simulation time short, there was no point in using traditional CFD methods here, either. Particleworks' mesh-free Moving Particle Simulation (MPS) method offers a great solution to the simulation of fluid flow and determining the cooling effect. Once the boundary conditions are established, the temperature field is easily solved.

Heat transfer in a piston

A general transient heat transfer problem can be formulated as below [2]:

$$\begin{cases} -\int_\Omega (\nabla\psi)^T \underline{k} \nabla T \, dV + \int_{\partial\Omega_q} \psi q'' dS + \int_\Omega \psi(\dot{E}_g - \rho\dot{u}) \, dV = 0 \\ T = T_0 \text{ on bounday } \partial\Omega_T. \end{cases}$$

This equation forms the basis of solving a temperature field with FEM.

The boundary condition of the convective heat flux of the second term in the equation above is expressed as [3]:

$$q'' = h(T_1 - T_2),$$

where h is the convective heat transfer coefficient.

Thermal boundary conditions

Fig. 2 summarises the combined heat transfer problem of piston cooling. Heat is transferred by convection and radiation from the hot gases inside the cylinder (temperature T_g) to the piston wall, which is at temperature Tw_1 by heat transfer coefficient h_g. Temperature T_g and coefficient h_g are assumed to be constant for the whole top surface of the piston crown.

This is a reasonably good approximation for gas engines where the heat load is more uniform due to premixed combustion. In diesel engines, the spatial distribution for the thermal load must consider the injection spray pattern. Surface heat from the top is conducted through the metal to the cooling oil on the side wall that is at temperature Tw_2. There, the heat is transferred to the oil which is at temperature T_0 by convective heat transfer coefficient h_0. In this application, the empirical correlation chosen for the thermal load is based on the so-called Woschni [4] formula which relates the instantaneous heat transfer coefficient of the cylinder to the piston movement, the cylinder gas temperature and pressure. The formula can be written as:

$$h_g = \frac{k_f}{D_c} Nu = K_1 D_c^{b-1} p_c^b w^b T_g^{K_2 - 1{,}62b}.$$

Information about valve timing and the compression ratio are also included in the Woschni formula. The gas temperature inside the cylinder is calculated using ideal gas law, and cylinder pressure is measured using a cylinder pressure sensor, which is available anyway in Wärtsilä gas engines.

The instantaneous heat transfer coefficient and the reference temperature are time-averaged over one full engine cycle using the following formulas:

$$\begin{cases} \bar{h}_g = \frac{1}{\Delta\phi} \int_{-360°}^{360°} h_g \, d\phi \\ \bar{T}_g = \frac{1}{\Delta\phi \, \bar{h}_g} \int_{-360°}^{360°} h_g \, T_g \, d\phi \end{cases}$$

Particleworks 6.1.1 implements a model for the calculation of the heat transfer coefficient. The model is based on the analytical results of a flat isothermal plate in parallel flow. Software is used to solve the cooling effect of the oil i.e. the spatial distribution of the heat transfer coefficient h_0 on the cooling gallery surfaces. Unlike the heat transfer coefficient, the reference temperature T_0 is considered to be one constant value over the area.

The solution procedure

The general principle of the iterative solution procedure and the coupling of Particleworks with FEM is shown in Fig. 3. First, the basic geometry and parameters of the engine being analysed must be determined. For example, the cooling oil mass flow m_0, the oil temperature at spray nozzle T_0,in, engine speed, piston geometry, piston movement, cylinder pressure, and the mass flow rate of the intake air are needed. Then a simulation is performed using Particleworks, which provides a time-

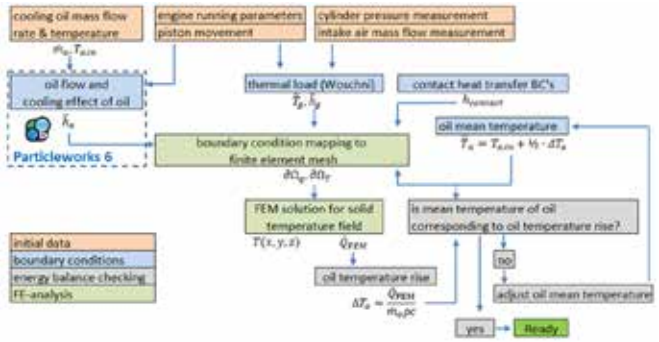

Fig. 3. General solution procedure.

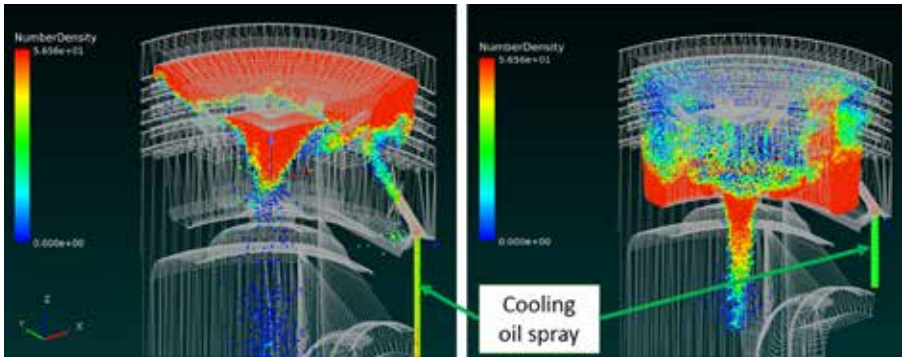

Fig. 4. Oil sloshing inside the piston cooling gallery.

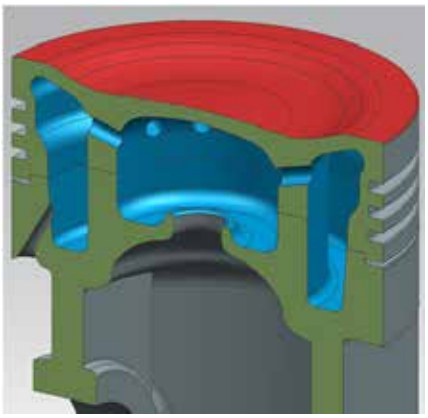

Fig. 5. Boundary conditions on different surfaces.

averaged spatial distribution of the heat transfer coefficient inside the cooling gallery. The reference temperature of the oil T_0 is guessed for the first round of the iteration.

At the same time, a script based on the Woschni correlation, which was developed in-house, outputs the thermal load, T_g and h_g, for the piston. The gap conductance $h_{contact}$ between the piston crown and the piston skirt is acquired by using simple methods like those described in [5] and [6], for example.

Once all the boundary conditions have been determined, they are mapped to the surface of a finite element mesh that describes the solid geometry of the piston. Fig. 5 shows that the thermal load is applied to the red area and the cooling effect is mapped to the blue areas. The grey area is treated as an insulated surface because it is assumed that the major part – at least 90% – of the heat flow goes through the red and blue surfaces. While there is obviously also heat flow through some grey surfaces, like the top land area, only major contributors are taken into account to keep the model simple.

After mapping the boundary conditions, a steady-state FE analysis is performed. The outputs of the solution are the solid temperature field of the piston and the heat flow Q_{FEM} through the piston. At the next stage, the rise in oil temperature equivalent to the heat flow Q_{FEM} is calculated. The new mean temperature of the oil based on this rise in oil temperature is then compared to the initial guess used for the first round of iteration. If the two values are different, the mean oil temperature is adjusted, and the FE analysis is performed again. This loop will continue until these two temperatures match. Usually two rounds are enough to obtain converged results. The ultimate result after the final loop is the piston's solid temperature field $T_{(x,y,z)}$.

engine load (BMEP)	cooling oil mass flow rate		
	high	Medium	low
100 %	nominal speed	nominal speed	nominal speed
75 %	nominal speed	nominal speed	nominal speed
50 %	nominal speed	nominal speed	nominal speed
10 %	nominal speed	nominal speed	nominal speed
100 %	-	-	0,95 x nominal
100 %	-	-	0,90 x nominal
100 %	-	-	0,85 x nominal

Table 1. Test matrix.

Validation results

To validate the model, a simple test series was run on a laboratory engine. This is a medium-bore Wärtsilä spark-ignited gas (SG) engine with a mean piston speed of 10,75m/s and a specific output of 18,5kW/litre. One cylinder of the engine was equipped with a special piston with thermocouple sensors. The schematic picture on the left hand side of Fig. 6 shows the locations of these temperature sensors.

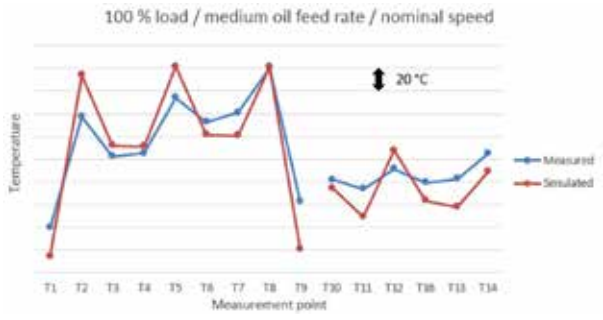

Fig. 7. Example result set from the validation measurements.

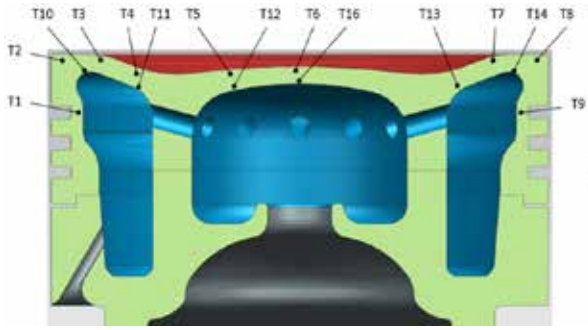

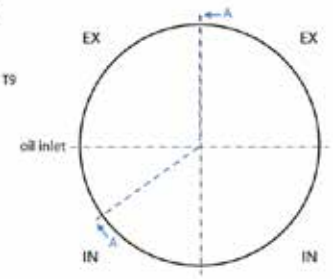

Fig. 6. Temperature sensor locations inside the piston.

The picture on the right hand side shows the oil inlet hole and the valve locations. All the sensors are located in section A–A. A test series was run according to Table 1 to see if the calculation model could handle changes in the engine load, the cooling oil's feed rate and the engine speed. Fig. 7 shows an example result set from a test point that was run with a 100% engine load, a medium oil-

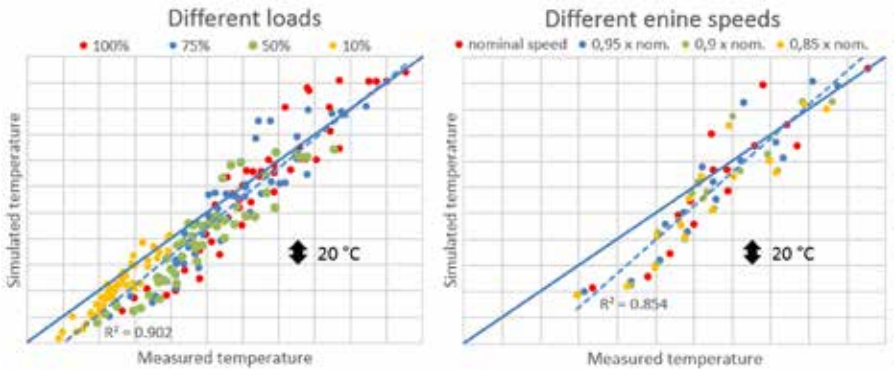

Fig. 8. Correlation between the simulation and measurement.

	MPS-method Particleworks	VOF-method
physical time (one piston stroke)	0,1 s	0,1 s
simulation time	5 h	24 h
number of CPU cores	12	160
particle diameter (MPS) average element size (VOF)	1,75 mm	2 mm

Table 2. Comparison of simulation time.

feed rate and a nominal engine speed. The simulated temperatures match well to the measured ones. The root mean square (RMS) error for 15 measurement points is 21,36°C which can be considered a good result. The model underestimates the piston ring groove temperatures (T1 and T9) – probably because no heat load was applied to the top land and the first ring groove areas. The simulation gives a substantially hotter temperature T2 than was found during measurement. This was caused by using uniform heat load in the simulation, which doesn't take into account the fact that the inlet-valve side of the piston is usually cooler than the exhaust-valve side. A future task will be to develop the heat-load distribution to include the effect of the valves. Temperatures T10–T16 which are located closer to the cooling gallery surfaces were generally hotter in measurement than in simulation. Sensor T15 wasn't working properly during the test run. Fig. 8 shows the correlation between the measured and the simulated temperatures. One dot represents one temperature measurement point. The different colours represent different engine loads, but they all include all three values for the cooling oil feed rate. On the left hand side, the engine load is varied and on the right hand side the engine speed is varied. The solid blue line shows the ideal correlation. The dashed blue line is a trendline fitted to all data points.

It can be noted that the model is able to follow the changes in engine load and the changes in oil feed rate. Especially the highest temperatures, which are usually the most interesting and important, are very near ideal blue line. On the other hand, the prediction of temperatures for varying engine speeds is not as accurate. Overall, the model provides reliable results. The RMS error in all cases is in range 7, or 24°C.

Conclusions

Particleworks CFD software, which utilizes the MPS method, is an effective tool for the simulation of free surface flow. While the heat transfer coefficient model implemented in the software might seem very simple at first, it calculates the cooling effect of the splashing fluid very accurately. The validation measurements showed that the model can predict the effect of the main parameters related to piston cooling. Thanks to the mesh-free nature of the method, the pre-processing time of the simulation is minimal. The whole pre-processing workflow, starting from the importation of the piston's 3D-geometry from the CAD software to setting up the simulation using Particleworks' GUI, can be done in only a couple of hours. Instead, traditional mesh-based methods require at least a few days for the pre-processing. Particleworks' actual simulation time is short, too. The post-processing was done with the features included in the program and self-made Excel macros.

Table 2 compares the simulation time between Particleworks and another commercial CFD software that uses the Volume of Fluid (VOF) method. Basically, a similar case was simulated using both types of software.

With Particleworks, the simulation time is 80% shorter and uses only a fraction of the CPU cores. This simulation time can be shortened even further by using Graphics Processing Unit (GPU) computing. In additional, the VOF method seemed quite unstable at the beginning so extra iterations were needed to get converged results. Even then, the method couldn't beat the accuracy of the MPS method. The time required to perform the analysis with the new model that was developed is quick enough to allow the evaluation of different piston cooling designs to be done parallel to rest of the piston design process. The new method has already been used in practice to solve the cooling problems being experienced with a specific design project for a new piston. The piston cooling gallery's geometry was unfavourable, and the oil wasn't flowing properly through the piston causing the piston to heat up more than expected, which ultimately led to a piston seizure. Once this design was simulated with Particleworks, the problem was discovered. A new design was simulated, and a geometry design change was implemented after which the problem disappeared.

Article from:
EnginSoft Newsletter Year 15 n.4
Winter 2018

References

[1] Mahle (2012). *Pistons and engine testing*, pp. 284.

[2] J. Bergheau, and R. Fortunier, "Finite element simulation of heat transfer", John Wiley & Sons, Incorporated, Hoboken, New Jersey, USA, pp. 279.

[3] F. Incropera, and D. DeWitt, "Introduction to heat transfer", 4th ed. John Wiley & Sons, Inc., New York, USA, pp. 892.

[4] G. Woschni, "A universally applicable equation for the instantaneous heat transfer coefficient in the internal combustion engine", available at: https://saemobilus.sae.org/content/670931.

[5] B. B. Mikić, "Thermal contact conductance; theoretical considerations", *International Journal of Heat and Mass Transfer*, Vol. 17(2), pp. 205-214. http://www.sciencedirect.com/science/article/pii/0017931074900829.

[6] A. Hasselström, and U. Nilsson, U. "Thermal contact conductance in bolted joints, Chalmers University of Technology", Department of materials and manufacturing technology, p 81. Available at: http://publications.lib.chalmers.se/records/fulltext/159027.pdf.

Thermal optimization of e-drives using moving particle semi-implicit (MPS) method

By L. Martinelli[1], M. Hole[1], D. Pesenti[2], M. Galbiati[2]
1. Drive System Design Ltd - 2. EnginSoft

A novel technique to model the temperature of windings in oil cooled e-machines has been developed. It aims to reduce the time taken to generate and solve thermal models by using a combination of particle based fluid modelling and steady state finite element (FE) thermal modelling. The fluid model is used to generate a heat transfer coefficient (HTC) map for the complex, multi-phase flow, which is applied to a finite element FE model of the e-machine. This would allow thermal modelling to take place at a concept design stage where rapid design iterations are required. By using this combined modelling approach, it was shown that it is possible to generate and solve models in under a week which show credible results. Further correlation work is underway to validate the models and results predicted.

Passenger Car Traction Motor[1]	2017	2025	2035
Cost ($/kW)[2]	10	5.8	4.5
Continuous power density (kW/kg)	2.5	7	9
Continuous power density (kW/l)	7	25	30
Drive cycle efficiency (%)[3]	86.5	92.5	93

1] All assume 350V / 450Amps @ 65degC inlet
2] Prices are 300% mark-up on material costs
3] Drive cycle based on WLTP

Fig. 1. APC Targets for Passenger Car Traction Motors [5].

1. Introduction

With major OEMs committing to increasing numbers of EVs and greater electrification, the total electric car stock could reach between 9 million and 20 million by 2020 [4]. To make this possible, the UK's Advanced Propulsion Centre (APC) have outlined target costs, power densities and efficiencies for passenger vehicle traction e-machines, as shown in Fig. 1 [5].

They also note that one key technological enabler is the closer integration of e-machines into transmissions and internal combustion engines (ICEs), and eventually fully integrated powertrains. This means that there will be a shared cooling and lubrication strategy within the transmission and e-machine, tending towards oil cooled e-machines. A passive (splash) lubrication regime is likely to maximise the efficiency of the integrated powertrain whilst minimising cost and weight but may not deliver sufficient cooling for high power density e-machines. Down-sized, low power electric pumps will be required to balance efficiency, mass and cooling.

With increasing power density motors, the loss density will also increase, meaning that more effective e-machine cooling will be required. Alongside more integration in powertrains, e-machine cooling becomes a factor in the lubrication design and it will become increasingly necessary to use fluid modelling to influence concept level designs.

Currently it is difficult to accurately model fluid flow within enclosed volumes such as transmissions and e-machines with traditional

computational fluid dynamics (CFD) methods due to the high computation time required. It is even less practical to model heat dissipation as the bulk temperature stabilises over a much greater timescales than the fluid flow, meaning even greater computation time is required. As a result, it is currently impractical to perform in the early stages of a new design where rapid iterations are required. This is currently a barrier at the concept stage to the optimisation of oil cooled e-machines.

It has been shown that modelling oil within enclosed volumes with rotating components, such as transmissions, can be performed effectively on modest hardware [2], [6]. This paper builds on this work to model multiphase fluid flow within an oil cooled e-machine. By combining this approach with FE it is possible to model the temperature distribution in the windings of an oil cooled e-machine in a compressed timescale, enabling faster design iterations and more power dense e-machines through thermal optimisation.

2. Thermal Modelling

2.1 Modelling Oil Within Powertrains

To understand the movement of oil within powertrains there are two established methods which are practiced:

- Clear case testing
- Finite volume computational fluid dynamics (CFD) modelling

Baffles, oil guides and pumps can be tested in clear cases to optimise the oil distribution. High temperature testing is not possible however due to the limitations of the materials used for clear casings - typically transparent thermoplastics such as acrylic. The clear case testing is useful once a design has matured to the extent that the rotating components are relatively well defined but cannot provide useful data during the concept design phase. It can take several months to procure rotating components and so there is often a requirement to commit to a design for clear case testing at the same time as procuring prototype test components. As such, if any significant issue is found during clear case testing there is a large cost, both in lost time and wasted material, associated with re-design and re-testing.

Finite volume CFD is of limited benefit in the design of automotive transmissions or electrified powertrains due to the extended run time required to generate results. Typically it can take several weeks of computation to generate a few seconds of real world data. Fluid flow will tend to stabilise within a few seconds in a powertrain but it may take several minutes to reach thermal steady state [6]. This could require months of simulation. As multiple input speeds would need to be modelled, it rapidly becomes impractical to use this type of CFD to model a single concept even on computers with high processing power.

An increasingly well correlated alternative method of CFD using particles is more suited to modelling fluids in confined volumes (2). This meshless CFD utilises a moving particle semi-implicit (MPS) method which allows simulation of single phase and multiphase fluid flow. With MPS the fluid is discretised as a series of particles whose interactions are calculated using conservation of momentum and mass. The Navier-Stokes equations are solved using the Lagrangian methodology [6]. The MPS method is able to account for surface tension, droplet break up, free surface fragmentation and coalescence. Solid bodies are represented by mathematical functions, called distance functions, and so a mesh is not required. The MPS solver can be run on graphics processing units (GPUs) to further reduce computation time. This method enables much faster solving of fluid models, for example it can take as little as a few days to simulate several seconds of real time data for a single speed automotive transmission on modest hardware, compared to weeks using finite volume CFD.

	Moving Particle Simulation	Mesh-Based CFD
Pre-process (geometry, meshing, setup)	< 1 day	2 weeks
CPU Time	5.0 [s] in 3 days	0.5 [s] in 4 weeks
Cores	12	32
GPU Time	5.0 [s] in 6 hours - v6 on K40 5.0 [s] in 3 hours - v6 on P100	

Fig. 2. Comparison of MPS and CFD solve times for a simple automotive transmission [6].

Fig. 2 shows a comparison of MPS vs CFD solve times for a simple automotive transmission. By combining the performance benefits of MPS with appropriate modelling simplifications, it may be possible to use this method as an iterative design tool, rather than a final validation.

2.2 Modelling Heat Transfer in Oil Cooled Motors

E-machine design software enables rapid iterations to develop high power density designs, with information on power curves and efficiency. A critical factor in increasing the power density of an e-machine is how much of the heat generated can be removed. Overheating can cause damage to the insulation and lead to short circuiting. The design of the cooling system will directly impact how much power the e-machine can produce in both continuous running and peak conditions.

There are several widely acknowledged and utilised methods for cooling E-machines in automotive transmissions:

- Water/glycol cooling jacket
- Direct oil spray onto the stator windings
- Oil or water/glycol in a hollow rotor shaft

The cooling effect of a water/glycol jacket can be calculated relatively easily as the channels are fully filled with water/glycol only. This means that correlations to empirical data is known to be accurate.

Oil sprayed directly onto the stator windings provides a greater challenge as the oil mixes with air in varying proportions over the entire surface of the windings. Empirical data is used to correlate to, however this is always a compromise as the data is inherently discontinuous, having been measured at a series of discrete points. As a result, the designs generated may not be as optimised as possible. By developing a more detailed method of modelling the temperatures on the surface of the e-machine windings it will be possible to increase its power density.

An MPS CFD method can be used to simulate the complex flow of the oil around the e-machine windings. From this it is possible to export the heat transfer coefficients (HTC). This can then be combined with the

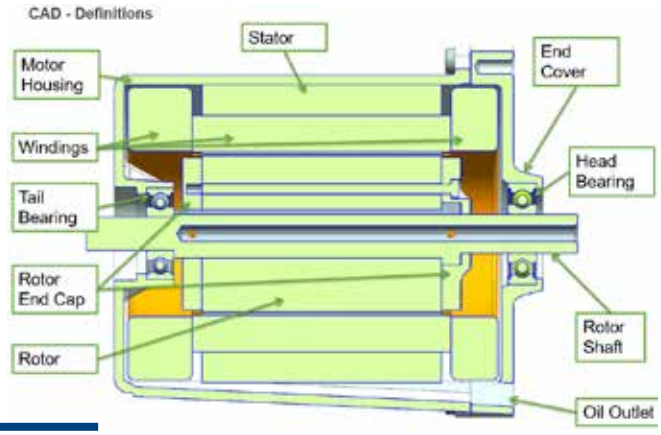

Fig. 3. e-machine Design.

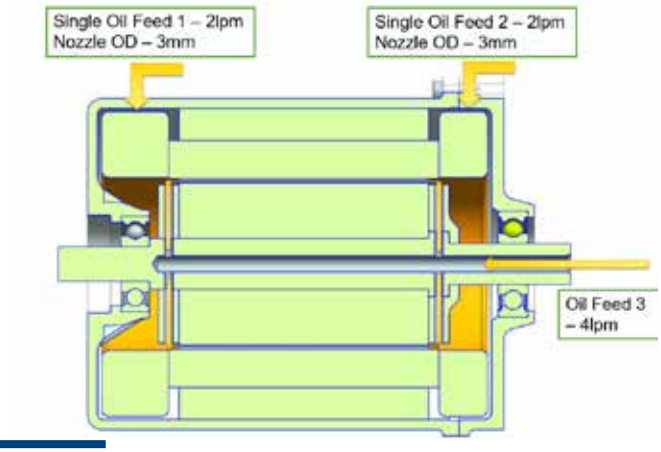

Fig. 4. Initial Oil Requirements.

power loss in the windings to model the temperature at the surface and give indications of poorly cooled areas.

2.3 Motor Design and Cooling Strategy

A high power density e-machine has been developed by DSD for an automotive application using state of the art e-machine design software. Initially a winding temperature prediction was carried out using correlation to empirical data. The data showed a step change in temperature under certain conditions which is due to the discrete nature of the empirical data.

The design, Fig. 3, uses a series of spray cooling jets to introduce oil onto the windings, which then drains down into a remote sump (not shown) allowing the oil to settle and de-aerate. An oil to air radiator is

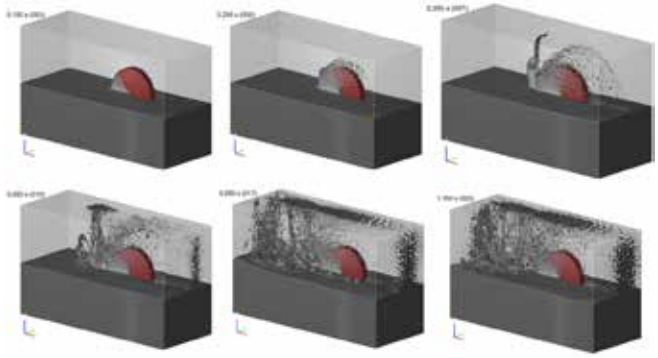

Fig. 5. Correlation model of single gear in oil [6].

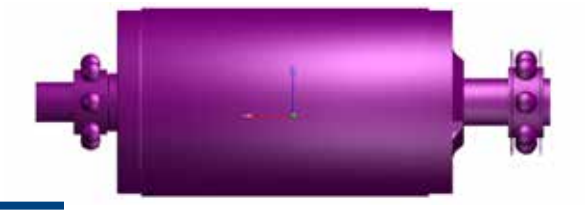

Fig. 6. Rotating Components.

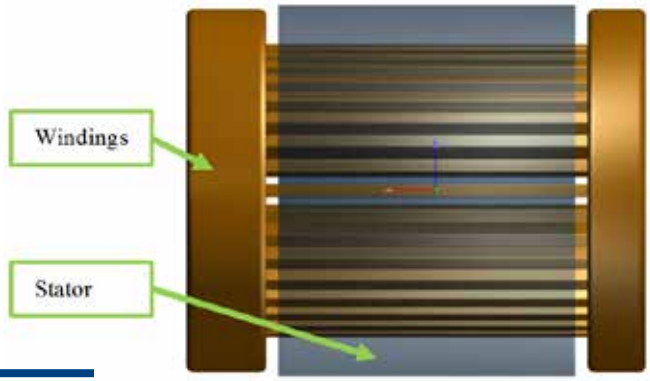

Fig. 7. Stationary Components.

used to cool the oil before it reaches the e-machine. A single oil spray nozzle feeds oil to each end of the windings from the highest point on the casing. A nozzle also feeds oil directly up the centre of the rotor shaft, with four radial drillings spreading this oil to the inside of the windings. The pump selected for this design is capable of supplying 8L/min of oil to the e-machine. An initial estimate of the required flow rate split is shown in Fig. 4.

This e-machine is required to run at the continuous high power and building an analytical model offers the opportunity to test the estimated oil cooling and optimise the cooling regime.

2.4 Modelling the System

It has previously been shown how the flow of oil using an MPS method can be correlated to test data [6]. Fig. 5 shows the model used in this test.

For the e-machine analysis a model was generated in Particleworks, using imported CAD. The solid components were imported as grouped bodies based on how they will behave within the model. The rotor was combined with the bearing inner races and elements into a single body as these will all rotate about the same axis (Fig. 6) to reduce pre-processing time. The stator and windings were imported as separate bodies so that information such as heat transfer coefficients could be

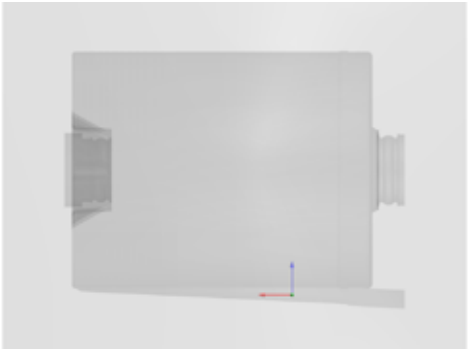

Fig. 8. Containment Volume.

Orifice	Flow Rate (L/min)	Percentage
Inlet	4	100
Outlet 1	1.0109	25.27
Outlet 2	1.0096	25.24
Outlet 3	0.9896	24.74
Outlet 4	0.9899	24.75

Table 1. Flow Rate at Inlet and Outlets.

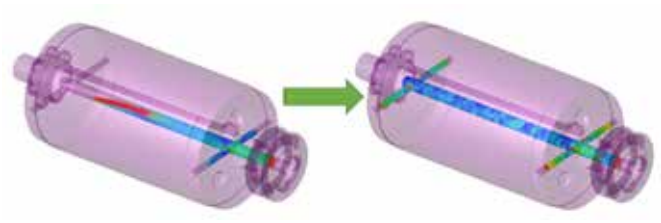

Fig. 9. Oil Flow through Rotor Shaft.

investigated for these components individually (Fig. 7).

The inner surface of the casing, including the bearing outer races, was extracted to create an oil tight containment volume, with the outer surface simplified to a cube (Fig. 8). This simplification was carried out to reduce the pre-processing time required to generate the distance functions for the solid body.

An initial model was generated which isolated the rotor assembly to calculate the oil flow through the radial drillings. The rotor shaft was placed within a cubic domain with an oil feed into the centre of the shaft. The rotor was set to rotate at 3,000rpm, with the oil fed at a rate of 4L/min.

Once the flow had become stable, the flow rate from each orifice was measured as shown in Table 1. Fig. 9 shows the rotor shaft before flow had stabilised and after flow had stabilised and the rotor becomes saturated.

As the flow rate of each orifice is approximately equal, a fixed flow rate equal to one quarter of the input flow will be used at each orifice in the complete model to reduce the computation time required to solve.

A complete model was generated, including the modelling simplification described above. For low speed applications it is possible to model an enclosed volume without air to significantly decrease the computation time required.

As the tip speed on the rotor shaft is between high speed and low speed, back to back models were generated with and without air to determine whether it was necessary. Fig. 10 shows the development of the oil flow in the model without air, coloured by velocity. The model shows, in the circled region, areas where oil doesn't appear to reach.

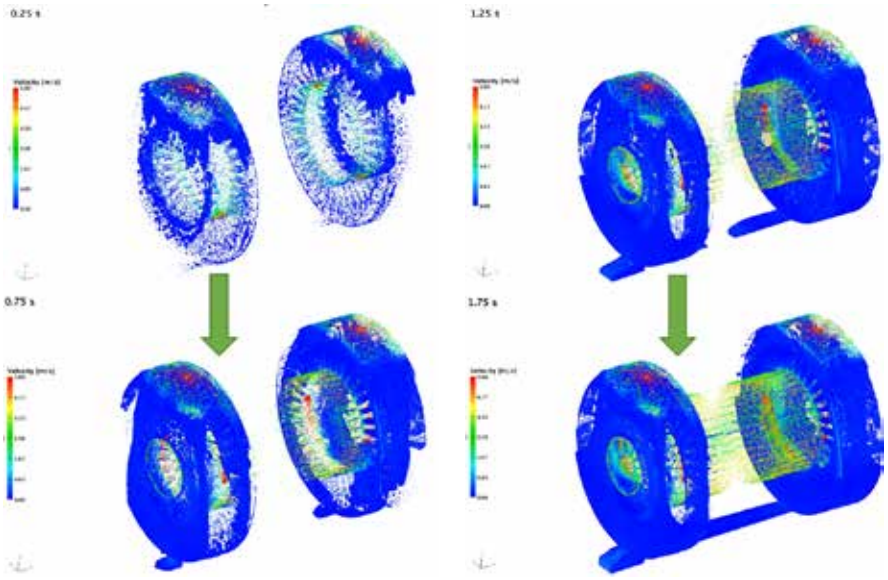

Fig. 10. Development of Oil Flow (Without Air).

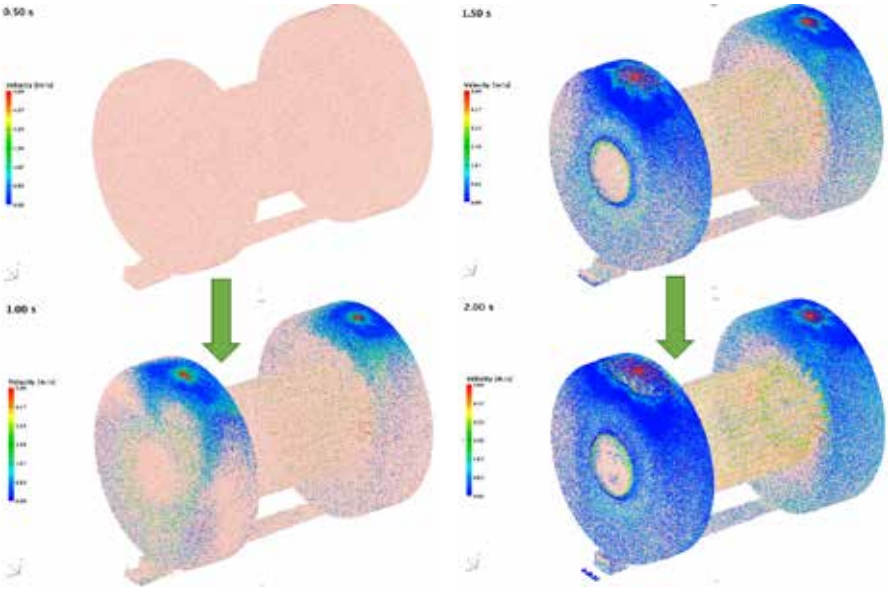

Fig. 11. Development of Oil Flow (with Air).

Fig. 11 shows the oil and air flow developing in the model with air, the air particles are coloured pink throughout whilst the oil is coloured by velocity. From the test described above, it was deemed that the model with air would provide a more accurate model of the fluid movement and hence the HTC. A comparison of the HTC map for the models without and with air is shown in Fig. 12 and Fig. 13. It can be seen that in the model without air the HTC is very low in the areas where oil isn't reaching in significant quantities.

This is to be expected as the model assumes a vacuum where there isn't oil. The model with air shows a more even distribution of HTC. This aligns with expectation well as the air will be dragged around as the rotor spins, meaning that it will also have a cooling effect on the windings. Although it would reduce

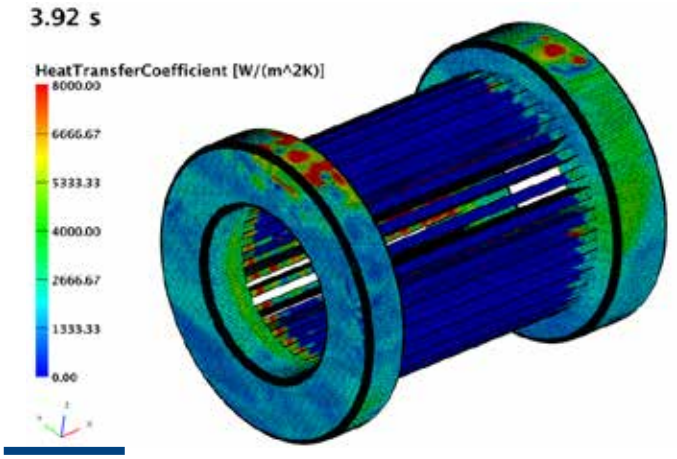

Fig. 12. HTC Map (without Air).

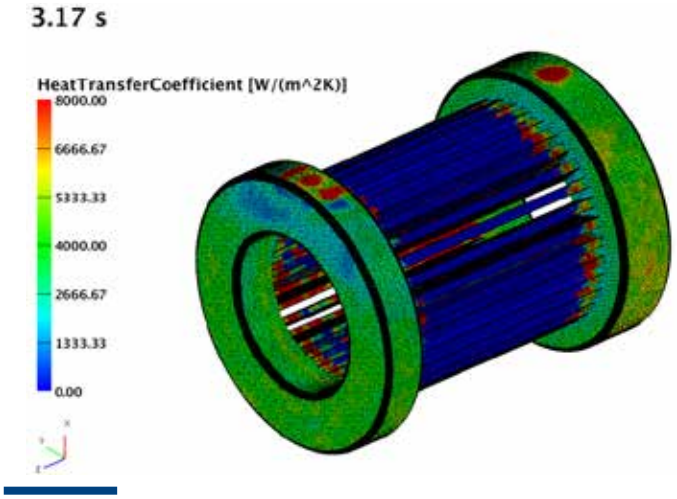

Fig. 13. HTC Map (with Air).

computation time further, it was deemed that modelling without air would not produce reliable results.

To check whether these results fall within the expected range, a hand calculation was performed using the Dittus-Boelter Correlation at the point of the top inlet. The HTC predicted at this point by hand calculation is within 10% of the HTC predicted by the model.

2.5 Temperature Mapping

The HTC map was exported from the model once the flow field had stabilised. This was then mapped onto a solid mesh in FE software. The power loss predicted in the windings, from the motor design software, was applied to the windings as a volumetric power loss. Whilst the losses vary over very short distances, for the purpose of developing a simplified design tool it was assumed that the power loss is equal across the windings. This simplification will help to minimise set up time for the thermal models.

It is impractical to model each individual wire in the motor windings at a concept level, especially when these are to analysed using FE. The insulation is very thin and would require a very fine mesh to capture

$$k_e = k_p \frac{(1+v_c)k_c + (1-v_c)k_p}{(1-v_c)k_c + (1+v_c)k_p}$$

Equation 1 - Hashkin & Shtrickman Approximation.

correctly, greatly increasing the number of elements in the model. This would require an impractically large amount of computation time to solve [7], [8].

$$c_e = \frac{PF(\rho_c c_c - \rho_p c_p) + \rho_p c_p}{PF(\rho_c - \rho_p) + \rho_p}$$

Equation 2. Specific Heat Capacity Estimation.

A method for estimating the bulk properties of a homogenised winding material has been validated by Simpson et al. [7]. The effective thermal conductivity, *ke*, of the winding material can be estimated using the Haskin and Shtrickman approximation:

Where *k* denotes thermal conductivity, v denotes volumetric ratio with *vc+vp=1*, and the subscripts *e* denotes effective, *c* denotes conductor and *p* denotes potting compound. The effective specific heat capacity, *ce*, of the bulk material can be estimated using:

Where *c, p,* and *PF* denote specific heat capacity, density and packing factor respectively. The subscripts *c* and *p* denote conductor and potting compound respectively. By applying these homogenised properties to the winding, the FE model can be significantly simplified with a small reduction in accuracy [7].

A steady state heat transfer problem was then carried out using the FE solver.

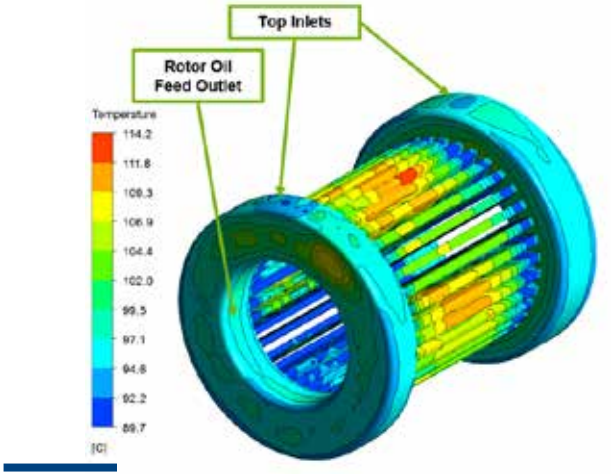

Fig. 14. Temperature Map (4L/min in Rotor Shaft).

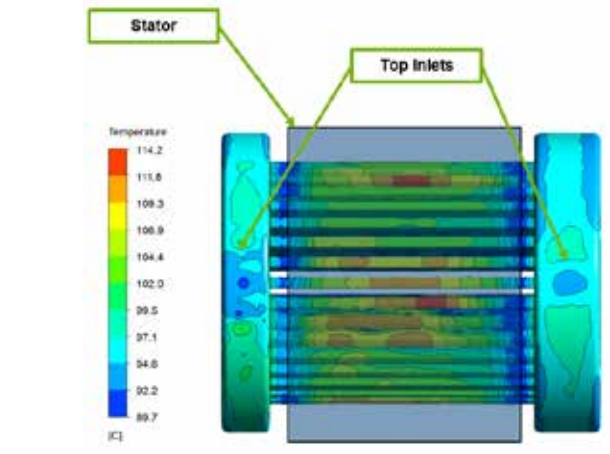

Fig. 15. Temperature Map (4L/min in Rotor Shaft) viewed from above.

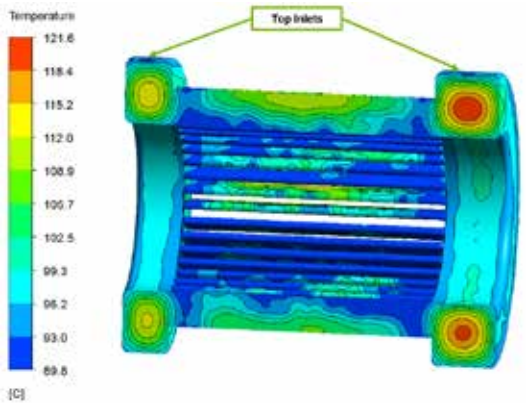

Fig. 16. Temperature Map (4L/min in Rotor Shaft) viewed in section.

3. Results

The results from the steady state heat transfer problem are shown in Fig. 14. The results show low temperatures in the expected areas, the areas where the oil inlets are situated are effectively cooled by the direct jets. The inner surface of the end windings also shows a well defined region of lower temperature where the rotor shaft oil feed exits.

Model Name	Oil in rotor shaft (L/min)	Oil in each top inlet (L/min)	Total oil in (L/min)
A	4	2	8
B	6	1	8
C	2	3	8

Table 1. Flow Rate at Inlet and Outlets

The windings which are situated within the stator show a higher temperature due to the lack of oil in this area (Fig. 15). Whilst this is expected due to the relatively low convective heat transfer in this area, the temperature may be lower in reality as there would be heat conduction through the stator which has not been accounted for.

The peak temperature is 124.9°C, found in the centre of windings (Fig. 16) whilst the average temperature across the entire windings is 103.6°C.

The model was iterated using different flow rates in each area to test whether further optimisation was possible with the current package and pump restrictions. The additional test points are summarised in Table 2. Model B shows a similar pattern of temperature distribution to model A

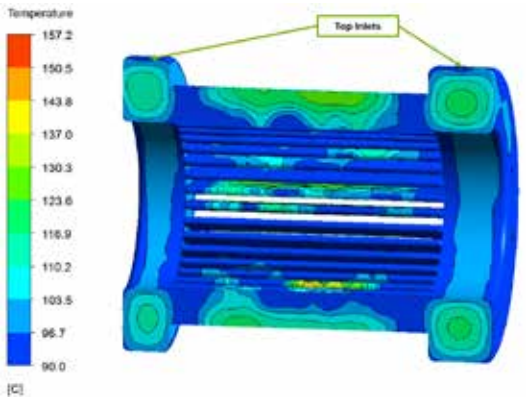

Fig. 17. Temperature Map (6L/min in Rotor Shaft).

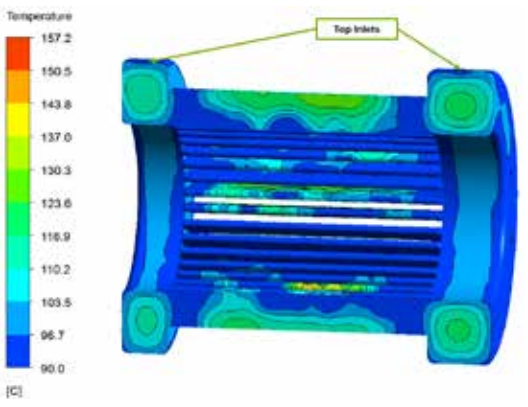

Fig. 19. Temperature Map (6L/min in Rotor Shaft) viewed in section.

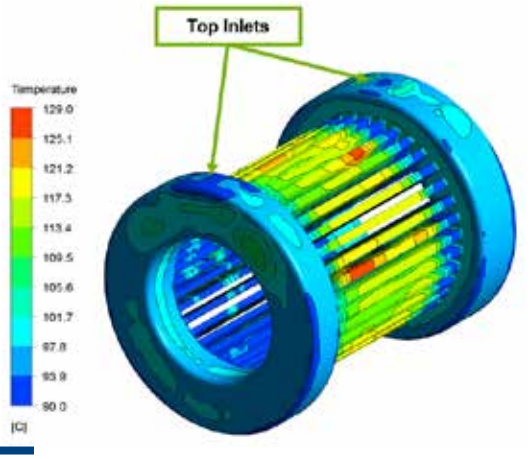

Fig. 20. Temperature Map (2L/min in Rotor Shaft).

(Fig. 17) but with generally slightly lower temperatures across the end windings.

As with model A, high temperatures are seen in the area covered by the stator (Fig. 18).

The peak temperature is 145.0°C, found in a very localised area in the section of windings covered by the stator (Fig. 19) whilst the average temperature across the entire windings is 105.1°C.

Model C also shows a similar temperature distribution to models A and B (shown in Fig. 20) Again, the windings show high temperatures in the area covered by the stator (Fig. 21).

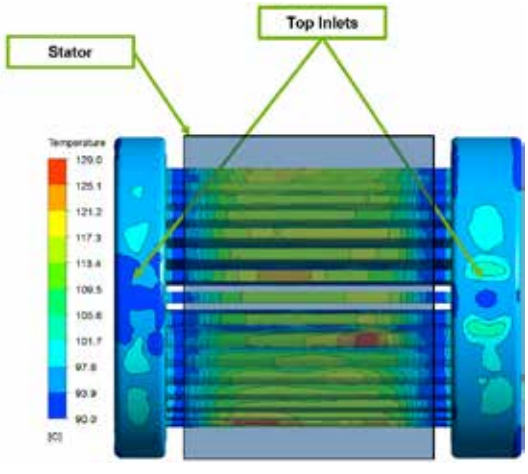

Fig. 21. Temperature Map (2L/min in Rotor Shaft) viewed from above.

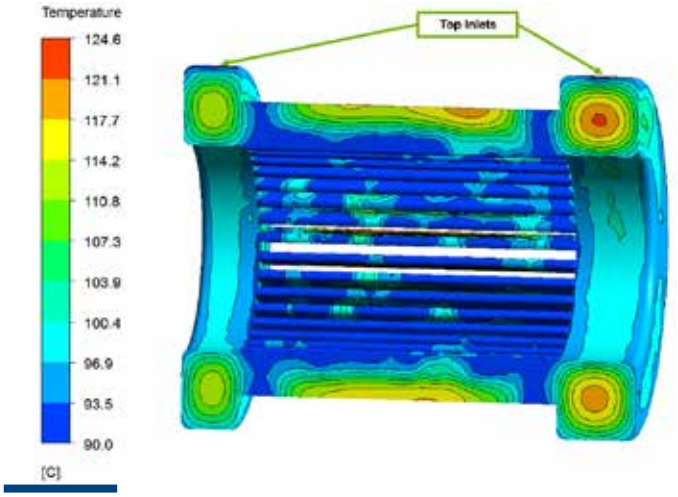

Fig. 22. Temperature Map (2L/min in Rotor Shaft) viewed in section.

Model	Peak Temp (°C)	Avg Temp (°C)
A	124.9	103.9
B	145.0	105.1
C	129.0	105.0
Standard Motor Design Software (Model A)	122.0	115.6

Table 3. Summary of Model Results.

In section view, it can be seen that in model C the highest temperature is found in the centre of the windings (Fig. 22).

The peak temperature is 129.0°C, whilst the average temperature across the entire windings is 105.0°C. The temperatures predicted by the standard motor design software for the same conditions as model A are shown in Table 3 along with the temperatures predicted using this novel method.

Model A, the initial estimation of flow requirements, appears to give the lowest peak temperature and lowest average temperature across the windings. This aligns with the expected trend from hand calculations. The peak temperature predicted is very similar to the standard motor design software, $<2.5\%$ difference. The average temperature predicted shows a larger difference, $\sim 10\%$.

Each MPS model was set up in under half a day, with approximately three days of solve time on modest computer hardware. A further day was required to postprocess and solve the steady state heat transfer. This means that a set of results can be obtained in under one week, much less than traditional finite volume CFD techniques.

4. Conclusions

A new method for solving the heat transfer prediction problem in an e-machine has been shown. The results have been benchmarked against other existing techniques.

A suitable assumption to merge the end windings into an equivalent mass has been carried out for the purpose of this concept study. For detailed motor analysis it is feasible to model the individual end windings, however this is at the expense of computation time. It is deemed that one inaccuracy in the models is the absence of conductivity to the stator. This is currently planned to be included in the model.

As the time taken to set up and solve the model is under one week, this technique offers a credible method to predict temperature at the early design stage. This will allow for a more informed comparison of different designs, enabling greater optimisation of e-machine thermal performance.
Machine testing is planned during 2018 to correlate models, and refine the process.

5. Glossary

APC: Advanced Propulsion Centre
CFD: Computational Fluid Dynamics
EV: Electric Vehicles
FE/FEA: Finite Element (Analysis)
GPU: Graphical Processing Unit
HTC: Heat Transfer Coefficient
ICE: Internal Combustion Engine
MPS: Moving Particle Semi-Implicit (method)
OEM: Original Equipment Manufacturer

References

[1] International Council On Clean Transportation. *EU CO2 Emission Standards for Passenger Cars and Light-Commercial Vehicles.* [Online] January 2014. [Cited: 28 March 2018.] https://www.theicct.org/sites/default/files/publications/ICCTupdate_EU-95gram_jan2014.pdf.

[2] "Low cost, low drag passive lubrication system developed with smoothed particle hydrodynamics". Berlin: CTI Symposium Automotive Transmissions, HEV and EV Drives, 2017.

[3] D. Block, and P. Brooker, *2015 Electric Vehicle Market Summary and Barriers.* [Online] 30 July 2016. [Cited: 28 March 2018.] http://www.fsec.ucf.edu/en/publications/pdf/FSEC-CR-2027-16.pdf.

[4] International Energy Agency. *Global EV Outlook 2017.* [Online] 2017. [Cited: 28 March 2018.] https://www.iea.org/publications/freepublications/publication/GlobalEVOutlook2017.pdf.

[5] Advanced Propulsion Centre UK. *APC Electric Machines Roadmap.* http://www.apcuk.co.uk. [Online] December 2017. [Cited: 03 April 2018.] http://www.apcuk.co.uk/wp-content/uploads/2017/12/EMC_Full_Pack.pdf.

[6] M. Galbiati, "Oil Splashing, Lubrication and Churning Losses Prediction by Moving Particle Simulation". NAFEMS World Conference 2017. [Online] June 2017. [Cited: 07 April 2018.] https://www.nafems.org/congress/presentation_downloads/.

[7] *Estimation of Equivalent Thermal Parameters of Electrical Windings.* N. Simpson, P. H. Mellor, and R Wrobel,

[8] *Estimation of Equivalent Thermal Conductivity for Impregnated Electrical Windings Formed from Profiled Rectangular Conductors.*

Article from:
EnginSoft Newsletter Year 15 n.3 - Autumn 2018

Prediction of oil splashing, lubrication and churning losses by moving particle simulation

By Salvatore Ruffino[1], Ragnar Skoglund[2], Massimo Galbiati[2]
1. Comer Industries - 2. EnginSoft

Lubrication, churning losses, and heat dissipation are key considerations in the design of gearboxes and transmission systems. These three aspects influence the functionality, life, and efficiency of the device but despite their importance the use of simulation to study these phenomena and support the design of transmission systems is very limited. This is because traditional mesh-based CFD (computational fluid dynamics) methods can only undertake the simulation of gearboxes or similar systems using complex meshing methods and time-consuming transient simulations that are incompatible with the design process. This paper shows how particle-based methods such as Moving particle Simulation (MPS) can simulate lubrication and oil splashing by completely eliminating mesh generation from the CFD process and dramatically reducing the simulation time, thanks to the semi-implicit scheme used by MPS for temporal integration. In particular, we show the results of the MPS method on a two-speed reduction gearbox, which is part of the rotor drive transmission of a forage harvester. The harvester's gearbox must work in a very wide range of rotation speeds and torque and good lubrication of all rotating components is mandatory to avoid breakdowns and overheating problems.

Gearboxes and transmissions systems are designed to maximize the efficiency of power transmission and ensure lubrication and heat dissipation. One of the causes of transmission losses are churning losses (the loss of power as a result of the resistance exerted by the oil on the gears). Gearbox design therefore seeks to minimize churning loss, while avoiding lubrication and overheating problems that affect system functionality. A prototype is, therefore, usually evaluated after the first design phase of a gearbox to assess the lubrication and heat dissipation. In these tests, lubrication can only be "measured" qualitatively by visually examining the oil distribution on the external walls of the gearbox. Quantitative measurements, such as the oil flow rate to the bearings, cannot be acquired, while the oil distribution inside the gearbox is impossible to visualize. When these tests produce negative results, either due to insufficient lubrication or overheating, a new iteration of design and prototyping must be undertaken, which is usually continued in a trial-and-error fashion until the objectives are met. This process is time- and resource-intensive and generally the right solution is only found from experience. To make this process faster and more efficient, Comer Industries, an Italian transmission systems manufacturer, decided to evaluate a new design process that integrates fluid dynamics simulation in the early stages of the design.

The purpose of this methodological test is not only to verify the feasibility and accuracy of the simulations, but also to understand if the simulation process could be compatible with the design phase of a real gearbox,

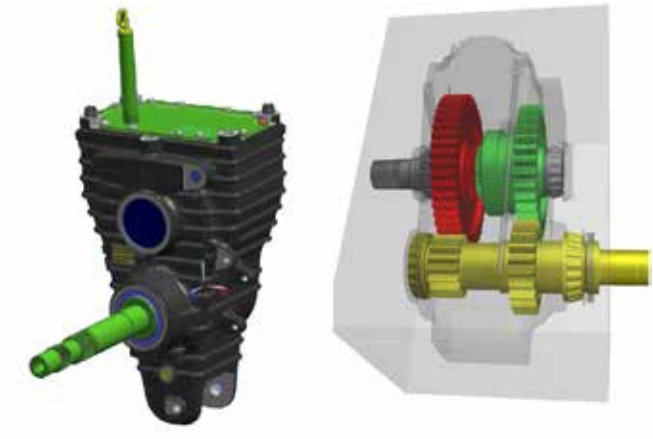

Fig. 1. Two-speed reduction gear box, part of the rotor drive transmission of a forage harvester.

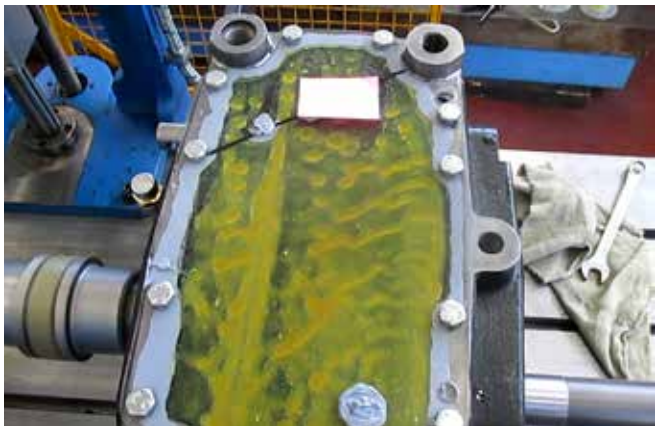

Fig. 3. Oil distribution on the upper cover of the gearbox during a lab test at Comer Industries.

Fig. 2. MPS model of the speed reduction gearbox with the initial oil volume at the bottom.

Fig. 4. Oil distribution in the gearbox, comparison of the original housing design (left) and new housing design (right). Oil reaches the upper cover and drops down onto the gears.

which lasts 2-3 weeks. During this phase, the aim is to produce a first design of the gearbox and to use fluid dynamics modelling to simulate and compare the performance of at least three designs in order to select the best one for physical prototyping and testing.

CFD modelling of a gearbox using moving particle simulation

The object of the modelling and simulation activity is a two-speed reduction gearbox, which is part of the rotor drive transmission for a forage harvester. The gearbox has to work in a very wide range of rotation speeds and torque, and good lubrication of all the rotating components is mandatory to avoid breakdowns and overheating problems. The objective of the design and simulation process is to modify and adapt the external housing of an existing gearbox to the new requirements of Comer Industries' customers. Lubrication in the new design must be at least as good as previous housing designs. The modelling and simulation activity is defined in two phases: the first phase will qualitatively compare the lubrication performance of the old and new housing designs; the second phase will study the effects on lubrication of design changes or changes in operating conditions. Fig. 1 shows the two-speed reduction gearbox with the input and output axes and the four gears. The CFD model is configured using Particleworks software, based on the moving particle simulation method, which is a mesh-less CFD method that allows incompressible single-phase and multi-phase flows to be simulated. In the MPS method fluids are represented by particles. The governing equations are expressed by the laws of conservation of mass and momentum. The Navier-Stokes equations are discretized by particle interaction models and solved with the Lagrangian method. The mesh-less nature of this CFD solver easily accounts for the effect of wall or body displacement on fluid flow without the complexity and effort of dealing with mesh movement, deformation, or overset, and without generating meshes for complex geometries such as a gearbox. The MPS method uses a semi-implicit algorithm [4]. When resolving a free-surface flow the MPS method considers the effect of surface tension, and calculates free-surface fragmentation, droplet break-up, and coalescence.

Comparison of lubrication efficiency for two housing designs

The first step of the simulation process is to compare the original and new housing designs in terms of oil distribution. The key factor in evaluating oil distribution and lubrication is the fact that the oil, initially located in the lower part of the gearbox (see Fig. 2) must be lifted by the lower gears to the upper gears. The upper gears then lift the oil up further to the upper cover of the housing. The oil is then pushed along the cover wall by the rotational effect of the gears and descends from the cover, thus lubricating the gears and bearings through special channels that collect the oil by gravity. This process and the efficiency of lubrication were verified experimentally for Comer Industries' original housing design.

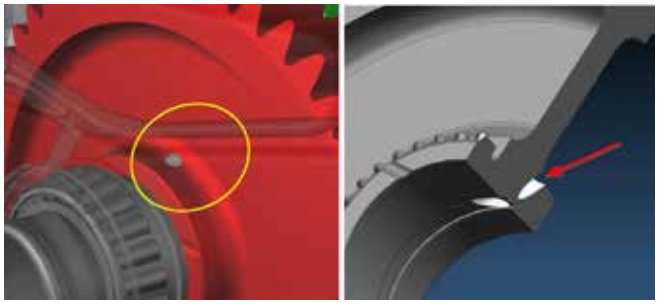

Fig. 5. Lubrication hole on one of the gears; the inclination of these holes according to the rotational direction can increase the gear lubrication.

Fig. 3 shows the top view of the original gearbox with a Plexiglas wall replacing the top of the prototype. Fig. 3 shows this Plexiglas wall covered with oil. This means that the action of the gears is able to lift the oil to the upper part of the wall, demonstrating that the lubrication is acceptable.
The left side of Fig. 4 shows the moving particle simulation of the original housing design. It shows the same behaviour and the same oil distribution on the cover wall. This is a first qualitative validation of the CFD model. The same type of simulation is also conducted on the new housing design. Fig. 4 shows that the oil behaviour in both the new and original gearbox designs is the same. The results of the two simulations show oil on the upper cover of the housing and oil droplets falling on the gears and entering the channels that lubricate the bearings. As a result, this first simulation phase concludes that the new design provides the same level of lubrication as the original one, and that no major modifications need to be made to the new housing.
It takes less than one week to simulate 5[s] of physical operational time of the Comer Industries gearbox using the MPS method. It takes 3-5 [s] to let the flow develop to evaluate the lubrication. Simulation time on 4 cores is 7.9 [days] using Particleworks software version 5.2.0 (Table 1). Using parallel computing on 8 cores cuts the simulation time in half to 4.1 [days], while using a GPU reduces the simulation time to 27 [hours]. It takes less than 1 hour to configure the MPS model starting from the CAD geometry, which is the time necessary to import the CAD geometry, to configure the rotational axis and speed of the gears, and the oil properties and level, and to select the proper numerical models. This fact in conjunction with the simulation time shown in Table 1 convinced Comer Industries that simulation was feasible within their normal design process and would allow them to compare the performance of at least three different designs in the space of two weeks.

	Simulation time [days] using Particleworks 5.2.0 Simulated physical time = 5.0 [s]	
Particle Size	CPU - 4 cores and 8 cores Intel Core i5-2400 - 3.10GHz	GPU NVIDIA Tesla K40 Intel Core i7 - 5930K - 3.50GHz
1.2 mm	7.9 [days] on 4 cores 4.1 [days] on 8 cores	1.1 [days]

Table 1: Simulation time using CPU-4 cores and GPU K40.

Investigating the effect of design changes and changes in operating conditions on lubrication

After the qualitative validation of the MPS model and the comparison between the original and the new housings, the focus of the study moved on to the effect of design changes to the lubrication holes found on the gears and to the effect of the initial oil level. In some instances, Comer Industries uses inclined rather than radial holes on the gears. These holes are inclined according to the direction of rotation; in theory, therefore, they should increase lubrication over radial holes by aiding oil capture as the gears rotate. This phenomenon cannot be verified on real prototypes because it is impossible to measure the rate of oil flow through these holes. CFD modelling, on the other hand, allows the calculation and comparison of the oil flow rates for different inclinations of the holes. The simulation of different geometries shows that the inclination of the hole can increase the oil flow and the lubrication of the system, as seen in Fig. 6, which compares the average oil flow in the lubrication holes when their direction is radial or inclined. Inclined holes in some locations increase the flow rate by more than 100% compared to radial holes.
Another factor affecting lubrication is the volume of oil in the gearbox. Reducing the oil volume can reduce churning losses and increase transmission efficiency, but may adversely affect lubrication. As a result, Comer Industries decided to simulate the effect of a 20% reduction in oil volume, from 2.0 litres to 1.6 litres. Fig. 7 shows that a 20% reduction in oil volume produces a 74% reduction in oil flow at the lubrication holes located on the gears. Therefore, the oil level cannot be reduced below a certain threshold without changing the oil pattern in the system and affecting lubrication.

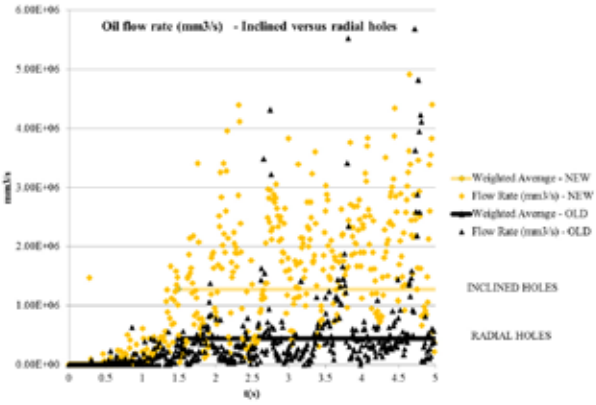

Fig. 6. Oil flow rate through the holes located on the gears, comparison between inclined and radial holes.

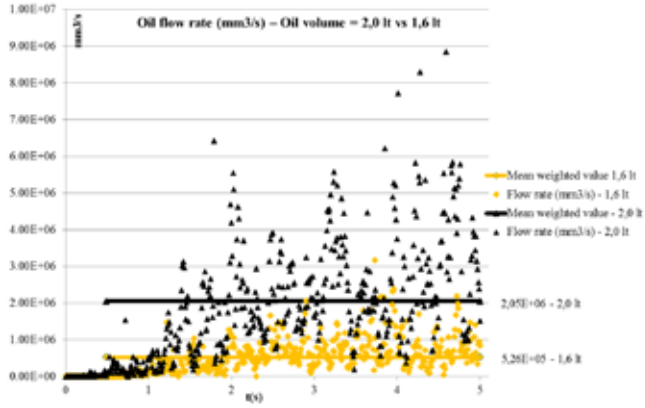

Fig. 7. Oil flow rate through the holes located on the gears, comparison between 2.0 litres of oil volume and 1.6 litres.

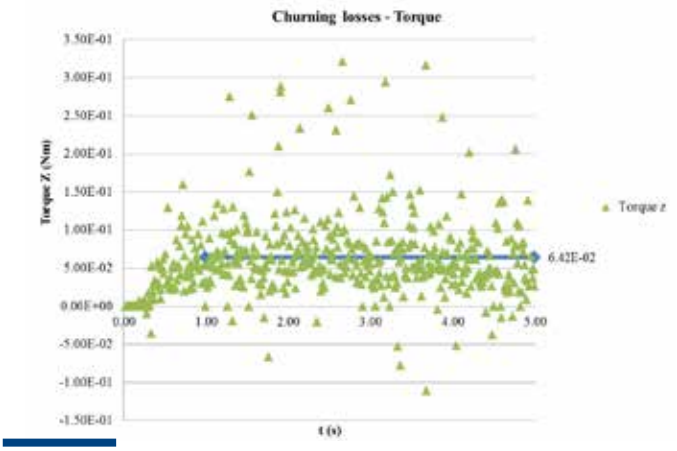

Fig. 8. Churning losses calculated on the first speed output gear.

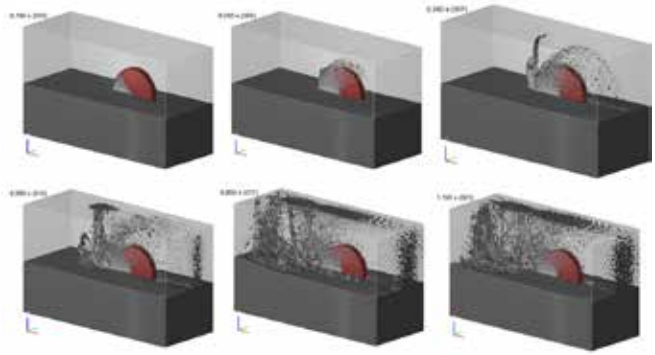

Fig. 9. Test case for validation of churning losses, single gear in a squared gear box.

Validation of churning losses

Churning loss is the torque exerted by the fluid on the gears and, like oil flow rate, cannot be measured in experimental tests, but can be calculated using MPS simulation. Fig. 8 shows the churning losses calculated on the first speed output gear. The average value calculated by the CFD model after the initial transient period is in line with Comer Industries' estimates. In order to fully validate the churning losses calculated with the MPS method, after the study of the two-speed reduction gearbox, a new and simpler geometry with a single gear is simulated, and the churning losses calculated are compared to the experimental data available for this simpler geometry. Fig. 9 shows the gearbox with the single gear and the oil pattern at 500rpm. Fig. 10 shows the total torque acting on the single gear and the torque components due to oil viscosity and pressure. The delta between the total torque calculated with the MPS method and the experimental churning losses is 10%. This last quantitative comparison completed the validation of the MPS method.

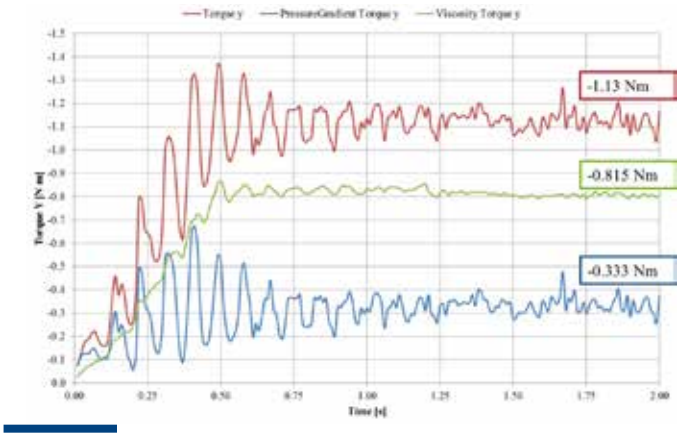

Fig. 10. Test case with a single gear in a squared gear box: total torque (red line), viscous torque (green) and pressure torque (blue).

Conclusions

Predicting oil splashing, lubrication, and churning losses early in the design of transmission systems helps optimize transmission performance, and reduces the number of design reviews and prototypes. While the benefits are evident to all industry players in this sector, the infeasibility of fluid dynamics modelling has been the main limiting factor to the adoption of simulation. For this type of application, the feasibility or infeasibility of CFD simulation is largely related to the geometric complexity of the transmission systems, the management of the mesh, and the solution methods used by traditional mesh-based solvers. Mesh-less particle-based methods like moving particle simulation eliminate the bottlenecks arising from geometric complexity and the management of the computational grid. Using this method reduces the time required to configure the CFD model from the 2-3 weeks required by a mesh-based software to 2-3 hours or less. Furthermore, the semi-implicit scheme applied by MPS for temporal integration reduces the computational time and resources required to run the simulations, while also leveraging the benefits of GPU-based calculation. For Comer Industries this means that simulation based on moving particle simulation is feasible within the standard design process and allows them to select the best design for the system by comparing at least three configurations in about two weeks. The advantage is that the solution chosen for prototyping will most likely not have problems with lubrication or overheating, which will have a positive impact on development costs and time to market.

About Comer Industries:

Comer Industries is one of the world's most important suppliers of agricultural, industrial and renewable energy machinery. The mechanical components manufactured by Comer Industries represent fundamental elements for the correct functioning of combine harvesters, tractors, ploughs, mowers, round balers, excavators, bulldozers and wind generators. Comer Industries' market is fully globalised and highly competitive, imposing the need to provide customers with products and services with unique standards of excellence all over the world.
Comer Industries employs 1,400 people, exports to all five continents and has seven locations in Europe, one in the United States, one in Brazil, two in China and one in India; between production plants and sales subsidiaries it reaches 54 countries with its products. In March 2019, the company opened to outside investors by listing on the AIM market of the Milan Stock Exchange.

Article from:
Newsletter EnginSoft Autumn 2017- Update January 2023


PROMETECH.
ENGINSOFT
Particleworks
EUROPE